2016

Applications Of Disposable Pipette Technologies With LC-MS/MS For Forensic And Clinical Analyses Of Biological Matrices

Kaylee R. Mastrianni
University of South Carolina

Applications of Disposable Pipette Technologies with LC-MS/MS for Forensic and Clinical Analyses of Biological Matrices

by

Kaylee R. Mastrianni

Bachelor of Science
Western New England University, 2012

Submitted in Partial Fulfillment of the Requirements

For the Degree of Doctor of Philosophy in

Chemistry

College of Arts and Sciences

University of South Carolina

2016

Accepted by:

Stephen L. Morgan, Major Professor

William E. Brewer, Committee Member

Scott Goode, Committee Member

Michael Myrick, Committee Member

Maria Marjorette Pena, Committee Member

Paul Allen Miller, Vice Provost and Interim Dean of Graduate Studies

DEDICATION

This work is dedicated to my loving husband, Chris, and parents, Martin and Laura McDonald, for their constant support and encouragement.

ACKNOWLEDGEMENTS

I would like to thank my family, without whom I would not be the person I am today. I'm also forever grateful to my husband for his patience, love, and support over the last four years.

I would like to express my sincere gratitude to my mentor, Dr. William E. Brewer, for his continuous support, motivation, and immense knowledge. I am indebted to him for providing the opportunity for me to research within my interest of toxicology. Working with him was both an honor and a pleasure.

I would also like to thank Dr. Stephen L. Morgan for the opportunity to work for him. His attention to detail and editorial ability has influenced the refinement of my writing skills.

ABSTRACT

Efficiently hydrolyzing glucuronide metabolites is an important step in the analysis of drugs in urine. Amitriptyline and cyclobenzaprine are both tricyclic compounds with tertiary aliphatic amine groups that are subsequently metabolized to a less common form of glucuronide metabolite, quaternary ammonium linked glucuronides (N^+- glucuronide). A collaborative study was conducted to investigate discrepancies in recoveries of these two commonly prescribed compounds in patient urine samples when hydrolyzed with different enzyme from four different commercially available *β*-glucuronidase sources.

Similarly, there is potential for 6-monoacetylmorphine to be converted to morphine during β-glucuronidase hydrolysis of urine samples. 6-monoacetylmorphine is a unique metabolite of heroin and thus a marker of heroin use. A collaborative study was performed to analyze the degree of 6-monoacetylmorphine (6-MAM) conversion by the same four commercially available β-glucuronidase enzymes in drug free spiked urine and patient urine samples.

Meconium is an important biological matrix in determining drug exposure of a newborn. A novel method for the quantitation of ten commonly prescribed benzodiazepines and/or their metabolites (7-aminoclonazepam, clonazepam, α-hydroxyalprazolam, alprazolam, nordiazepam, diazepam, midazolam, oxazepam, lorazepam, and temazepam) in meconium was developed using enzymatic hydrolysis,

WAX-S dispersive pipette extraction (DPX) tips, and LC-MS/MS. The proposed method minimizes sample volume and sample preparation time. A successful blind study with a corresponding laboratory verified the effectiveness of the method.

As marijuana continues to be decriminalized, the need for analyses to determine marijuana impairment for driving under the influence cases rises. An analytical procedure was developed and validated for the analysis of Δ^9-tetrahydrocannabinol (THC) and its metabolites, 11-hydroxy-Δ^9-tetrahydrocannabinol (11-OH-THC) and 11-nor-9-carboxy-Δ^9-tetrahydrocannabinol (THC-COOH), in whole blood using liquid chromatography tandem mass spectrometry (LC-MS/MS). An automated DPX method was employed on a Hamilton NIMBUS96 platform to extract the analytes of interest. A full well plate (96) of samples could be extracted in less than three minutes. The method was fully validated according to the Scientific Working Group of Forensic Toxicology (SWGTOX) guidelines. This method resulted in a successful patient sample comparison with a local forensic toxicology lab, South Carolina Law Enforcement Division.

The measurement of free catecholamines and metanephrines in the clinical laboratory is important for the diagnosis of tumors, such as pheochromocytoma. We have developed an automated, high throughput DPX sample preparation procedure for the selective extraction of norepinephrine, epinephrine, dopamine, normetanephrine, and metanephrine in urine. The method was assessed for linearity, sensitivity, precision, accuracy, carryover, matrix effects and recovery. Using diphenyl borinic acid for complexation and styrene divinyl benzene for extraction enabled high recoveries and reduced ion suppression. The simple and high throughput nature of this method would be ideal for

clinical laboratories experiencing high demand for catecholamine and metanephrine urine analysis.

Determining the limit of detection (LOD) for a toxicological analytical method is an important component of method validation. However, with growing applications in an increasing variety of applications, the recommendation for determining an LOD from relevant data have evolved in varying directions. Specifically, guidelines often do not clarify the ambiguities and the effects of different choices associated with the estimate of uncertainty (standard deviation) for signal-to-noise LOD criteria. Further, LOD is based on fitting calibration relationship by the method of least squares which require assumptions (e.g., constant variance) that are rarely addressed. In addition to clarifying these ambiguities, the application of tolerance intervals for limits of detection determinations is discussed for forensic dye analysis.

.

TABLE OF CONTENTS

LIST OF TABLES

LIST OF FIGURES

CHAPTER 1

VARIATIONS IN ENZYMATIC HYDROLYSIS EFFICIENCIES FOR AMITRIPTYLINE AND CYCLOBENZAPRINE IN URINE

Abstract

A collaborative study was conducted to investigate discrepancies in recoveries of two commonly prescribed compounds, amitriptyline and cyclobenzaprine, in patient urine samples when hydrolyzed with different enzymes from different sources. A two- to ten-fold increase in analyte recoveries was seen for patient samples hydrolyzed using a recombinant *β*-glucuronidase (IMCSzyme™) over samples hydrolyzed with *β*-glucuronidase from *Haliotis rufescens*. We report outcomes from four commercially available *β*-glucuronidase enzymes (IMCSzyme™, *Patella vulgata*, *Helix pomatia*, and *Haliotis rufescens*) on patient samples that tested positive for amitriptyline and cyclobenzaprine. Our results confirm reduced hydrolysis of glucuronides by *β*-glucuronidases isolated from mollusks, but near complete conversion when using the recombinant enzyme. Our premise is systematic differences in hydrolysis efficiencies due to varying substrate affinity among enzyme subtypes potentially impacts accuracy and reliability of measurements.

Introduction

Amitriptyline and cyclobenzaprine are both tricyclic compounds with tertiary aliphatic amine groups that are subsequently metabolized to form quaternary ammonium linked glucuronides (N^+- glucuronide). Amitriptyline is a tricyclic antidepressant that was first introduced in the 1950s (1). Amitriptyline is currently a widely used tricyclic antidepressant. Cyclobenzaprine is also a tricyclic compound, initially marketed under the name Flexeril™ in 1977 (2). The drug is a skeletal muscle relaxant commonly prescribed for acute neck and back pain as well as fibromyalgia treatment (2). Due to its high potential for abuse, cyclobenzaprine is monitored by many toxicology and pain management laboratories (3-8).

Cyclobenzaprine and amitriptyline are structurally related and hence metabolize similarly. Both can be demethylated, oxidized, hydroxylated at the aromatic carbons, and glucuronidated (9-11). The glucuronides formed are quaternary ammonium-linked (Figure 1.1). Only trace levels of parent compound are found in urine due to the extensive metabolism. A pharmacokinetic study showed free unconjugated amitriptyline in urine at approximately 1% of the initial dose, while amitriptyline glucuronide accounts for 58% of the urinary metabolites at approximately 25% of the dose taken (9). Similarly, cyclobenzaprine N^+-glucuronide can be present in urine with concentrations up to 50% of the dose (10). Ideally, glucuronides could be targeted directly for monitoring amitriptyline or cyclobenzaprine use. Glucuronides typically require extended liquid chromatography run times, and exhibit poor recoveries with solid phase extractions and low ionization efficiencies with in electrospray mass spectrometry. Hydrolysis of the glucuronides should lead to increased concentrations of the parent compounds, providing

better sensitivity and accuracy for monitoring these drugs. Unfortunately, the quaternary ammonium linked glucuronides are less common than primary or secondary glucuronides and have proven to be difficult to hydrolyze with *β*-glucuronidase enzymes isolated from mollusks (10, 12-13).

After observing large discrepancies between samples hydrolyzed with *Haliotis rufescens* and IMCSzyme™, a more comprehensive study was conducted to monitor the hydrolysis of patient samples positive for cyclobenzaprine or amitriptyline with four different sources of *β*-glucuronidase enzyme: IMCSzyme™ (genetically engineered *E. Coli*), *Patella vulgata* (limpet), *Helix pomatia* (Roman snail), and *Haliotis rufescens* (red abalone). Patient samples were analyzed before and after hydrolysis with each of the enzymes and conversion of glucuronide conjugates was monitored by the increase in free (unconjugated) parent compound. The objective of this study was to evaluate the hydrolysis of quaternary ammonium-linked glucuronide metabolites with each of the named target enzymes.

Materials and Methods

Reagents and Standards

Amitriptyline, amitriptyline-d_3, and cyclobenzaprine drug standards were purchased from Cerilliant Corporation (Round Rock, TX). The amitriptyline glucuronide standard had a listed concentration of 1000 ng/mL and was provided by TLC Pharmaceutical Standards (Ontario, Canada). Disposable pipette extraction (DPX) tips were provided by DPX Technologies, LLC (Columbia, SC); the 1 mL RP-S tips contain styrene divinyl benzene sorbent with salt. IMCSzyme™ was obtained from Integrated MicroChromatography

Systems, LLC (Columbia, SC). *Haliotis rufescens β*-glucuronidase was purchased from Campbell Science (Logan, UT). *Helix pomatia* and *Patella vulgata* enzymes were purchased from Sigma Aldrich (St. Louis, MO). All solvents were LC-MS Optima grade, from Fisher Scientific (Waltham, MA).

Specimens

Five urine samples positive for amitriptyline and five urine samples positive for cyclobenzaprine were obtained from PSO laboratory (Lansing, MI); all samples were anonymously coded. All ten samples were analyzed in the initial method comparison study using *Haliotis rufescens* (with results obtained by PSO Lab), and IMCSzyme™ (analyzed several days later). Further studies of the hydrolysis of spiked samples using other enzymes were conducted and presented herein. Patient samples, one positive for amitriptyline and one positive for cyclobenzaprine, were also analyzed using the various enzymes for direct comparison.

Sample Preparation

The following procedures were used for both the method comparison and the consequent enzyme hydrolysis comparison. Urine samples were prepared by aliquoting 200 µL into a 2 mL micro centrifuge tube (VWR, Radnor, PA). A master mix solution containing 10 µL of 1000 ng/mL amitriptyline-d_3 in methanol, 50 µL of hydrolysis buffer, and 40 µL of enzyme were added to the urine. Rapid hydrolysis buffer was provided by the vendor for IMCSzyme™ and 1 M sodium acetate at pH 4.5 was used for the other three enzymes. IMCSzyme™ had an activity of > 50 kU/mL, while *Helix pomatia, Patella vulgata,* and *Haliotis rufescens* were > 100 kU/mL. Samples were heated and vortexed at 60 °C and

550 RPM for 30 min. with IMCSzyme™ and 1 h for the other enzymes using a Labnet VorTemp™ 56 Benchtop Incubator/Shaker (Woodbridge, NJ). These hydrolysis time and temperature were consistent with manufacturer specifications.

Subsequent to hydrolysis, 500 µL acetonitrile was added to each sample, and disposable pipette extractions were performed by aspirating and dispensing the sample solutions in and out of the DPX (RP-S) tips. The extraction produces two distinct layers, aqueous solution containing salts on the bottom and acetonitrile containing analytes of interest on the top. After transferring a 300 µL portion of the top acetonitrile layer to a vial, and adding 700 µL water, the samples were ready for analysis.

Calibrators and Controls

All calibrators and controls were prepared in drug-free urine, obtained from healthy volunteers. The calibration design used for the method comparison study included eight concentration points at 0, 50, 100, 250, 500, 1000, and 2000 ng/mL of amitriptyline and cyclobenzaprine. Calibrations were done in duplicate to account for the difference in buffer pH needed for IMCSzyme™ (pH ~7.4) and *Haliotis rufescens*, *Patella vulgata*, and *Helix pomatia* (pH ~4.5).

Instrumental Analysis

Analyses were performed using a Thermo TSQ Vantage™ triple quadrupole mass spectrometer (Milwaukee, WI) coupled to an Agilent 1100 Series HPLC (Agilent Technologies, Waldbronn, Germany) equipped with an Agilent Poroshell EC-C18 column (3.0 x 50 mm, 2.7 µm). Sample injections of 20 µL were made using a 6 port

(0.25 mm) Cheminert C2V injection valve (Houston, TX) incorporated on a dual rail GERSTEL MPS autosampler (Linthicum, MD).

The mobile phase was composed of 0.1% formic acid in water (A) and 0.1% formic acid in acetonitrile (B). The gradient started at 70% A for 0.5 min., ramped to 5% A at 3 min., held at 5% A at 3.5 min, and then changed back to 70% A. The total run time was 6 min. Eluent was diverted to waste during the intervals of 0-0.75 and 4.5-6 min. after the injection. The column flow rate was 0.4 mL/min. Mass spectrometer parameters were: electrospray voltage, 4000 V; auxillary gas pressure, 60 psi; sheath gas pressure, 47 psi; vaporizer temperature, 400 °C; auxillary gas temperature, 24 °C; capillary temperature 350 °C. The selected ion pairs for multiple reaction monitoring (MRM) for each analyte can be found in Table 1.1.

Results and Discussion

Comparative Study with 10 Patient Samples

Researchers at PSO laboratory recognized a discrepancy between hydrolysis results of *Haliotis rufescens* and IMCSzyme™ in a number of patient samples, and donated samples to the University of South Carolina (USC) for further investigation. Patient sample results comparing IMCSzyme™ and *Haliotis rufescens* are summarized in Table 1.2, showing the concentrations of the unhydrolyzed parent compound (amitriptyline/ cyclobenzaprine) and concentrations of the parent compound after hydrolysis (hydrolyzed). The amount of glucuronide conjugates can be calculated from hydrolyzed versus unhydrolyzed concentration of the parent compound. The IMCSzyme™ and *Haliotis rufescens* unhydrolyzed sample concentration should be the same. Differences,

however, can potentially be attributed to hydrolysis in the two month storage time between analyses.

IMCSzyme™ and *Haliotis rufescens* produced different hydrolyzed parent compound concentrations, ranging over almost an order of magnitude. For example, in patient sample 42756, the hydrolyzed concentration of cyclobenzaprine using IMCSzyme™ was 4153.0 ng/mL; the hydrolyzed concentration using *Haliotis rufescens* was only 450.4 ng/mL. The amount of glucuronide conjugates hydrolyzed by the *Haliotis rufescens* was consistently lower in all samples compared to that produced by IMCSzyme™. Thus, enzyme choice (*Haliotis rufescens* for PSO, and IMCSzyme™ for this method) significantly impacted the amount of glucuronide converted. Consequently, further experiments were performed evaluate the ability of four commercially available *β*-glucuronidase enzymes to hydrolyze this unique class of glucuronides.

Glucuronides were monitored using the same product ions as the parent compounds shown in Table 1.1. These measurements enabled qualitative assessment of the glucuronide decrease as a result of hydrolysis, and to monitor consistency of the relationship between the parent compound peak area increase and glucuronide peak area decrease as a result of hydrolysis. The ratio (Δ[Parent]/Δ[Glucuronide]), shown in Table 1.3, can be employed to ascertain the likelihood that the increase in parent compound is a direct result of glucuronide decrease. If the ratio remains consistent throughout the patient samples, then it is likely that the parent compound peak area increase is a direct result of the glucuronide peak area decrease. However, if the ratios are highly variable, then it is likely there is a confounding factor causing the parent compound increase. Ratios for IMCSzyme™ data were consistent (approximately 6 for cyclobenzaprine and

18 for amitriptyline) except when the glucuronide peak areas for unhydrolyzed compounds were low (~30,000 area counts). This occurred for patient samples 48675 and 42746, which were most likely outside the linear dynamic range. We therefore concluded that the observed parent compound peak intensity increases were a direct result of glucuronide hydrolysis.

Hydrolysis of Amitriptyline Glucuronide Standard in Drug Free Urine

Drug-free urine was spiked with the acquired amitriptyline glucuronide standard. However, the concentration of amitriptyline glucuronide standard that was provided was inaccurate for two reasons. After "complete" hydrolysis (where no glucuronide peak was detected), the yield of amitriptyline did not match the manufacturer's specified amitriptyline glucuronide concentration. Further, amitriptyline was also present in the glucuronide standard solution, thus suggesting degradation had occurred. Therefore, calibration for product amounts was not conducted, and the peak areas of both compounds were monitored before and after hydrolysis.

The four sources of *β*-glucuronidase chosen here include a genetically engineered *β*-glucuronidase and three different types of sea snail sources. The goal of this work was not to find the optimum hydrolysis conditions for different enzymes, but rather, to compare their relative hydrolysis efficiencies. For that reason, the manufacturer recommendations for hydrolysis conditions were followed as described in the Experimental section.

Average peak areas for amitriptyline and amitriptyline glucuronide before and after hydrolysis with each of the enzymes are shown in Table 1.4. Percent hydrolysis was calculated as

$$\% \text{ hydrolysis} = (1 - A/B) \times 100\% \qquad \text{(Equation 1)}$$

where *A* is the average ratio (n = 3) of amitriptyline glucuronide peak area to internal standard peak area for post-hydrolysis, and *B* is the average ratio (n = 3) of amitriptyline glucuronide peak area to internal standard peak area for pre-hydrolysis.

IMCSzyme™ achieved 99.3% hydrolysis in 30 min. of incubation. The three mollusk enzymes (*Helix pomatia*, *Haliotis rufescens*, and *Patella vulgate*) produced 6.3%, 23.2%, and 31.4% hydrolysis, respectively, in 1 h. of incubation. The incubation times employed are based on manufacturer recommendations and common laboratory procedures for the respective enzymes. Amitriptyline glucuronide peak area decrease and amitriptyline peak area increase, when comparing pre-and post-hydrolysis chromatograms for each enzyme, as shown in Table 1.4.

Hydrolysis of Patient Samples by Four Different Enzymes

Further experiments to estimate the percent glucuronidation in actual patient samples were performed for the same four enzymes. In this case, however, the percent glucuronidation was calculated based on monitoring changes in the concentration of the parent compound (amitriptyline or cyclobenzaprine). The calculated percent glucuronidation for each enzyme can be compared to average ratios reported in the literature for parent and glucuronide metabolites in human urine. We assume that if calculated glucuronidation percentages are similar to reported averages, then the enzyme likely converted close to all of the available glucuronide.

The patient samples chosen for comparison of hydrolysis capability were patient sample 49187 (positive for cyclobenzaprine), and 42748 (positive for amitriptyline).

Samples (n = 2) were analyzed for amitriptyline or cyclobenzaprine before hydrolysis (unhydrolyzed), and after hydrolysis (hydrolyzed) for each of the four enzymes. The N^+-glucuronide metabolites of cyclobenzaprine and amitriptyline were resistant to hydrolysis with *Helix pomatia*, *Patella vulgata*, and *Haliotis rufescens*, but not with IMCSzyme™.

Table 1.5 shows total parent compound (amitriptyline/cyclobenzaprine) concentration (ng/mL) prior to hydrolysis ("unhydrolyzed"), and after hydrolysis ("hydrolyzed") with each of the four *β*-glucuronidase enzymes. Based on these values, the percent glucuronidation is calculated as the percentage of glucuronide metabolite compared to amount of total parent compound after hydrolysis, and represents the relative amount of hydrolyzed glucuronide produced by each enzyme. Hence, the percent glucuronidation increases with the increase in hydrolysis of the glucuronide metabolites.

Of the four enzymes tested, IMCSzyme™ converted the highest amount of amitriptyline N^+-glucuronide during hydrolysis (95.3%). The other enzymes exhibited glucuronidation percentages ranging from 57.8-67.5 %. The glucuronidation percentage with IMCSzyme™ hydrolysis is consistent with reported amitriptyline and amitriptyline glucuronide concentrations from metabolism studies in the literature. Using a hot alkali treatment (2 M sodium hydroxide at 100 °C for 15 min.), Dahl-Puustinen, *et al*. (14) found free amitriptyline concentration in urine to be 0.45 ± 0.46 % of total dose, while amitriptyline glucuronide was found to be 8.2 ± 3.2 % of total dose. These values represent an average of 94.8 % glucuronidation. Other studies report that excreted amitriptyline N^+-glucuronide is 5-10 % of the administered dose, and that free amitriptyline constitutes 0.2-0.4% of the dose (10). These results imply 92-98 % binding of glucuronide conjugates. Lastly, Rana, *et al.* (1) reported an average of 90 %

glucuronidation for amitriptyline in urine using K12 *β*-glucuronidase from *E. coli* at 52 °C for one h.

Our results show that the concentration of cyclobenzaprine post-hydrolysis with IMCSzyme™ was much higher than the post-hydrolysis cyclobenzaprine concentrations for the other enzymes. The IMCSzyme™ post-hydrolysis concentration of cyclobenzaprine was 2322.6 ± 16 ng/mL, while the concentration of free cyclobenzaprine in the unhydrolyzed sample was 144.4 ± 11 ng/mL, which correlates to a glucuronidation percentage of 93.8%. The other three enzymes had percentages that ranged from 52.0-72.9%. The IMCSzyme™ glucuronidation percentage is comparable to the free cyclobenzaprine and cyclobenzaprine glucuronide ratios found in the literature. Hucker, *et al.* (11) reported 1.7 % of metabolites in urine as free cyclobenzaprine and 34.0% was attributed to the N^+-glucuronide during the first 24 h. after administration–an average glucuronidation percentage of 95.2%. Between 24 and 48 h. 1.1 ± 0.6 % of metabolites in urine was free cyclobenzaprine, and 24.1 ± 6.9% was cyclobenzaprine glucuronide, corresponding to an average glucuronidation percentage of 95.6%. Hucker's study was carried out over five days. Cyclobenzaprine was present for the first 48 h. while cyclobenzaprine glucuronide was present for all five days. High hydrolysis efficiency from IMCSzyme™ for cyclobenzaprine glucuronide increases sensitivity and provides a longer window of detection for the parent compound.

We employed drug-free urine spiked with amitriptyline glucuronide standard to provide known reference samples for testing hydrolysis efficiency for the four different enzymes. Percent hydrolysis ranged from 6.3% with *Helix pomatia* in one h., to 99.3% with IMCSzyme™ in 30 min. This amitriptyline glucuronide standard hydrolysis study

was performed at a relatively low level (~1000 ng/mL) of amitriptyline glucuronide at which the enzymes perform optimally. However, patient samples often have a much greater glucuronide concentration. Thus, when comparing the post-hydrolysis glucuronide amounts in both the patient sample study and the glucuronide standard study, the three snail sourced enzymes performed more poorly. For example, *Patella vulgata* hydrolyzed approximately 30% of the amount that IMCSzyme™ did in the low glucuronide spiked urine. However, in patient samples, *Patella vulgata* only hydrolyzed approximately 13% of that hydrolyzed by IMCSzyme™ (based on post-hydrolysis amitriptyline concentrations). Use of IMCSzyme™ provided ratios of parent compound to glucuronide most consistent with the literature reports of average human excretion patterns (6, 10-11). The other three enzymes convert less amitriptyline and cyclobenzaprine glucuronide, even under more rigorous conditions (*i.e.*, longer hydrolysis time and higher activity). This variation of hydrolysis based on enzyme source for N^+-glucuronides is consistent with previous literature. Kowalczyk, *et al.*, compared the ability of three different enzymes (bovine liver, *E. coli*, and *Helix pomatia*) to hydrolyze two cyclic and two acyclic quaternary ammonium-linked glucuronide metabolites. This work showed that the enzymes hydrolyzed the compounds to different degrees and adjustment of buffer pH and amount of enzyme did not achieve complete hydrolysis (13).

Conclusion

Although variation in hydrolysis of these quaternary ammonium-linked glucuronides with enzyme source is evident, the high degree of hydrolysis with IMCSzyme™ provides a reliable β-glucuronidase source for amitriptyline and cyclobenzaprine N^+-glucuronide

hydrolysis. Hydrolysis efficiencies may vary due to many factors, including impurities in the enzyme solution, and/or differing binding affinities for this specific class of glucuronides. Large discrepancies in the hydrolysis efficiency of different enzymes is of great practical significance due to the potential for incomplete hydrolysis of samples. Insufficient hydrolysis results in limited sensitivity and positive samples may fall below limits of detection and/or limits of quantitation. Results presented here demonstrate that enzyme choice and/or optimal hydrolysis conditions should be evaluated specifically for N^+-glucuronides. Other combinations of N^+-glucuronide metabolites of different drugs (30+ known) and sources of *β*-glucuronidase may produce different hydrolysis results.

For both amitriptyline and cyclobenzaprine, *Helix pomatia, Patella vulgata,* and *Haliotis rufescens* produced lower hydrolysis efficiencies for amitriptyline N^+-glucuronide and produce glucuronide percentages in patient samples well below literature reported human metabolism ratios of these drugs. IMCSzyme™ hydrolysis resulted in calculated glucuronidation percentages closer to the literature averages in half the hydrolysis time. Based on the data reported, we conclude that IMCSzyme™ is more efficient at hydrolyzing these N^+-glucuronide metabolites (at the conditions tested) and could improve the sensitivity of the analysis of these compounds.

References

1. Rana, S., Uralets, V., Ross, W. (2008) A new method for simultaneous determination of cyclic antidepressants and their metabolites in urine using enzymatic hydrolysis and fast GC-MS. *Journal of Analytical Toxicology*, **32**, 355-363.
2. Cimolai, N. (2009) Cyclobenzaprine: a new look at an old pharmacological agent. *Expert Reviews in Clinical Pharmacology*, **2**, 255-263.
3. Spiller, H., Winter, M., Mann, K., Borys, D., Muir, S., Krenzelok, E. (1995) Five-year multicenter retrospective review of cyclobenzaprine toxicity. *Journal of Emergency Medicine*, **13**, 781-785.
4. Chabria, S. (2006) Rhabdomyolysis: a manifestation of cyclobenzaprine toxicity. *Journal of Occupational Medicine and Toxicology*, **1**, 1-2.
5. Spiller, H., Cutino, L. (2003) Fatal cyclobenzaprine overdose with postmortem values. *Journal of Forensic Science*, **48**, 883-884.
6. Linden, C., Mitchener, J., Lindzon, R., Rumack, B. (1983) Cyclobenzaprine overdosage. *Clinical Toxicology*, **20**, 281-288.
7. O'Riordan, W., Gillette, P., Calderon, J., Stennes, R. (1986) Overdose of cyclobenzaprine, the tricyclic muscle relaxant. *Annals of Emergency Medicine*, **15**, 592-593.
8. Lebby, T., Dugger, K. (1990) Skeletal muscle relaxant ingestion. *Veterinary and Human Toxicology*, **32**, 133-135.
9. Breyer-Pfaff, U. (2004) The metabolic fate of amitriptyline, nortriptyline, and amitriptylinoxide in man. *Drug Metabolism Reviews*, **36**, 723-746.

10. Hawes, E. (1998) N+-glucuronidation, a common pathway in human urine of drugs with a tertiary amine group. *Drug Metabolism and Disposition*, **26**, 830-837.
11. Hucker, H., Balletto, A., Arison, B., Zacchei, A. Arison, B. (1978) Physiological disposition and metabolism of cyclobenzaprine in the rat, dog, rhesus monkey, and man. *Drug Metabolism and Disposition*, **6**, 659-672.
12. Fischer, D., Breyer-Pfaff, U. (1995) Comparison of procedures for measuring the quaternary N-glucuronides of amitriptyline and diphenhydramine in human urine with and without hydrolysis. *Journal of Pharmacy and Pharmacology*, **47**, 534-538.
13. Kowalczyk, I., Hawes, E., McKay, G. (2000) Stability and enzymatic hydrolysis of quaternary ammonium-linked glucuronide metabolites of drugs with an aliphatic tertiary amine-implications for analysis. *Journal of Pharmaceutical and Biomedical Analysis*, **22**, 803-811.
14. Dahl-Puustinen, M., Aberg-Wistedt, A., Bertilsson, L. (1989) Glucuronidation of Amitriptyline in Man *in Vivo*. *Pharmacology and Toxicology*, **65**, 37-35.

Table 1.1

Ions selected for multiple reaction monitoring.

Analyte	Ions	
	Parent	Products
Amitriptyline	278	91.1, 233.0
Amitriptyline d_3	281	190.9, 233.0
Amitriptyline glucuronide	454.2	91.1, 233.0
Cyclobenzaprine	275.9	215.9, 231.0
Cyclobenzaprine glucuronide	452.2	215.9, 231.1

Table 1.2
Comparison of patient sample cyclobenzaprine and amitriptyline concentrations (ng/mL) prior to hydrolysis (unhydrolyzed), and after hydrolysis (hydrolyzed) in after use of IMCSzyme™ and *Haliotis rufescens (red abalone)* (NF = not found).

Cyclobenzaprine

	IMCSzyme™	
Patient Sample	Unhydrolyzed	Hydrolyzed
42756	1407	4153
48675	3618	3918
48678	NF	NF
48735	298	2985
49187	167	2715
	Haliotis rufescens	
Patient Sample	Unhydrolyzed	Hydrolyzed
42756	29	450
48675	214	661
48678	NF	87
48735	81	170
49187	33	182

Amitriptyline

	IMCSzyme™	
Patient Sample	Unhydrolyzed	Hydrolyzed
42746	7	95
42748	117	2253
42753	47	799
48663	587	4175
48665	35	1542
	Haliotis rufescens	
Patient Sample	Unhydrolyzed	Hydrolyzed
42746	6	11
42748	67	85
42753	26	76
48663	312	496
48665	20	191

Table 1.3

Comparison of peak areas for parent (cyclobenzaprine/amitriptyline) and glucuronide conjugates before and after hydrolysis with IMCSzyme™ as described in Sample Preparation (NF = Not Found, N/A = Not Applicable).

	Cyclobenzaprine glucuronide		Cyclobenzaprine		
Patient Sample	Unhydrolyzed	Hydrolyzed	Unhydrolyzed	Hydrolyzed	Δ[Parent]/ Δ[Glucuronide]
42756	820983	1182	2904217.4	7440808.8	5.5
48675	31197	NF	10290532	11237703	30.4
48678	NF	NF	930.5	2799.9	N/A
48735	1305618	912	665501.5	9123170.9	6.5
49187	735546	929	380286	6597721.7	8.5
	Amitriptyline glucuronide		Amitriptyline		
Patient Sample	Unhydrolyzed	Hydrolyzed	Unhydrolyzed	Hydrolyzed	Δ[Parent]/ Δ[Glucuronide]
42746	31269	NF	5114	308288	9.7
42748	372287	4938	480017	6824697	17.3
42753	162822	1823	199265	3072325	17.9
48663	696569	11806	2158599	15531667	19.5
48665	247575	233	133743	4702824	18.5

Table 1.4

Average peak areas (n = 3) before and after hydrolysis with *Helix pomatia*, *Haliotis rufescens*, *Patella vulgata*, and IMCSzyme™ and subsequent calculated percent hydrolysis.

	Average Peak Area			% Hydrolysis
	Am. Gluc.	*Amitriptyline*	*Am. Gluc./I.S.*	
Helix pomatia				
Pre-Hydrolysis	126093.1	11987.6	0.293	**6.3**
Post-Hydrolysis	123873.1	34786.1	0.274	
Haliotis rufescens				
Pre-Hydrolysis	116697.4	13315.4	0.255	**23.2**
Post-Hydrolysis	92136.2	96844.6	0.196	
Patella vulgata				
Pre-Hydrolysis	112592.8	12715	0.244	**31.4**
Post-Hydrolysis	76658.2	137821.6	0.168	
IMCSzyme™				
Pre-Hydrolysis	107857.2	16285.1	0.194	**99.3**
Post-Hydrolysis	500.3	356913.9	0.001	

Table 1.5

Amitriptyline and cyclobenzaprine concentrations (mean ± standard deviation, ng/mL) (n = 2) post-hydrolysis for each enzyme and the calculated percent glucuronidation based on concentrations of parent drug pre-hydrolysis (N/A = not applicable).

	Amitriptyline	
	Total Parent Concentration	% Glucuronidation
Unhydrolyzed	88.4 +/- 2.1	N/A
IMCSzyme™	1892.6 +/- 21.4	95.3
Helix pomatia	209.3 (one rep)	57.8
Patella vulgata	245.8 +/- 2.8	64.0
Haliotis rufescens	271.9 +/- 3.1	67.5
	Cyclobenzaprine	
	Total Parent Concentration	% Glucuronidation
Unhydrolyzed	144.4 +/- 10.9	N/A
IMCSzyme™	2322.6 +/- 16.1	93.8
Helix pomatia	300.9 (one rep)	52.0
Patella vulgata	523.7 +/- 3.6	72.4
Haliotis rufescens	532.8 +/- 3.7	72.9

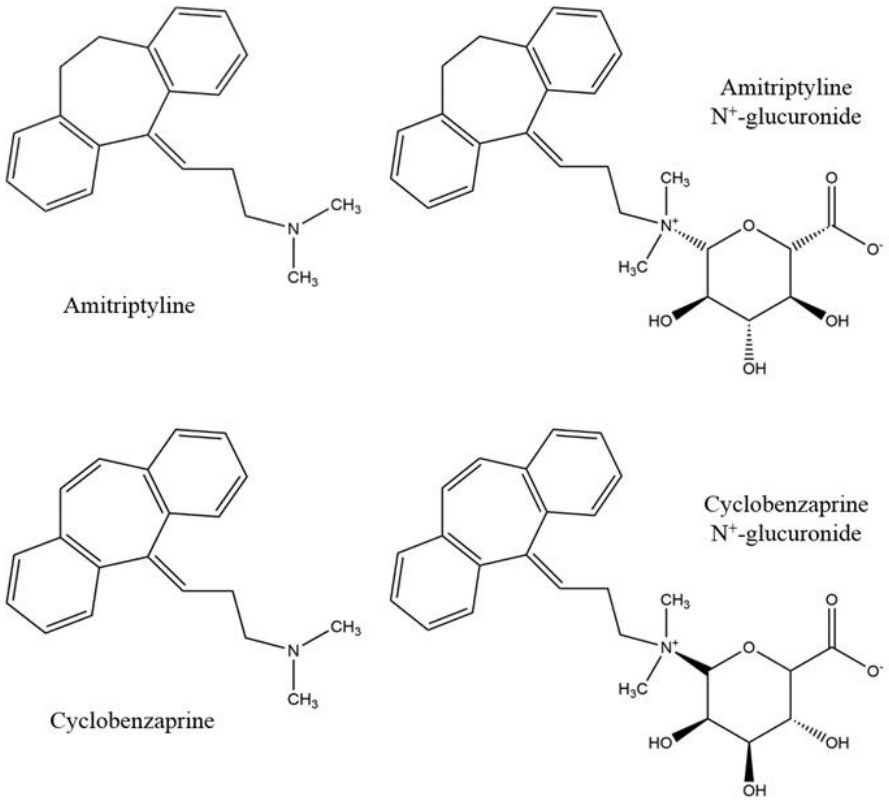

Figure 1.1 Structures of amitriptyline, cyclobenzaprine, and their N^+-glucuronides.

CHAPTER 2

ASSESSMENT OF 6-MONOACETYLMORPHINE CONVERSION DURING HYDROLYSIS WITH DIFFERENT β-GLUCURONIDASES

Abstract

There is potential for 6-monoacetylmorphine, a unique metabolite of heroin, to be converted to morphine during β-glucuronidase hydrolysis of urine samples. Loss of 6-monoacetylmorphine from the sample under analysis is detrimental to the determination of heroin use. Therefore, laboratories are forced to analyze opiate positive urine samples before and after hydrolysis to limit false negative heroin results. The increase in samples to analyze propagates backlog and increases cost.

A collaborative study was performed to determine the degree of 6-monoacetylmorphine (6-MAM) conversion by four commercially available β-glucuronidase enzymes (IMCSzyme™, *Haliotis rufescens*, *Helix pomatia*, and *Patella vulgata*) in drug free spiked urine and patient urine samples. The hydrolysis was performed at the specified temperature at 0, 1, and 2 h hydrolysis time intervals. 6-MAM and morphine levels were compared at each time interval to determine the amount of 6-MAM loss and corresponding morphine increase. The extent of 6-MAM conversion varied for each β-glucuronidase from 3 to 47% over 2 h. Choosing a β-glucuronidase that minimizes 6-MAM conversion would help conserve valuable resources.

Introduction

Heroin (3,6-diacetylmorphine) was first synthesized in 1874 as an antitussive. Heroin use drastically increased after the Vietnam War; approximately 42% of returning service members reported use. Heroin eventually became a Schedule I Substance, but there are still approximately 980,000 "hard core" users in the United States and 1.2-1.5 million total users (1). Due to its illicitness and highly adverse side effects, urine drug testing is routine for workplace, pre-employment, pre-trial, and criminal/death investigations, and in other situations in which effects of impairment are observed with individuals who are subsequently suspected of illicit drug use.

Due to the very short half-life of heroin (~2-8 min), detection of abuse using urine must rely on its metabolites (2, 3-9). Drug testing for heroin first began by monitoring for morphine, a known metabolite of heroin (Fig. 2.1). However, morphine is also a metabolite of codeine, and can also be found as a result of poppy seed ingestion, thus producing an increased likelihood of false positives for heroin presence. In 1994, the Department of Defense and the Department of Health and Human Services mandated testing for 6-monoacetylmorphine (6-MAM) because it is a metabolite exclusively for heroin (1, 10).

Today, analysis of opiates often includes hydrolysis via a β-glucuronidase for removal of the glucuronide moiety from glucuronidated metabolites for increased sensitivity. Unfortunately, a significant problem lies with the use of β-glucuronidase enzymes and their potential to convert 6-MAM to morphine. Initial 6-MAM levels in urine are often low as a result of a half-life of 10-40 min and a detection window of 2-24

h after intake (9). If 6-MAM conversion via the β-glucuronidase is significant, then 6-MAM may fall below detection limits, and definitive heroin use may be inconclusive. To avoid inaccurate quantitation of 6-MAM and morphine as a result of conversion during hydrolysis, laboratories have to analyze both hydrolyzed and unhydrolyzed opiate positive samples to monitor potential 6-MAM loss and morphine increase. This extra sample load requires time and money.

It is generally understood that β-glucuronidase enzymes effectively hydrolyze glucuronide conjugates, which is their primary purpose in opiate positive samples. However, their ability to convert 6-MAM to morphine undesirably has not been evaluated. Herein, we compare four commercially available β-glucuronidase enzymes, *Haliotis rufescens*, *Helix pomatia*, *Patella vulgata*, and IMCSzyme^{TM}, for their ability to convert 6-MAM to morphine using both controlled samples and patient samples.

Materials and Methods

Reagents and Standards

Morphine, 6-Monoacetylmorphine, and codeine-d_6 drug standards were purchased from Cerilliant Corporation (Round Rock, TX). Disposable pipette extraction (DPX) tips (type RP-S) were provided by DPX Technologies, LLC (Columbia, SC). IMCSzyme^{TM} was obtained from Integrated MicroChromatography Systems, LLC (Columbia, SC). *Haliotis rufescens* β-glucuronidase was purchased from Campbell Science (Logan, UT). *Helix pomatia* and *Patella vulgata* enzymes were purchased from Sigma Aldrich (St. Louis, MO). All solvents were LC-MS Optima grade, from Fisher Scientific (Waltham, MA).

Specimens

Spiked urine was used for direct analysis of 6-MAM conversion to morphine for all of the enzymes. Three urine samples positive for 6-MAM were obtained from PSO laboratory (Lansing, MI), all samples were anonymously coded, and used to compliment and confirm 6-MAM conversion in patient samples.

All calibrators and controls were prepared in drug-free urine. The two calibration curves consisted of morphine and 6-MAM at 0, 10, 50, 100, 500, and 1000 ng/mL. One calibration curve was prepared with the buffer solution appropriate for *Haliotis rufescens*, *Helix pomatia*, and *Patella vulgata* (pH 4.5) with sucrose in place of the enzyme. The other calibration curve was prepared with IMCSzyme^{TM} and its appropriate buffer at pH 7.4. Quality control samples were also prepared using drug-free urine. Six total quality controls positive for 6-MAM were used, three at 10 ng/mL and three at 100 ng/mL.

Hydrolysis and Sample Preparation

Hydrolysis of 200 µL urine was performed by adding 100 µL of the hydrolysis solution containing hydrolysis buffer (0.2 M potassium phosphate buffer at pH 7.4 for IMCSzyme^{TM}) and 1M sodium acetate buffer at pH 4.5 for the other three enzymes, in addition to a β-glucuronidase and codeine-d_6 internal standard at a ratio of 2:2:1, respectively. Samples were heated and mixed at 55 °C using a Labnet VorTemp^{TM} 56 Benchtop Incubator/Shaker (Woodbridge, NJ). Subsequently, 400 µL acetonitrile was added to each sample, and the solution was extracted using DPX-RP-S tips. This extraction results in separation of acetonitrile (containing drugs of interest) from water (containing salts and many interferences), after which 50 µL of the top acetonitrile layer was transferred to a 96-well plate. The solvent was evaporated and reconstituted with 200

µL of water/methanol (95/5). Hydrolysis with the 3 other enzymes was performed similarly, except the hydrolysis was carried out at 55°C using NaOAc buffer (167 mM, pH of 4.5).

For the controlled samples, the 6-MAM and morphine concentrations were monitored at time 0, after 1 h of incubation, and after 2 h of incubation with each enzyme. For the patient samples, each sample was hydrolyzed according to the manufacturer specified hydrolysis time, which was 30 min for IMCSzyme^{TM} and 2 h for the other three enzymes.

Instrumental Analysis

Analyses were performed using a Thermo TSQ Vantage triple quadrupole system (Milwaukee, WI) with an Agilent 1100 HPLC (Santa Clara, CA) equipped with an Agilent Poroshell EC-C18 column (3.0 × 50 mm, 2.7 µm). Sample injections of 20 µL were made using a 6 port (0.25 mm) Cheminert C2V injection valve (Houston, TX) incorporated on a dual rail GERSTEL MPS autosampler (Linthicum, MD).

The mobile phase used 0.1% formic acid in water (mobile phase A), and 0.1% formic acid in acetonitrile (mobile phase B) with a gradient from 95% A for 0.5 min, ramped to 5% A at 3 min, held at 5% A at 3.5 min, and then changed back to 95% A, for a run time of 6 min. The eluent was diverted to waste during the intervals of 0-0.75 and 4.5-6 min after the injection. The column flow rate was 0.4 mL/min. Electrospray voltage was 4000 V, and gas pressure was 60 psi. The selected MRMs were 286.1 to 152.1/165.1 (morphine), 462.0 to 285.8/200.89 (morphine glucuronide), 306.0 to 217.9/164.9/182.9 (codeine-d_6), and 327.9 to 165/201.9 *m/z* (6-MAM).

Results

Hydrolysis of Spiked 6-MAM Samples

Four enzymes were used to individually hydrolyze a previously drug-free urine sample spiked with 6-MAM for 0, 1, and 2 h. Nine samples were prepared for each enzyme, three samples for each length of hydrolysis. Therefore, any conversion could be monitored as a function of time. Of these four enzymes, three (*Haliotis rufescens*, *Helix pomatia*, and *Patella vulgata*) resulted in a decrease of 6-MAM and simultaneous increase in morphine after just 1 h.

The comparison of chromatograms (Figure 2.2) clearly shows that the *Helix pomatia* enzyme converts 6-MAM to morphine during the hydrolysis process. The amount of conversion appears to have a roughly linear relationship with length of hydrolysis. Over the course of two h. of hydrolysis, 6-MAM area counts decreased by half and morphine area counts reached a high of almost 11,000.

Figure 2.3 shows data from the analysis of 6-MAM spiked urine samples before and after hydrolysis with all four of the enzymes: IMCSzyme™, *Patella vulgata* (Sigma Aldrich, St. Louis, MO), *Haliotis rufescens* (Campbell science), and *Helix pomatia* (Sigma Aldrich). The concentration of 6-MAM stayed relatively constant when using IMCSzyme™ and approximately 10 ng/mL of morphine was detected after two hours. Because IMCSzyme™ only requires 30 min for glucuronide hydrolysis, any further morphine production would be minimized. The other enzymes come with recommendations of two hours for hydrolysis, and significant conversion to morphine occurs during that time. For example, *Haliotis rufescens* converted approximately 10% of

the starting 6-MAM concentration and produced about 28 ng/mL of morphine after two h of incubation. *Patella vulgata* converted over 30% of the 6-MAM and 75 ng/mL of morphine was detected after two h. Most severely, incubation for two h with *Helix pomatia* resulted in 47% loss in 6-MAM and a morphine level of 120 ng/mL. The concomitant 6-MAM loss and morphine increase suggests that the enzyme is responsible for the conversion.

Hydrolysis of 6-MAM Positive Patient Samples

The hydrolysis procedure used for the control samples was repeated with patient samples positive for 6-MAM. The exception being that these samples were hydrolyzed using the manufacturer specified hydrolysis time for each enzyme. (*Haliotis rufescens*, *Helix pomatia*, and *Patella vulgata*: 2 h; IMCSzyme^{TM}: 30 m). Each patient sample was analyzed prior to hydrolysis ("Unhydrolyzed") and was also separated into four different aliquots to be hydrolyzed with each of the four enzymes. Table 2.1 illustrates the significant conversion of 6-MAM to morphine in patient samples. The increase in morphine is unreliable as an indicator for the 6-MAM conversion due to the probable presence of morphine glucuronides prior to hydrolysis; however, the 6-MAM concentration should not fluctuate as a result of enzyme hydrolysis. Any variation of 6-MAM concentration can thus be attributed to enzyme conversion as shown with the controlled samples. In the case of *Helix pomatia* hydrolysis of patient sample 3741, almost half of the initial detected 6-MAM is lost in the time necessary for the enzyme to hydrolyze morphine glucuronides (two h). Both *Patella vulgata* and *Haliotis rufescens* also showed significant conversion to morphine, while IMCSzyme^{TM} converted very little. Patient sample 3637 obviously contained morphine and morphine glucuronides, but

reduction in 6-MAM was still apparent when *Helix pomatia* and *Patella vulgata* enzymes were used. Lastly, in patient sample 3627, 6-MAM concentrations increased with some of the enzymes which could possibly be attributed to the presence of acetate buffer as noted by Heideloff, *et al*. (11). However, notable morphine increases for *Helix pomatia*, *Patella vulgata*, and *Haliotis rufescens* occurred.

Conclusion

Significant conversion of 6-MAM to morphine occurs with the use of *Helix pomatia, Patella vulgata* and *Haliotis rufescens* enzymes for morphine glucuronide hydrolysis. This conversion is seen in the quality control samples as well as the patient samples. Depletion of 6-MAM to morphine using these enzymes would reduce the likelihood of detecting conclusive heroin use. IMCSzyme^{TM} demonstrates efficient hydrolysis of morphine glucuronide with negligible conversion of 6-MAM to morphine. While some conversion may occur after two h of incubation, only 30 min is needed for optimal morphine glucuronide hydrolysis with IMCSzyme^{TM}. Conversion of 6-MAM to morphine should be considered when using β-glucuronidase hydrolysis for analysis of heroin metabolites.

References

1. Smith, M., Shimomura, E., Summers, J., Paul, B. (2001) Urinary Excretion Profiles for Total Morphine, Free Morphine, and 6-Acetylmorphine Following Smoked and Intravenous Heroin. *Journal of Analytical Toxicology*. **25**, 504-514.
2. Cone, E., Welch, P. (1991) Forensic Drug Testing for Opiates: I. Detection of 6-Acetylmorphine in Urine as an Indicator of Recent Heroin Exposure; Drug and Assay Considerations and Detection Times. *Journal of Analytical Toxicology*, **15**, 1-7.
3. Boerner, U., Abbott, S., Roe, R. (1975) The Metabolism of Morphine and Heroin in Man. *Drug Metabolism Reviews*. **4**, 39-73.
4. Mitchell, J., Paul, B. (1991) Forensic Drug Testing For Opiates. II. Metabolism and Excretion Rate of Morphine in Humans After Morphine Administration. *Journal of Analytical Toxicology*. **15**, 49-53.
5. Yeh, S., Gorodetzky, C., McQuin, R. (1976) Urinary Excretion of Heroin and Its Metabolites in Man. *Journal of Pharmacology and Experimental Therapeutics*. **196**, 249-256.
6. Zuccaro, P., Ricciarello, R., Pichini, S., Pacifici, R., Altieri, I., Pellegrini, M. Ascenzo, G. (1997) Simultaneous Determination of Heroin, 6-Monoacetylmorphine, Morphine, and its Glucuronides by Liquid Chromatography-Atmospheric Pressure Ionspray-Mass Spectrometry. *Journal of Analytical Toxicology*. **21**, 268-277.
7. Cone, E., Jufer, R., Darwin, W. (1996) Forensic Drug Testing for Opiates. VII. Urinary Excretion Profile of Intranasal (Snorted) Heroin. *Journal of Analytical Toxicology*. **20**, 379-392.

8. Aderjan, R., Skopp, G. (1998) Formation and Clearance of Active and Inactive Metabolites of Opiates in Humans. *Therapeutic Drug Monitoring*. **20**, 561-569.
9. Von Euler, M., Villen, T., Svensson, J., Stahle, L. (2003) Interpretation of the Presence of 6-Monoacetylmorphine in the Absence of Morphine-3-glucuronide in Urine Samples: Evidence of Heroin Abuse. *Therapeutic Drug Monitoring*. **25**, 645-648.
10. Bogusz, M., Maier, R., Driessen, S. (1997) Morphine, Morphine-3-Glucuronide, Morphine-6-Glucuronide, and 6-Monoacetylmorphine Determined by Means of Atmospheric Pressure Chemical Ionization-Mass Spectrometry-Liquid Chromatography in Body Fluids of Heroin Victims. *Journal of Analytical Toxicology*, **21**, 346-355.
11. Heideloff, C., Gabler, J., Yuan, C., Zhang, L., Wang, S. (2014) In Vitro Conversion of Morphine to 6-Acetylmorphine in Urine Samples during Enzymatic Hydrolysis. *Clinical Chemistry*. **60**, 1234-1235.

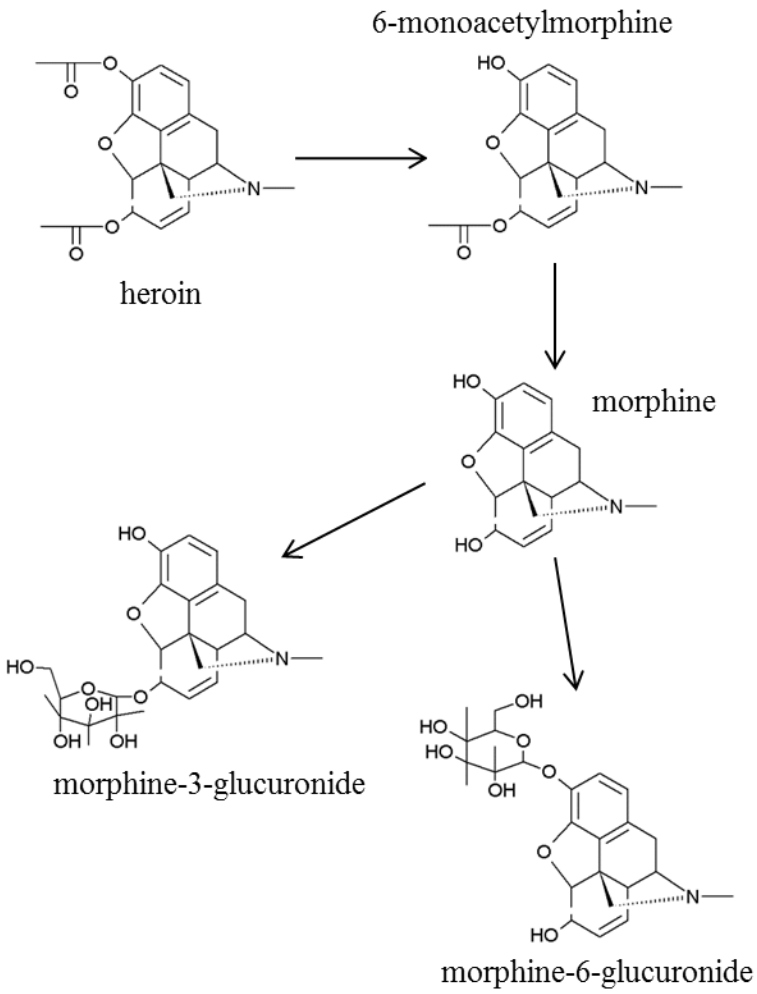

Figure 2.1. Metabolic pathway of heroin.

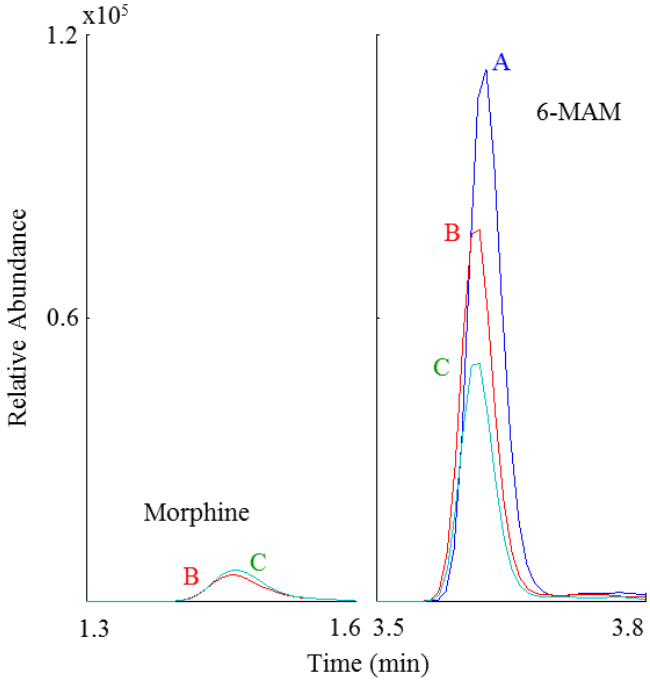

Figure 2.2. Morphine and 6-MAM intensities after *Helix pomatia* hydrolysis for 0 hours (A), 1 hour (B), and 2 hours (C) of 6-MAM spiked drug-free urine.

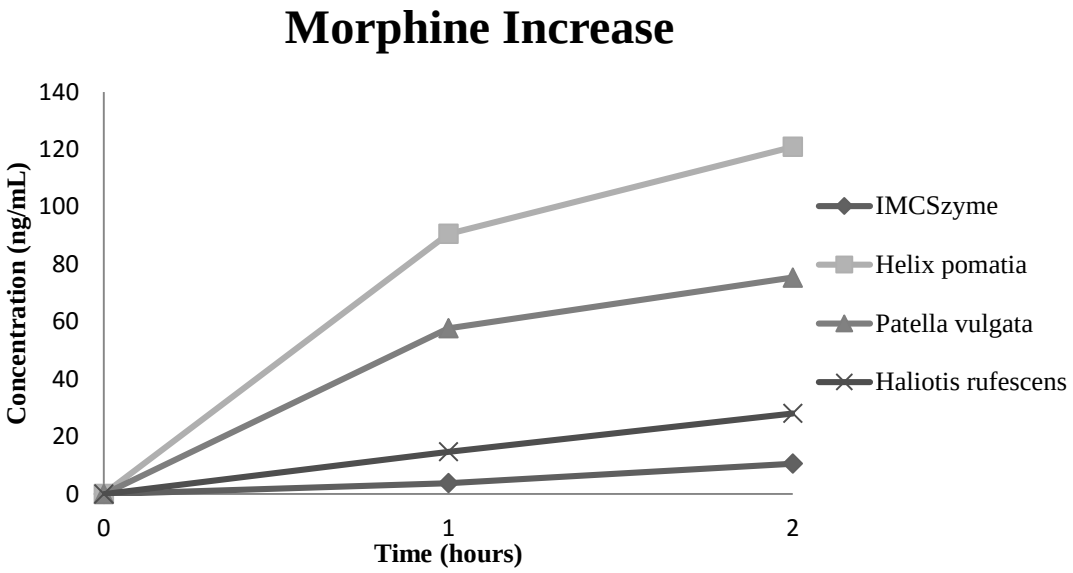

Figure 2.3. Concentration (ng/mL), of 6-MAM and morphine after 0, 1, and 2 h. of incubation with the respective enzyme in previously drug free urine spiked with 6-MAM.

Table 2.1
Concentration (ng/mL) of 6-MAM and morphine in patient samples, 3741, 3637, and 3627, after hydrolysis of respective enzyme compared to the unhydrolyzed sample.

	3741	
Hydrolysis	**6-MAM**	**Morphine**
Unhydrolyzed	91.3	0
IMCSzyme™	88.6	1.8
Helix pomatia	37.3	41.1
Patella vulgata	71.0	15.8
Haliotis rufescens	58.8	14.3
	3637	
Hydrolysis	**6-MAM**	**Morphine**
Unhydrolyzed	781.7	4006.3
IMCSzyme™	743.1	44042.5
Helix pomatia	424.4	62093.7
Patella vulgata	522.5	51581.1
Haliotis rufescens	801.6	47031.6
	3627	
Hydrolysis	**6-MAM**	**Morphine**
Unhydrolyzed	57.2	0
IMCSzyme™	65.0	4.3
Helix pomatia	73.4	48.6
Patella vulgata	103	27.4
Haliotis rufescens	103.4	10.2

CHAPTER 3

INNOVATIVE METHOD FOR MONITORING BENZODIAZEPINES IN MECONIUM: VALIDATION AND INTERLABORATORY COMPARISON

Abstract

A novel method for the quantitation of ten commonly prescribed benzodiazepines and metabolites (7-aminoclonazepam, clonazepam, α-hydroxyalprazolam, alprazolam, nordiazepam, diazepam, midazolam, oxazepam, lorazepam, and temazepam) in meconium was developed using enzymatic hydrolysis, WAX-S dispersive pipette extraction (DPX) tips, and liquid chromatography tandem mass spectrometry (LC-MS/MS). The method requires only 25 mg of meconium, limits pre-hydrolysis preparation to a dilution with water, and uses DPX tips for a quick (< 60 s) and effective sample clean-up post-hydrolysis. Calibrations were linear over a range of 5 ng/g to 1000 ng/g with correlation coefficients above 0.99 for each benzodiazepine. All intraday, interday, and total imprecision measures were below 13 % RSD. A blind study with a corresponding laboratory based on 35 positive patient samples produced an R^2 value of 0.9206 for quantitative results, and perfect agreement for qualitative results

Introduction

Benzodiazepines are a schedule IV class of psychotropic drugs commonly used for their depressant properties (1). Benzodiazepines are one of the most prescribed drug classes to women of reproductive age and to pregnant women (2, 3). However, the US Food and Drug Administration (FDA) classifies most benzodiazepines as pregnancy category "C", which have shown adverse effects on animal fetus, but there are no studies in humans, or "D", which have shown conclusive evidence of negative effects on human fetus (4). Benzodiazepines have the ability to cross the placenta and accumulate in the fetus, potentially causing adverse effects such as cleft palates and withdrawal symptoms (2, 4-6). Maternal prescription, prenatal prescriptions, misuse of non-prescribed medications and administration during birth to the mother and/or to the newborn are possible sources of fetal exposure to benzodiazepines. Thus, detection of benzodiazepine use is critical both for monitoring compliance and misuse/abuse by pregnant women, and for identifying potential health risks and treatment options for exposed newborns.

Meconium is the black, tarry stool of a newborn passed 1-5 days after birth. Meconium is an ideal toxicological matrix for identifying *in utero* drug exposure because it acts as a repository for xenobiotics including drugs of abuse from the 12-16th week of gestation until birth (7-9). Drugs accumulate in the meconium as a function of fetal swallowing of bile or urine and fetal biliary excretion. Once deposited, the meconium and drugs therein remain fixed until passed after birth, although the potential for drug degradation has been noted (7).

Due to its large window of detection and the easy, non-invasive collection, meconium has become a matrix of choice for determining fetal exposure to drugs (10). However, analysis of meconium is difficult. Meconium is a complex heterogeneous mixture composed of epithelial cells, mucus, lanugo, bile acids and salts, sugars, lipids, proteins, pancreatic and intestinal secretions, and more (1, 7, 9). As a result of this complexity, use of meconium as a biological matrix to monitor drug use by liquid chromatography/mass spectrometry is problematic because of the potential for significant matrix effects. Reducing matrix effects requires sample preparation methods that can extract target analytes from the endogenous biological interferents, a task that is often time consuming and labor intensive. Further, benzodiazepines are extensively metabolized, producing many glucuronide conjugates. Enzymatic hydrolysis with β-glucuronidases is employed to convert glucuronides back to the free parent compound for improved detection (11). Unfortunately, enzyme hydrolysis adds time and complexity to the analysis of meconium. The objective of our present research is to minimize both meconium matrix effects and sample preparation time by using minimal sample, performing hydrolysis *in situ*, preparing samples with dispersive pipette extraction (DPX) tips, and analyzing benzodiazepines with liquid chromatography tandem mass spectrometry.

The method was evaluated for imprecision (total, interday, and intraday), accuracy, extraction recovery, and linearity, and limits of detection and quantitation were estimated for each of the ten benzodiazepines and/or metabolites analyzed (7-aminoclonazepam, clonazepam, α-hydroxyalprazolam, alprazolam, nordiazepam, diazepam, midazolam, oxazepam, lorazepam, and temazepam). A blind study of 35

patient samples was performed with a collaborating lab (ARUP Laboratories, Salt Lake City, UT) that independently determined benzodiazepine concentrations using alternative β-glucuronidase hydrolysis, solid phase extraction, and LC-MS/MS.

There are a few publications regarding the analysis of benzodiazepines in meconium using LC-MS/MS (1, 9, 12), and one paper that reports analysis of meconium for nicotine, cocaine, and metabolites using DPX tips for sample preparation (13). The objective of this study was to develop and validate a simple and reliable method for the analysis of benzodiazepines in meconium using LC-MS/MS.

Experimental

Reagents and Standards.

Drug standards and deuterated internal standards (7-aminoclonazepam, clonazepam, α-hydroxyalprazolam, alprazolam, nordiazepam, diazepam, midazolam, oxazepam, lorazepam, temazepam, 7-aminoclonazepam-d_4, midazolam-d_4, oxazepam-d_5, lorazepam-d_4, clonazepam-d_4, temazepam-d_5, and diazepam-d_5) were purchased from Cerilliant Corporation (Round Rock, TX). Fisher Scientific (Waltham, MA) Optima LC/MS grade acetonitrile and formic acid were used.

DPX WAX-S tips were purchased from DPX Technologies, LLC (Columbia, SC). IMCSzyme™ was obtained from Integrated MicroChromatography Systems, LLC (Columbia, SC). Blank meconium, used for all controls and calibrators, was donated by ARUP Laboratories (Salt Lake City, UT) and previously found to be negative using established preliminary and confirmatory methods (10). Patient samples for the blind

study (also donated by ARUP) had been previously analyzed and all patient identification was removed prior to donation.

Instrumental Analysis.

Analyses were performed using a Thermo TSQ Vantage triple quadrupole system (Thermo Fisher Scientific Inc, Waltham, MA) with an Agilent 1100 HPLC system (Agilent Technologies, Santa Clara, CA) equipped with an Agilent Poroshell EC-C18 column (3.0 x 50 mm, 2.7 µm). Sample injections of 20 µL were made using a 6 port (0.25 mm) Cheminert C2V injection valve incorporated on a dual rail MPS autosampler (Gerstel Inc., Linthicum Heights, MD).

The mobile phase was composed of 0.1% formic acid in water (A) and 0.1% formic acid in acetonitrile (B). The initial gradient was 70% A for 0.25 min, which then ramped to 5% A at 5 min. The gradient remained at 5% A for 1 min, and then switched back to 70% A for a total run time of 6.5 min. The eluent was diverted to waste during the intervals of 0-0.5 and 5-6.5 min after injection. The column flow rate was 0.4 mL/min. The electrospray voltage and the gas pressure were set at 4000V and 60 psi, respectively. Selected multiple reaction monitoring transitions (MRMs) and retention time windows are listed in Table 3.1.

Methods

Sample Preparation.

Meconium samples were weighed (25 mg) and transferred into 2 mL micro centrifuge tubes (VWR, Radnor, PA) containing 215 µL of water from an 18.2 MΩ, Millipore

(Billerica, MA) Direct-Q 3 Ultrapure Type 1 water purification system. The mixture was vortexed using a Fisher Scientific (Waltham, MA) Vortex-Genie at speed 10 until homogenously distributed/dissolved in the water. A solution consisting of 75 µL of pH 7.5, 0.1 M potassium phosphate buffer, 50 µL of IMCSzyme™ β-glucuronidase enzyme (50,000 units/mL), and 10 µL of 500 ng/mL internal standards (7-aminoclonazepam-d_4, midazolam-d_4, oxazepam-d_5, lorazepam-d_4, clonazepam-d_4, temazepam-d_5, and diazepam-d_5) in water was added. This mixture was then incubated for 1 h at 55°C using a Labnet VorTemp™ 56 Benchtop Incubator/Shaker (Woodbridge, NJ). Following hydrolysis, 600 µL of acetonitrile was added to the mixture to precipitate proteins. This mixture was vortexed for ~20 s and centrifuged for 5 min using a Becton Dickinson (Franklin Lakes, NJ) Clay Adams brand Compact II Centrifuge. The supernatant (~950 µL) was removed and placed into a clean round bottom shell glass vial. The solution was taken in and out of a DPX-WAX-S tip (20 mg 55-65 µm resin/40 mg salt) twice. This step separates the acetonitrile and water layers and facilitates transfer of analytes into the acetonitrile supernatant, and binds matrix components to the resin to reduce matrix effects. The top acetonitrile layer (~500 µL) was then transferred to a new vial suitable for solvent evaporation. Solvent evaporation was performed with a Sybron Thermolyne™ Dri-Bath (Barnstead/ Thermolyne Corp., Dubuque, IA) at temperature setting 8 with N_2 gas flow. After evaporation, the residue was reconstituted in 100 µL of 10/90 methanol/water (v/v) and analyzed by LC-MS/MS.

Results and Discussion

Because meconium is available in a finite quantity, minimizing sample mass required for analysis is desirable to conserve patient specimens for other analyses. Past methods have used 1 g of meconium and required pre-hydrolysis preparation including mechanical homogenization and 15 min of centrifugation (1). Our methodology uses 25 mg of meconium and requires dilution with water and vortexing until homogenized pre-hydrolysis. Hydrolysis is performed with IMCSzyme^{TM}, which is a genetically engineered β-glucuronidase enzyme optimized for rapid hydrolysis. Morris, *et. al*. previously reported use of IMCSzyme^{TM} for complete hydrolysis of benzodiazepines in urine in less than 5 min (14). IMCSzyme^{TM} was chosen because it hydrolyzes benzodiazepines efficiently, and because it is highly purified and will not complicate the matrix further. Performing the hydrolysis *in situ* was an important goal to minimize overall pre-hydrolysis preparation and to avoid protein precipitation prior to hydrolysis. Protein precipitation can trap analytes of interest in clusters of folded proteins, often discarded or out of reach of enzyme, reducing the availability of target compounds. If protein precipitation were performed prior to hydrolysis, an additional solvent evaporation step would have been required because β-glucuronidases have poor performance in high organic content solutions. Thus, we proposed hydrolysis with β-glucuronidase *in situ* followed by protein precipitation with acetonitrile for increased efficiency.

Following hydrolysis and protein precipitation, the supernatant was transferred to a clean vial, and the solution was extracted using dispersive pipette extraction (DPX).

DPX is a solid phase extraction method that incorporates loosely contained sorbent in a pipette tip between a frit at the narrow bottom end of the tip and a barrier at the wider top end. By using loose sorbent, DPX tips increase surface area available for analyte contact, which produces high extraction efficiency. The tips allow for simple and fast clean-up methods, typically taking less than 60 s to complete. In summary, a "dirty" solution is aspirated into the tip, then air drawn into the tip (to effect vigorous mixing of sample solution and sorbent), and a clean solution is eluted. The process permits rapid equilibration and selective retention of the matrix components, leaving the analytes of interest in the clean eluted solution. In this case, using WAX-S tips, the clean solution contains 2 layers, with the upper acetonitrile layer containing the analytes with high recovery.

Method Validation.

Extraction recovery, ion suppression, imprecision (interday, intraday, and total), analytical measurement range, and limits of detection and quantitation were evaluated to validate the performance of the method.

Extraction recovery was estimated by comparing three replicate extractions of fortified samples to three replicate matrix matched (analyte spiked post-extraction) samples. Three blank meconium samples were fortified with the ten benzodiazepine standards and then analyzed according to the above procedure. Three blank meconium samples were also analyzed according to the same procedure, but were fortified just before solvent evaporation. The samples were fortified to theoretically have the same final concentration as the pre-fortified samples (*i.e.*, accounting for the total dilution

factor). These samples are referred to as "matrix matched" samples and represent 100% recovery. Extraction recovery was calculated by taking the average response in the pre-fortified samples, dividing by the average response in the matrix matched samples for each benzodiazepine, and expressed as a percentage. Ion suppression was similarly calculated, but the matrix matched samples were compared to three "neat" replicates. The neat replicates did not contain any meconium and were simply the final solvent composition (100 µL of 10% methanol in water (v/v)) spiked to the same concentration as the matrix matched samples. The average response in the neat sample was then compared to the average response of the matrix matched for each benzodiazepine, and then multiplied by 100 to express ion suppression as a percent. The recovery and ion suppression percentages for the benzodiazepines of interest are listed in Table 3.2. All recoveries were greater than 50% (55% to 81%) and percent ion suppression did not exceed 45% for any analyte, with 7 of the 10 benzodiazepines having less than 20% ion suppression.

Linearity was assessed by analyzing samples at ten concentration points (5, 10, 25, 50, 75, 100, 250, 500, 750, 1000 ng/g) with four replicates at each point. The correlation coefficients and subsequent linear regression analysis equations for each benzodiazepine are shown in Table 3.3. The calibrations for all compounds produced coefficients of determination (R^2) above 0.994 with slopes ranging from 0.9948 to 1.0414. Limit of detection (LOD) and the limit of quantitation (LOQ) estimates for each benzodiazepine are also listed. LOD was calculated as 3.33 times the standard deviation of four replicate measurements at the concentration of the lowest non-zero calibrator (5 ng/g) divided by the slope of the calibration line. The LOQ was calculated as 10 times the

same standard deviation divided by the slope of the calibration line. The LODs ranged from 0.5 to 2.1 ng/g, and the LOQs ranged from 1.5 to 6.4 ng/g. For ease of use, the LOD and LOQ were administratively set to 5 ng/g and 10 ng/g, respectively.

A precision study was performed over three days with three replicate samples at concentrations of 100 ng/g and 1000 ng/g each day, for a total of nine samples at each concentration. The average intraday imprecision (expressed as percent relative standard deviation, %RSD) was based on the average of each day's concentration standard deviation. The intraday precision did not exceed 10% RSD. The average interday imprecision was 10.2 % or lower for each benzodiazepine at each concentration. Lastly, the total imprecision, which is the square root of the sum of the squares of the interday and intraday imprecision at each concentration for each benzodiazepine, ranged from 2.3 to12.2 % RSD. Values of zero for the interday imprecision represent a negligible imprecision when compared to the intraday imprecision, thus total imprecision is simply equal to the intraday imprecision (15).

Case Samples and Blind Study.

Meconium case samples that had been previously analyzed were provided by ARUP. These patient samples (35 in total, with 89 positive benzodiazepines) were analyzed using the lab's existing validated meconium method involving a mechanical homogenization process, enzyme hydrolysis (post protein precipitation), solid phase extraction, and a different LC-MS/MS system than used in our work, similar to that described previously (16). These patient samples were analyzed in our laboratory in triplicate by our method delineated above. Relative standard deviations (% RSD) for the

measurements of each benzodiazepine in each set of patient samples ranged from 0.04% to 40% with an average %RSD of 8%.

The correlation coefficient for measured benzodiazepine concentrations determined by our method against the previously estimated results determined by the corresponding lab's results was 0.9206 (Figure 3.2). Additionally, every benzodiazepine found in each patient sample by ARUP was also found by our method (100% qualitative correlation). Further observations concerning individual benzodiazepines are also possible. Seven out of the ten individual analytes of interest exhibited great correlation with $R^2 > 0.93$. The three analytes that fell below an R^2 of 0.93 were alpha-hydroxyalprazolam (0.8206), alprazolam (0.8178), and 7-aminoclonazepam (0.4387). 7-aminoclonazepam likely had a low correlation due to a low number of positive samples (n = 6), but a recent presentation suggests it may also be due to degradation during the time between ARUP analysis and our analysis (17). The presentation reported that 7-aminoclonazepam decreased by 48% at 4 °C after storage for two weeks. Lower correlation of alpha-hydroxyalprazolam and alprazolam may be affected by the lack of respective internal standard. Seven out of ten of the analytes had slopes ranging from 0.91-1.3, indicating that our results were not systematically higher or lower than the ARUP previously reported values. The overall success of this blind study validates the application of this quick and easy method compared to a more intricate, lengthy method.

Conclusions

The method reported here is based on simple vortexing for sample homogenization, use of fast and reliable IMCSzyme™ for hydrolysis *in situ* that reduces hydrolysis time to

one hour, and use of a single WAX-S DPX tip for rapid sample clean-up. The final extract consists of a clean and analyte rich acetonitrile solution, which is solvent evaporated and reconstituted in 10% methanol. The method minimizes sample preparation and solvent evaporation times. LODs and LOQs were below 5 and 10 ng/g, respectively. Coefficients of determination for the calibrations with each benzodiazepine were above 0.99 for the ten-point calibration (5-1000 ng/g) with four replicates at each point. Results from 35 positive patient samples using our method, compared to the results from our collaborating laboratory using a different analytical protocol, produced an overall correlation of 0.9206. While the percent recovery and ion suppression outcomes were not ideal, they are acceptable given the difficult and complex nature of meconium and the level of precision, linearity, and sensitivity achieved by the method. DPX tip extraction and the straightforward nature of the method also enables automation of the sample preparation and analysis protocol. The success of the blind study indicates that analytical approach espoused herein, consisting of a combination of fast hydrolysis coupled with a simple clean-up scheme, offers an effective analytical approach for the analysis of benzodiazepines in meconium.

References

1. Marin, S.J. (2008) Quantitation of Benzodiazepines in Urine, Serum, Plasma, and Meconium by LC-MS-MS. *Journal of Analytical Toxicology*, **32**, 492-498.
2. Iqbal, M.M., Sobhan, T., Ryals, T. (2002) Effects of commonly used benzodiazepines on the fetus, the neonate, and the nursing infant. *Psychiatric Services*, **53**, 39-49.
3. Garcia-Algar, O., Lopez-Vilchez, M.A., Martin, I., Mur, A., Pellegrini, M., Pacifici, R., Rossi, S., Pichini, S. (2007) Confirmation of gestational exposure to alprazolam by analysis of biological matrices in a newborn with neonatal sepsis. *Clinical Toxicology*, **45**, 295-298.
4. (2012) Bcnc.org.uk. Benzodiazepine use in pregnancy. http://www.bcnc.org.uk/BZ_pregnancy.pdf (accessed 1 January 2015)
5. Bar-Oz, B. (2003) Comparison of Meconium and Neonatal Hair Analysis for Detection of Gestational Exposure to Drugs of Abuse.*Archives of Disease in Childhood. Fetal and Neonatal Edition*, **88**, F98-F100.
6. Wilkner, B.N., Stiller, C., Bergamn, U., Asker, C., Kallen, B. (2007) Use of benzodiazepines and benzodiazepine receptor agonists during pregnancy: neonatal outcome and congenital malformations. *Pharmacoepidemiology and Drug Safety*, **16**, 1203-1210.
7. Gareri, J., Klein, J., Koren, G. (2006) Drugs of abuse testing in meconium. *Clinica Chimica Acta*, **366**, 101-111.

8. Williamson, S. (2006) Determination of the Prevalence of Drug Misuse by Meconium Analysis. *Archives of Disease in Childhood. Fetal and Neonatal Edition*, **91**, F291-F292.
9. Gray, T., Shakleya, D., Huestis, M. (2009) A liquid chromatography tandem mass spectrometry method for the simultaneous quantification of 20 drugs of abuse and metabolites in human meconium. *Analytical and Bioanalytical Chemistry*, **393**, 1977-1990.
10. McMillin, G.A., Wood, K.E., Strathmann, F.G., Krasowski, M.D. (2015) Patterns of Drugs and Drug Metabolites Observed in Meconium; What Do They Mean? *Therapeutic Drug Monitoring*, 37, 568-80.
11. Nakamura, M. (2011) Analyses of benzodiazepines and their metabolites in various biological matrices by LC-MS(/MS). *Biomedical Chromatography*, **25**, 1283-1307.
12. Pichini, S., Cortes, L., Marchei, E., Solimini, R., Pacifici, R., Gomez-Roig, M., Garcia-Algar, O., (2016) Ultra-high-pressure liquid chromatography tandem mass spectrometry determination of antidepressant and anxiolytic drugs in neonatal meconium and maternal hair. *Journal of Pharmaceutical and Biomedical Analysis*, **118**, 9-16.
13. Bordin, D., Alves, M., Cabrices, O., Campos, E., De Martinis, B. (2013)A Rapid Assay for the Simultaneous Determination of Nicotine, Cocaine, and Metabolites in Meconium Using Disposable Pipette Extraction and Gas Chromatography-Mass Spectrometry. *Journal of Analytical Toxicology*, **38**, 31-38.

14. Morris, A.A., Chester, S.S., Strickland, E.C., McIntire, G.L. (2014) Rapid enzymatic hydrolysis using a novel β-glucuronidase in benzodiazepine urinalysis. *Journal of Analytical Toxicology*, **38**, 610-614.

15. Krouwer, J., Rabinowitz, R. (1984) How to Improve Estimates of Imprecision. *Clinical Chemistry*, **30**, 290-292.

16. Marin S and McMillin G**.** (2010). LC-MS/MS Analysis of 13 Benzodiazepines and Metabolites in Urine, Serum, Plasma and Meconium. In Hammett-Stabler C, Garg U (Eds.), *Clinical Applications of Mass Spectrometry* (pp. 89-105). Totowa NJ: Humana Press.

17. Wu, F. Marin, S. Clark, C., McMillin, G. Stability of 21 cocaine, opioid and benzodiazepine drug analytes in meconium at three temperatures. Presented at: 51st Annual Academy of Clinical Laboratory Physicians and Scientists Meeting; 2016 Jun 2-4; Birmingham, AL.

Table 3.1
Mass transitions and retention time windows for the ten benzodiazepines and deuterated internal standards.

Compound	Ion mass, *m/z*	Quantifier, *m/z*	Qualifier, *m/z*	Retention time (min)
7-Aminoclonazepam	285.8	249.90	221.90	1.28-1.32
Midazolam	325.7	290.80	208.80	3.23-3.29
α-hydroxyalprazolam	324.7	296.84	175.94	3.49-3.53
Alprazolam	308.8	164.94	280.85	3.65-3.68
Oxazepam	286.7	240.94	268.81	3.66-3.68
Nordiazepam	270.7	139.97	164.93	3.71-3.75
Lorazepam	321.0	274.78	302.77	3.73-3.78
Clonazepam	315.7	269.80	213.90	3.78-3.81
Temazepam	300.7	254.86	282.81	3.99-4.00
Diazepam	284.7	153.97	192.97	4.18-4.20
7-Aminoclonazepam-d_4	289.8	121.00	225.90	1.26-1.30
Midazolam-d_4	329.7	294.90	247.70	3.23-3.28
Oxazepam-d_5	291.7	245.87	287.82	3.65-3.67
Lorazepam-d_4	328.9	278.80	306.70	3.72-3.75
Clonazepam-d_4	319.7	273.80	217.80	3.78-3.81
Temazepam-d_5	305.7	259.87	287.82	3.96-3.99
Diazepam-d_5	289.7	153.99	197.96	4.14-4.18

Table 3.2
Mean percent recovery and mean percent ion suppression for benzodiazepines.

Compound	% Recovery	% Ion Suppression
Nordiazepam	60.33	13.21
Diazepam	54.97	27.19
7-Aminoclonazepam	64.23	38.20
Oxazepam	54.51	2.00
Temazepam	63.57	19.73
Alprazolam	80.74	6.54
Clonazepam	68.46	12.98
Lorazepam	56.32	1.69
α-hydroxyalprazolam	80.95	6.03
Midazolam	77.95	42.82

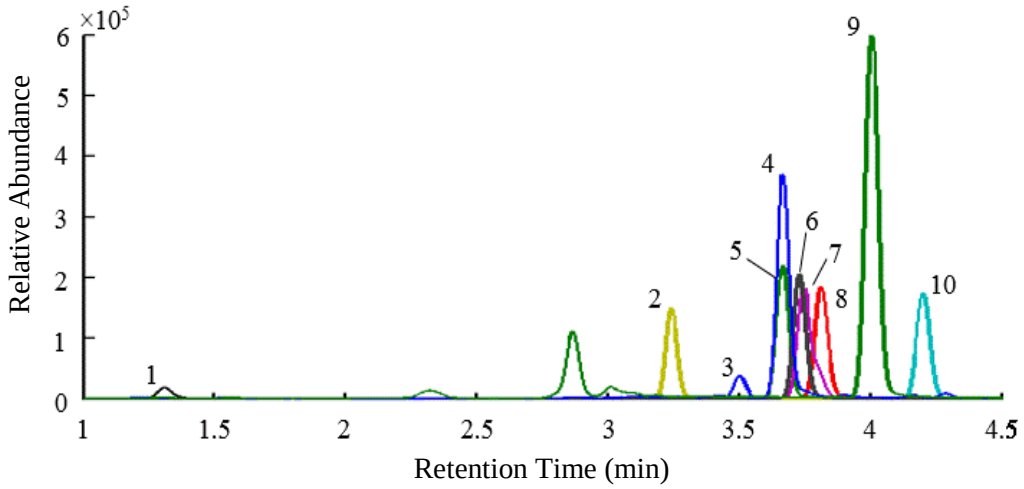

Figure 3.1 A chromatogram of a 100 ng/g spiked meconium sample analyzed according to the same procedure. Peak identities are: (1) 7-aminoclonazepam, (2) Midazolam, (3) α-hydroxyalprazolam, (4) Oxazepam, (5) Alprazolam, (6) Nordiazepam, (7) Lorazepam, (8) Clonazepam, (9) Temazepam, and (10) Diazepam.

Table 3.3
Linear regression results and limits of detection and quantitation.

Compound	R^2	Equation	LOD (ng/g)	LOQ (ng/g)
7-Aminoclonazepam	0.9997	y = 0.0048x - 0.0047	1.5	4.4
Midazolam	0.9965	y = 0.0043x - 0.0430	0.5	1.5
α-hydroxyalprazolam	0.9948	y = 0.0003x - 0.0008	1.8	5.3
Alprazolam	0.9953	y = 0.0038x - 0.0055	1.6	4.8
Oxazepam	0.9956	y = 0.0031x - 0.0123	1.2	3.7
Nordiazepam	0.9971	y = 0.0037x + 0.0028	1.9	5.8
Lorazepam	0.9979	y = 0.0014x + 0.0043	2.1	6.4
Clonazepam	0.9993	y = 0.0051x - 0.0048	1.4	4.2
Temazepam	0.9950	y = 0.0039x - 0.0163	0.6	1.8
Diazepam	0.9984	y = 0.0059x - 0.0213	0.7	2.1

Table 3.4

Average within-run precision, average between-run precision, and total precision for two concentrations (100 and 1000 ng/g) expressed in percent relative standard deviation (%RSD).

	Within Run Imprecision		Between Run Imprecision		Total Imprecision	
Compound	100	1000	100	1000	100	1000
7-Aminoclonazepam	3.9	1.8	0.0	2.6	3.9	3.2
Midazolam	6.4	1.3	0.0	1.6	6.4	2.0
α-hydroxyalprazolam	11.8	10.0	2.9	0.0	12.2	10.0
Alprazolam	5.7	4.5	0.0	1.5	5.7	4.7
Oxazepam	3.3	3.1	2.0	2.5	3.8	3.9
Nordiazepam	6.5	4.8	7.9	2.7	10.3	5.5
Lorazepam	5.0	2.5	3.8	10.0	6.3	10.4
Clonazepam	1.9	2.5	1.2	1.2	2.3	2.8
Temazepam	5.0	2.4	0.0	3.4	5.0	4.2
Diazepam	4.0	3.2	0.7	0.0	4.1	3.2

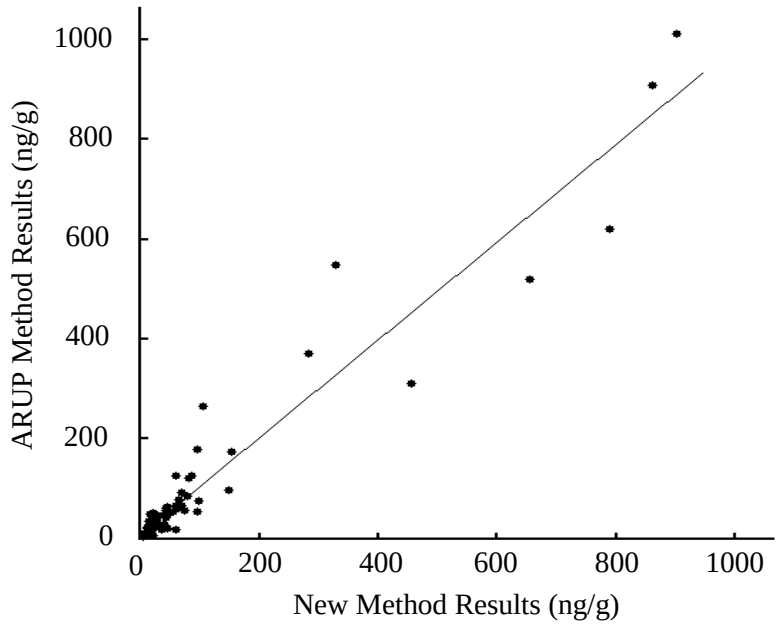

Figure 3.2. Correlation of positive patient sample results from the proposed method and the ARUP method. The fitted straight line is $y = 0.9816x + 6.5126$, with a coefficient of determination of $R^2 = 0.9206$.

CHAPTER 4

ANALYSIS OF Δ^9-TETRAHYDROCANNABINOL AND ITS TWO MAIN METABOLITES IN WHOLE BLOOD USING AUTOMATED DISPERSIVE PIPETTE EXTRACTION AND LC-MS/MS

Abstract

An analytical procedure was developed and validated for the analysis of Δ^9-tetrahydrocannabinol (THC) and its metabolites (11-hydroxy-Δ^9-tetrahydrocannabinol (11-OH-THC) and 11-nor-9-carboxy- Δ^9-tetrahydrocannabinol (THC-COOH)) in whole blood using LC-MS/MS. An automated dispersive pipette extraction (DPX) using a unique liquid-liquid solid-phase extraction was employed on a Hamilton NIMBUS96 platform to extract the analytes of interest. Extraction time was less than 3 min with a total LC-MS/MS run time of 5.6 min. The method was fully validated in accordance with the Scientific Working Group of Forensic Toxicology (SWGTOX) guidelines for limit of detection (0.22 ng/mL THC, 0.25 ng/mL 11-OH-THC and 0.62 ng/mL THC-COOH), limit of quantitation, carryover, extraction efficiency (93-100%), matrix effects (8-30%), linearity (0.5-50 ng/mL), within and between-run precision (CV <7.5%), and accuracy (mean relative bias <5%). An interlaboratory comparison of patient samples in collaboration with a local forensic toxicology lab method resulted in a correlation coefficient of 0.9901 between results from the two labs.

Introduction

Cannabis is the most widely abused illicit drug in the US. According to the National Survey on Drug Use and Health, 18.9 million people admitted to marijuana use in the previous month. Between 2007 and 2012, the rate of marijuana use rose from 5.8% to 7.3% (1). As the use of marijuana increases, it becomes more prevalent in clinical and forensic case work, particularly in impaired driving cases. After legalization in Washington State in 2015, the percent of cannabinoid positive cases went from 28 to 40% (2). Colorado also reported an increase in cannabinoid positive case samples after legalization in 2012 (3). The National Highway Traffic Safety Administration (NHTSA) reported in 2007, that 8.6% of nighttime drivers tested positive for cannabinoids – a rate almost four times higher than those with blood alcohol levels equal to or above 0.8 g/L (4). Recent use of marijuana is associated with 2-6 times increased risk of crashing while driving, depending on dose, than when unimpaired (5). From 1992 to 2009, 20,000 US drivers involved in fatal car crashes tested positive for cannabinoids (5).

Δ^9-Tetrahydrocannabinol (THC) is the main psychoactive ingredient in cannabis (marijuana). After smoking, THC is rapidly absorbed into the blood stream. THC is metabolized into two main metabolites, the active metabolite, 11-hydroxy-Δ^9-tetrahydrocannabinol (11-OH-THC) and the inactive metabolite, 11-nor-9-carboxy- Δ^9-tetrahydrocannabinol (THC-COOH). THC affects mental processes, ranging from altered perception of time and distance to hallucinations (6), owing to the risk of use while driving. Peak THC effects are 20-30 min after use, when blood levels are the highest, levels are low after 3 h and become baseline after 4 h (7, 8). Blood is routinely the matrix of choice when determining drug or alcohol impairment. Colorado and Washington states

have both legalized recreational marijuana use and adopted a 5 ng/mL THC blood concentration as the driving under the influence of drugs (DUID) level (3, 9). Unfortunately, blood draws are not done at the "scene" and can take up to hours after the time of the incident. DUI data shows that 42 and 70% of all cannabinoid-positive traffic arrests tested below 5 ng/mL THC in blood. Detection and quantification of THC and its metabolites in blood at low levels (< 5ng/mL) are imperative in determining time of THC use and potential impairment.

Previously published LC-MS/MS methods for the analysis of THC and its metabolites in blood require at least 0.25 mL of blood (10), but most require 0.5 mL or more (6, 11-16) or derivatization (17) to achieve necessary sensitivity. These methods often necessitate tedious sample preparation, e.g., use of SPE columns (11-13, 15-16), intricate online SPE (6), or liquid-liquid extraction (10, 14). Our aim was to develop a method that minimizes sample volume and automates a fast and easy dispersive pipette extraction procedure to obtain sensitive quantitation of THC, 11-OH-THC and THC-COOH in whole blood using LC-MS/MS.

Experimental Methods

Reagents and Standards.

All drug standards (Δ^9-Tetrahydrocannabinol, 11-hydroxy-Δ^9-tetrahydrocannabinol, 11-nor-9-carboxy- Δ^9-tetrahydrocannabinol, Δ^9-Tetrahydrocannabinol-d_3, and 11-nor-9-carboxy- Δ^9-tetrahydrocannabinol-d_3) were purchased from Cerilliant Corporation (Round Rock, TX). DPX WAX-S tips were purchased from DPX Technologies, LLC (Columbia, SC).

Instrumental Analysis.

Analyses were performed using a Thermo TSQ Vantage™ triple quadrupole mass spectrometer (Milwaukee, WI) coupled to an Agilent 1260 Series HPLC (Agilent Technologies, Santa Clara, CA) equipped with an Agilent Poroshell EC-C_{18} column (3.0 × 50 mm, 2.7 µm) with column temperature held at 50 °C. Sample injections of 20 µL were made using a 6 port (0.25 mm) Cheminert C2V injection valve (Houston, TX) incorporated on a dual rail GERSTEL MPS autosampler (Linthicum, MD).

The mobile phase was composed of 0.1% formic acid in water (A) and 0.1% formic acid in methanol (B). The gradient started at 40% B, ramped to 90% B at 1.3 min, and 91% B at 3.5 min, after which the composition was ramped quickly ramped to 98% B at 3.6 min, where it remained until 4.6 min and was re-equilibrated to 40% B. The total run time was 5.6 min. Eluent was diverted to waste during the intervals of 0-1.5 min after injection. The column flow rate was 0.5 mL/min. Mass spectrometer parameters were: electrospray voltage, 5000 V/-4500V; auxillary gas pressure, 25 psi; sheath gas pressure, 35 psi; vaporizer temperature was 330 °C, and capillary temperature was 400 °C. Ion transitions monitored for each compound are listed in Table 4.1.

Sample Preparation.

Aliquots of 100 µL of each sample (calibrator, control, blank, patient sample) were transferred to a 2 mL micro centrifuge tube (VWR, Radnor, PA). Internal standard in methanol was added (10 µL) and the tubes were vortex mixed. Acetonitrile (300 µL) was added and the tubes were vortexed using a Fisher Scientific (Waltham, MA) Vortex-Genie at speed 10 and then centrifuged for 10 min at 13,300 RPMs using a Thermo

Scientific Sorvall Legend Micro 17 centrifuge (Milwaukee, WI). For the interlaboratory comparsion, the forensic samples were prepared up to protein precipitation at the State Law Enforcement Division to avoid any biological hazards at the University of South Carolina. The protein precipitated forensic samples were brought back to the university for centrifugation and further analysis. The supernatant (350 µL) was transferred to a 2.2 mL well plate, which was then placed on the Hamilton NIMBUS96 system (Reno, NV) for the automated solid-phase extraction procedure. The NIMBUS system was loaded with DPX WAX-S tips (10 mg WAX resin and 20 mg salt), 300 µL CO-RE tips, a reservoir of 0.1 M formic acid, and an additional empty well plate. The NIMBUS system uses the CO-RE tips to add 50 µL of 0.1 M formic acid to the well plate containing the sample supernatant. The 1 mL DPX WAX-S tips are then used to aspirate and dispense the sample solution three times, thus allowing extraction of matrix and subsequent partitioning of the acetonitrile and the aqueous phase. The CO-RE tips are used to transfer 100 µL of the supernatant (acetonitrile layer) to a clean well plate, which is then transferred to the LC-MS/MS for injection.

Method Validation

Linearity and Sensitivity.

The method was validated according to SWGTOX guidelines (18). Linear least squares regression with a 1/x weighting was used as a calibration model for each analyte and spanned 0.5 ng/mL to 50 ng/mL with seven calibration points and five replicates at each point. Carryover was evaluated by running an extracted blank matrix sample after each high calibrator (n = 5). The sensitivity was determined by calculating the limits of

detection and quantitation. The limit of detection (LOD) was calculated using the standard deviation of the y-intercept (s_y) and the average slope (avg_m):

$$LOD = (3.3\ s_y)/avg_m$$

The limit of quantitation (LOQ) was similarly quantified with a multiple of 10 instead of 3.3. The average slope and standard deviation of the y-intercept were taken from the five separate runs of the calibration plot.

Accuracy and Precision.

The accuracy and precision of the method were determined by evaluating three different concentrations (2 ng/mL, 10 ng/mL, and 25 ng/mL) in triplicate over 5 separate runs. The accuracy was calculated as the (mean concentration measured – fortified concentration) divided by the fortified concentration × 100%. The within-run precision was determined by taking the standard deviation of a single run of samples at a single concentration divided by the mean calculated value of that single run × 100%. The between-run precision was determined by taking the standard deviation of all observations for each concentration divided by the grand mean for each concentration × 100%.

Extraction Efficiency and Matrix Effects.

Matrix effects were determined using the post-extraction addition technique. An unextracted neat solution of a low concentration (1 ng/mL 11-OH-THC, 5 ng/mL THC, and 10 ng/mL THC-COOH) and a high concentration (2 ng/mL 11-OH-THC, 20 ng/mL THC, and 40 ng/mL THC-COOH) were injected six times each (set 1). These results were compared to pooled blank blood spiked with analyte at the appropriate

concentration post-extraction in triplicate (set 2). Matrix effects were then calculated as the mean area of set 2 divided by the mean area of set 1 subtracted from 1 and multiplied by 100%. A negative value represents ion suppression, while a positive value represents ion enhancement. Extraction efficiency was determined by comparing the matrix matched samples (set 2) to a set of samples that were fortified after protein-precipitation and centrifugation, but before extraction (set 3). Extraction efficiency was calculated as the mean area of set 3 divided by the mean area of set 2 multiplied by 100%. Finally, loss during the protein precipitation step was also determined. In this case, the post-precipitation spiked samples (set 3) were compared to a set of samples where the blood was fortified before any processing (set 4). Protein precipitation loss was also calculated as the mean area of set 4 divided by the mean area of set 3 × 100%.

Results and Discussion

LC-MS/MS parameters.

Various liquid chromatography and mass spectrometry parameters were evaluated, but the most noteworthy differences involved the spray voltage and the choice of organic mobile phase. The difference in analyte signal when switching from low (3500/-3500V) to high (5000/-4500V) spray voltage was significant. The 11-THC-OH analyte showed the largest difference with a 2.5-fold increase in signal intensity after switching from low to high voltage. Similarly, the THC peak doubled in intensity, but the THC-COOH peak showed a 33% increase. The change of organic mobile phase (B) from acetonitrile to methanol also resulted in significant increases in signal intensity for all analytes. The 11-THC-OH peak exhibited the largest signal increase of over 8 ×. The THC signal

increased by almost 4 times, and THC-COOH signal increased by about 2.5 times. The reduced surface tension of methanol and the increased spray voltage both helped to increase ionization efficiency, with a concomitant increase in both signal intensity and sensitivity.

Stability in Plastic Time Study.

It is well known that THC has a tendency to fall out of solution and/or be retained on the surfaces of its container, particularly plastic. In the method presented here, plastic well plates were utilized throughout sample preparation. Most importantly, plastic well plates hold the eluent during LC-MS/MS analysis. With a run time of 5.6 min, a full well plate could take 9 h. A study was performed to evaluate analyte loss due to the use of plastic well plate containers at room temperature in the eluent conditions (~100% acetonitrile). Samples were extracted in triplicate at three different concentrations (1, 10, 25 ng/mL) for each analyte. The extracted samples were injected immediately at time 0, and then again at 6, 12, and 24 h. Concentrations did not vary by more than 15% except at 1 ng/mL for THC-COOH, which decreased by 35% after 12 h; however, no further loss was observed at 24 h. As a result of this study, well plates were used throughout this study, but calibrators were re-injected at the end of the runs to ensure stability.

Linearity and Sensitivity.

Calibration fitting resulted in average coefficients of determination (R^2) values of 0.9984 for THC, 0.9980 for 11-OH-THC, and 0.9966 for THC-COOH. The average slope and y-intercept standard deviation values were used to determine the LODs and LOQs for each compound (0.66 ng/mL for THC, 0.75 ng/mL for 11-OH-THC, and 1.8 ng/mL for THC-

COOH) as described above (Table 4.2). The limit of quantitation for each compound was well below the recommended cut-off level for DUID confirmation in blood of 1, 5, and 1 ng/mL for THC, THC-COOH, and 11-OH-THC, respectively (19). Chromatograms of the parent-to-quantifier transition response for each of the analytes at the suggested cut-off levels are shown in Figure 4.1.

Accuracy and Precision.

Accuracy, within-run precision, and between-run precision were determined and shown in Table 4.3. The method exhibited a minimum bias of 0.02% at 25 ng/mL for 11-OH-THC, and a maximum of 4.7% at 2 ng/mL of THC. The within-run and between-run precision was ascertained from the same replicate analyses. The average within-run precision had a maximum of 6.8% at 2 ng/mL of THC, and the between-run precision had a maximum at 2 ng/mL of THC at 7.5%.

Extraction Efficiency and Matrix Effects.

Low concentrations of analyte are most susceptible to large matrix effects. Ion suppression for THC was 31% at 5 ng/mL, but only 12% at 20 ng/mL. The 11-OH-THC analyte elicited ion suppression at 1 ng/mL of 6% and 2% at 2 ng/mL. THC-COOH had negligible matrix effects, showing ion suppression at 10 ng/mL of 3% but ion enhancement at 40 ng/mL of 3%. The DPX extraction post-protein precipitation was very efficient at >93% at both concentrations for all compounds. The loss of analyte during the protein precipitation step also varied with concentration. There was approximately 30% loss of all compounds at 25 ng/mL, but 15%, 19%, and 8% of THC, 11-OH-THC and THC-COOH, respectively, were lost at 2 ng/mL.

Interlaboratory Comparison.

A successful sample comparison was completed with the South Carolina Law Enforcement Division (SLED). SLED uses a method that requires 1 mL of blood and employs solid-phase extraction cartridges and GC-MS analysis. Twenty-eight forensic samples were compared. Each sample was analyzed in triplicate using the DPX method described above. The coefficient of determination (R^2) for the comparison of 11-OH-THC positive samples was 0.9965 (n = 3) (Figure 4.2), THC-COOH R^2 was 0.9836 (n = 27) (Figure 4.3), and THC produced an R^2 of 0.9960 (n = 16) (Figure 4.4). When all positive results were combined, the overall correlation was 0.9901 (Figure 4.5). A chromatogram of the parent to quantifier ion transitions for each of the analytes in patient sample 13 is shown in Figure 4.6. The calculated percent difference in triplicate analysis of each sample compared to the reported concentration from SLED did not exceed 20% for any case sample. The relative standard deviation of the triplicate extractions of patient samples did not exceed 15%. SLED detection cut-off values were 2 ng/mL for each analyte. Our LOQs were considerably lower and resulted in more positive 11-OH-THC and THC samples than SLED identified.

Conclusion

The LC-MS/MS method developed in this study minimizes required sample volume, and provides sensitive quantitation of THC, 11-OH-THC and THC-COOH in whole blood. Notably, our method simplifies sample preparation for the analysis of THC and its metabolites in blood with an automated dispersive pipette extraction without subsequent dilution or solvent evaporation. The extraction process is rapid, minimizes matrix effects

(<30%), and maximizes recoveries (>93%). LODs and LOQs were below 0.75 ng/mL and 2 ng/mL, respectively. These outcomes clearly provide the necessary sensitivity to meet laboratory cut-off with minimal imprecision (<8%). All calibrations were linear (R^2 > 0.99) over two orders of magnitude (0.5-50 ng/mL). Lastly, a successful comparison of forensic case sample using our new method with a local toxicology laboratory verifies the effectiveness of this new quick and easy method.

References

1. Substance Abuse and Mental Health Services Administration, Results from the 2013 National Survey on Drug Use and Health: Summary of National Findings, NSDUH Series H-48, HHS Publication No. (SMA) 14-4863. Rockville, MD: Substance Abuse and Mental Health Services Administration, 2014.
2. Couper, F., Peterson, B. (2014) The prevalence of marijuana in suspected impaired driving cases in Washington state. *Journal of Analytical Toxicology*, **38**, 569-574.
3. Urfer, S., Morton, J., Beall, V., Feldmann, J., Gunesch, J. (2014) Analysis of Δ9-tetrahydrocannabinol Driving Under the Influence of Drugs Cases in Colorado from January 2011 to February 2014. *Journal of Analytical Toxicology*, **38**, 575-581.
4. Compton, R., Berning, A. (2009) Results of the 2007 national roadside survey of alcohol and drug use by drivers. COT HS 811 175. NHTSA, Washington, DC.
5. Masten, S., Guenzburger, G. (2014) Changes in driver cannabinoid prevalence in 12 U.S. states after implementing medical marijuana laws. *Journal of Safety Research*, **50**, 35-52.
6. Jagerdeo, E., Schaff, J., Montgomery, M., LeBeau, M. (2009) A semi-automated solid-phase extraction liquid chromatography/tandem mass spectrometry method for the analysis of tetrahydrocannabinol and metabolites in whole blood. *Rapid Communications in Mass Spectrometry*, **23**, 2697-2705.
7. Huestis, M.A. (2007) Human cannabinoid pharmacokinetics. *Chemistry and Biodiversity*, **4**, 1770–1804.

8. Grotenhermen, F. (2003) Pharmacokinetics and pharmacodynamics of cannabinoids. *Clinical Pharmacokinetics*, **42**, 327–360.
9. Wood, E., Brooks-Russell, A., Drum, P. (2016) Delays in DUI blood testing: Impact on cannabis DUI assessments. *Traffic Injury Prevention*, **17**, 105-108.
10. Fernandez, M., Boeck, G., Wood, M., Lopez-Rivadulla, M., Samyn, N. (2008) Simultaneous analysis of THC and its metabolites in blood using liquid chromatography-tandem mass spectrometry. *Journal of Chromatography B*, **875**, 465-470.
11. Coulter, C., Miller, E., Crompton, K., Moore, C. (2008) Tetrahydrocannabinol and two of its metabolites in whole blood using liquid chromatography-tandem mass spectrometry. *Journal of Analytical Toxicology*, **32**, 653-658.
12. Schwope, D., Scheidweiler, K. (2011) Direct quantification of cannabinoids and cannabinoid glucuronides in whole blood by liquid chromatography-tandem mass spectrometry. *Analytical and Bioanalytical Chemistry*, **401**, 1273-1283.
13. Elian, A., Hackett, J. (2009) Solid-phase extraction and analysis of THC and Carboxy-THC from whole blood using a novel fluorinated solid-phase extraction sorbent and fast liquid chromatography-tandem mass spectrometry. *Journal of Analytical Toxicology*, **33**, 461-468.
14. Fabritius, M. et al. (2013) Comparison of cannabinoid concentrations in oral fluid and whole blood between occasional and regular cannabis smokers prior to and after smoking a cannabis joint. *Analytical and Bioanalytical Chemistry*, **405**, 9791-9803.

15. Jamey, C., Szwarc, E., Tracqui, A., Ludes, B., (2008) Determination of cannabinoids in whole blood by UPLC-MS-MS. *Journal of Analytical Toxicology*, **32**, 349-354.
16. Simoes, S., Ajenjo, A., Dias, M. (2011) Qualitative and quantitative analysis of THC, 11-hydroxy-THC, and 11-nor-9-carboxy-THC in whole blood by ultra-performance liquid chromatography/tandem mass spectrometry. *Rapid Communications in Mass Spectrometry*, **25**, 2603-2610.
17. LaCroix, C., Saussereau, E. (2012) Fast liquid chromatography/tandem mass spectrometry determination of cannabinoids in micro volume blood samples after dabsyl derivatization. *Journal of Chromatography B*, **905**, 85-95.
18. Scientific Working Group for Forensic Toxicology (2013) Standard Practices for Method Validation in Forensic Toxicology. *Journal of Analytical Toxicology*, **37**, 452-474.
19. Logan, B., Lowric, K., Turri, J., Yeakel, J., Limoges, J., Miles, A., Scarneo, C., Kerrigan, S., Farrell, L. (2013) Recommendations for Toxicological Investigation of Drug-Impaired Driving and Motor Vehicle Fatalities. *Journal of Analytical Toxicology*, **37**, 552-558.

Table 4.1. Selected ion transitions			
Compound	Precursor	Quantifier	Qualifier
THC-COOH	343	299.06	244.99
THC-COOH d3	346	301.89	N/A
11-OH-THC	331	312.99	193.10
THC	315	192.98	123.03
THC d3	318	196.00	N/A

Table 4.2. The standard deviation of the y-intercept (S_y), average slope (n=5) (Avg_m), limit of detection (LOD) in ng/mL, limit of quantitation (LOQ) in ng/mL, and the average coefficient of determination (R^2) (n = 5).

	S_y	Avg_m	LOD	LOQ	Avg R^2
THC	0.001	0.014	0.22	0.67	0.9984
11-OH-THC	0.006	0.074	0.25	0.75	0.9980
THC-COOH	0.003	0.016	0.62	1.8	0.9966

Table 4.3. The accuracy, within-run precision, and between-run precision calculated as described above.			
	Accuracy		
	2 ng/mL	10 ng/mL	25 ng/mL
THC	4.7%	0.7%	-0.2%
11-OH-THC	-1.3%	-2.8%	0.02%
THC-COOH	3.6%	0.7%	-0.4%
	Within-Run Precision		
	2 ng/mL	10 ng/mL	25 ng/mL
THC	6.8%	4.6%	2.8%
11-OH-THC	5.0%	3.5%	1.8%
THC-COOH	6.4%	4.5%	3.0%
	Between-Run Precision		
	2 ng/mL	10 ng/mL	25 ng/mL
THC	7.5%	5.6%	2.9%
11-OH-THC	6.6%	6.0%	3.5%
THC-COOH	7.0%	4.4%	3.1%

Table 4.4. Extraction efficiency, precipitation loss and matrix effects percentages for THC, 11-OH-THC, and THC-COOH at multiple concentrations.						
	Extraction Efficiency		Precipitation Loss		Matrix Effects	
Concentration	2 ng/mL	25 ng/mL	2 ng/mL	25 ng/mL	Low	High
THC	94	99	15	30	-31	-12
11-OH-THC	100	99	19	28	-6	-2
THC-COOH	93	96	8	29	-3	+3

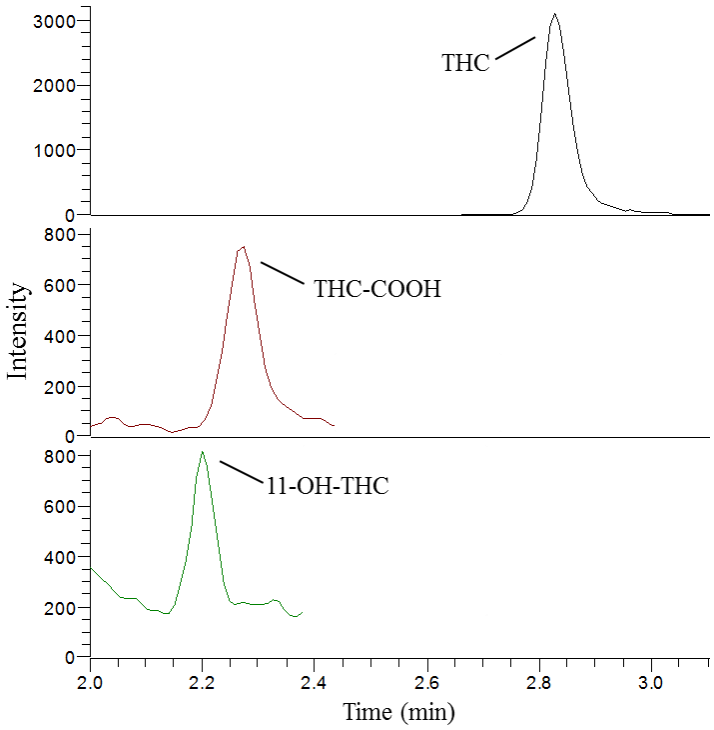

Figure 4.1. Chromatograms of calibrators at previously reported suggested cut-offs for THC (1 ng/mL), THC-COOH (5 ng/mL), and 11-OH-THC (1 ng/mL).

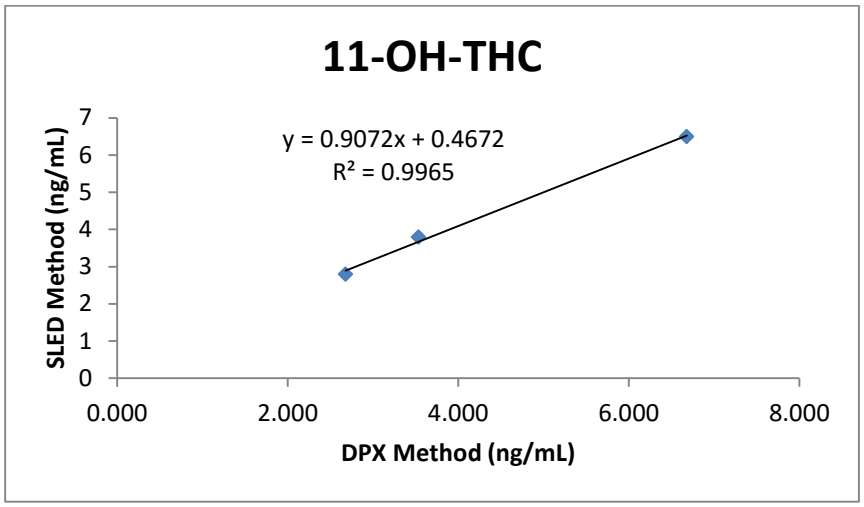

Figure 4.2. Correlation of 11-OH-THC positive case samples between the SLED and DPX method.

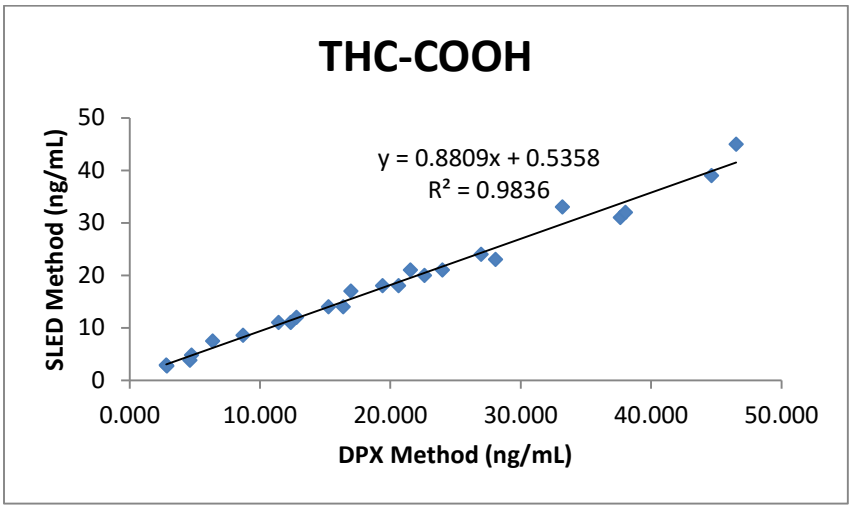

Figure 4.3. Correlation of THC-COOH positive case samples between the SLED and DPX method.

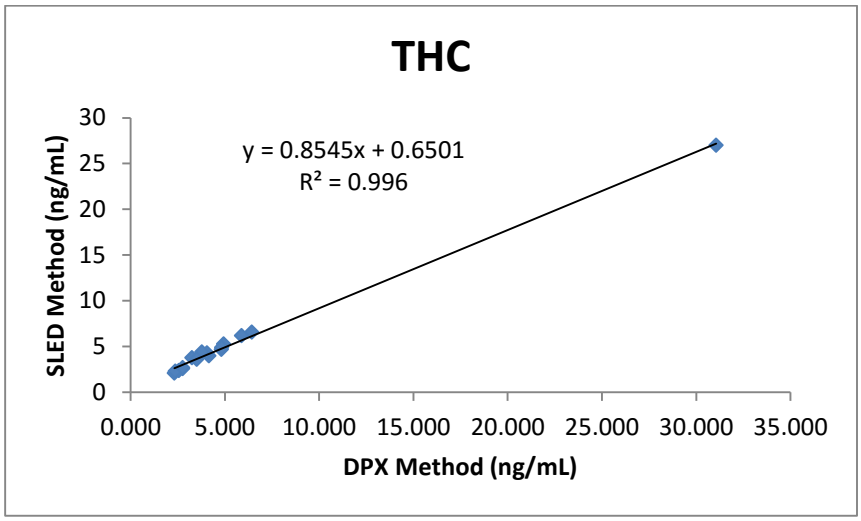

Figure 4.4. Correlation of THC positive case samples between the SLED and DPX method.

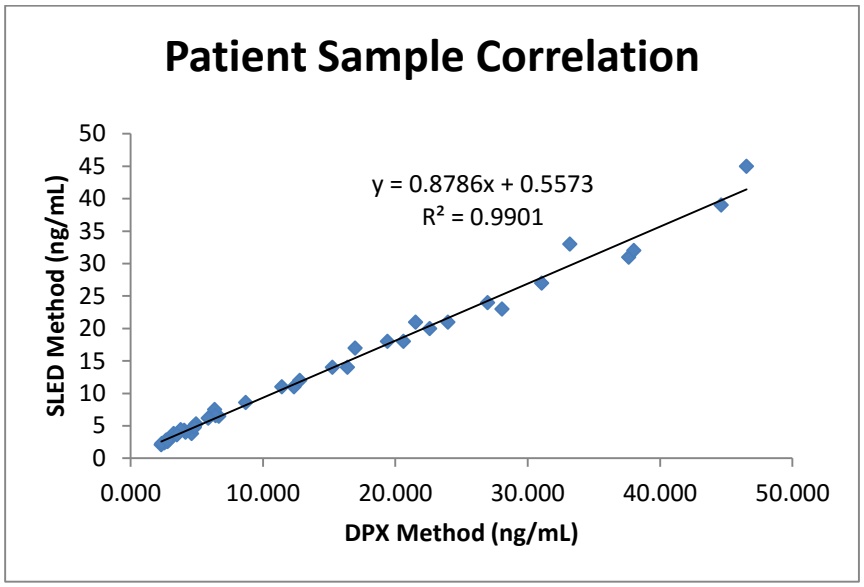

Figure 4.5. Correlation of all positive case samples between the SLED and DPX method.

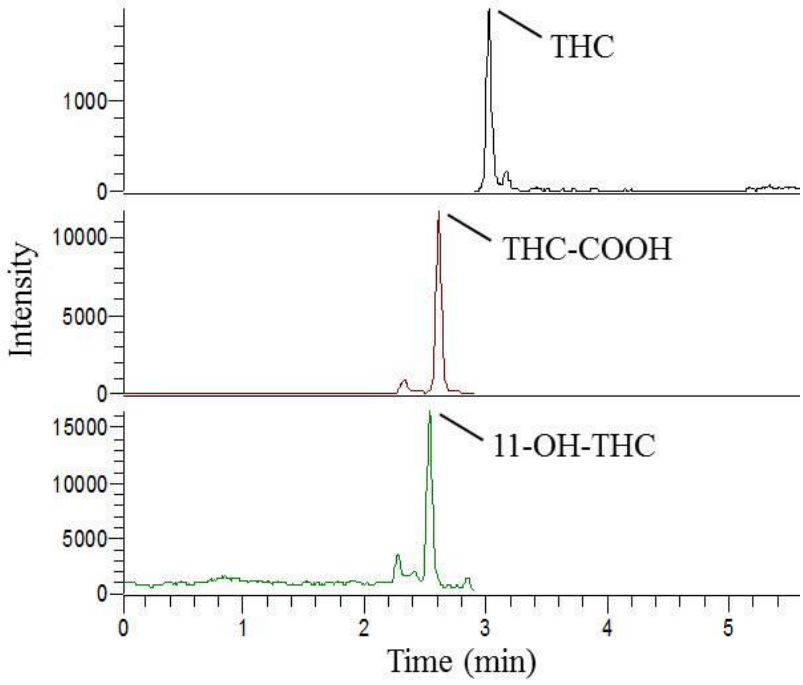

Figure 4.6. Chromatogram of patient sample 13 with 31 ng/mL THC, 77 ng/mL THC-COOH, and 6.7 ng/mL 11-OH-THC.

Table 4.5.
Patient Sample (PS) Results in ng/mL ± standard deviation (n = 3).

	11-OH-THC		THC-COOH		THC	
PS	DPX	SLED	DPX	SLED	DPX	SLED
1			21.5 ± 0.42	21	2.6 ± 0.24	2.4
2			15.3 ± 0.47	14	4.2 ± 0.61	4
3			8.7 ± 0.59	8.6		
4			4.7 ± 0.15	4.8		
5	2.7 ± 0.29	2.8	37.6 ± 0.95	31	4.9 ± 0.36	5.3
6			44.6 ± 0.47	39	4.1 ± 0.29	4.3
7			24.0 ± 0.73	21	6.4 ± 0.18	6.6
8			12.4 ± 0.49	11		
9			20.6 ± 1.2	18		
10	3.5 ± 0.24	3.8	27.0 ± 2.0	24	4.8 ± 0.21	4.7
11			4.6 ± 0.20	3.8		
12			17.0 ± 0.63	17		
13	6.7 ± 0.22	6.5	77.0 ± 2.6	>50	31.0 ± 2.3	27
14			6.4 ± 0.29	7.5		
15			2.8 ± 0.28	2.9		
16			19.4 ± 1.1	18	2.32 ± 0.15	2.1
17			22.6 ± 0.38	20	5.9 ± 0.26	6.2
18			16.4 ± 1.4	14	3.3 ± 0.41	3.8
19			12.8 ± 0.78	12		
20			38.0 ± 2.2	32		
21			76.0 ± 0.41	>50	2.77 ± 0.22	2.6
22			28.0 ± 0.38	23	2.4 ± 0.18	2.3
23			63.4 ± 0.64	>50	3.8 ± 0.27	4.4
24			<2	<2		
25			46.5 ± 0.77	45	2.8 ± 0.56	2.7
26			11.4 ± 0.23	11	4.8 ± 0.34	4.9
27			2.8 ± 0.34	2.7		
28			33.2 ± 0.77	33	3.5 ± 0.19	3.6

CHAPTER 5

AUTOMATED DISPERSIVE PIPETTE EXTRACTION OF DIPHENYL BORINATE COMPLEXED FREE CATECHOLAMINES AND METANEPHRINES IN URINE WITH LC-MS/MS ANALYSIS

Abstract

The measurement of free catecholamines and metanephrines in the clinical laboratory is important for the diagnosis of tumors, such as pheochromocytoma, a cancer of the adrenal gland. We have developed an automated, high throughput procedure, with a short LC-MS/MS analysis time, for the selective extraction of norepinephrine, epinephrine, dopamine, normetanephrine, and metanephrine in urine. An automated, high throughput extraction was achieved using dispersive pipette extraction (DPX) tip technology on an automated sample preparation system. The method was assessed for linearity, sensitivity, precision, accuracy, carryover, matrix effects and recovery. Using diphenyl boronic acid for complexation and styrene divinyl benzene for extraction enabled high recoveries (>81%) and reduced ion suppression (<39%). A pentafluorophenylpropyl column was found to provide adequate chromatographic separation prior to analysis on a triple quadrupole mass spectrometer with positive electrospray ionization. The method was linear over a broad range from 0.5 ng/mL to 1000 ng/mL, with precision below 8% CV, and limits of detection below 0.25 ng/mL for all analytes. External quality controls were

tested and quantitative results fell within the manufacturer specified concentration ranges. The simple and high throughput nature of this method would be ideal for clinical laboratories experiencing high demand for catecholamine and metanephrine urine analysis.

Introduction

The catecholamines, epinephrine, norepinephrine, and dopamine, are bioamines that play an integral role as neurotransmitters in the central and peripheral nervous system. Screening for catecholamines and their O-methylated metabolites, metanephrine and normetanephrine, is a widely accepted approach for diagnosis of catecholamine secreting tumors, such as pheochromocytomas, neuroblastomas, and paragangliomas (1-5). These tumors arise from adrenal and extra-adrenal chromaffin cells and are characterized by the over-production of catecholamines (6). Generally, pheochromocytomas are benign, but the potent effects on the cardiovascular system caused by excess catecholamines can have potentially fatal outcomes (7). Correct and timely diagnosis is crucial. Unlike analysis in plasma, it is recommended that both metanephrines and catecholamines be measured in urine (8). Urine analysis is not necessarily invasive, and urine usually exhibits sufficiently high levels of the target compounds. Catecholamines and metanephrines undergo phase II metabolism, primarily via sulphation. Whiting, *et al*. reported one-third of norepinephrine and one-half of epinephrine in urine were present in the free form, while metanephrines were present in the free form to a lesser extent (8). Previously, acid hydrolysis has been used to assess the amount of total catecholamine and metanephrines in urine to boost sensitivity. However, free fractionated metanephrines have been

proposed for enhanced diagnostic accuracy (9); with LC-MS/MS, methods for quantitation of free metanephrine have been implemented (5-6).

Catecholamines are characterized by a monoamine-linked benzene ring with two vicinyl hydroxyl groups (catechol) (2). Epinephrine is a secondary amine, while norepinephrine and dopamine are primary amines. The catechol group makes the catecholamines vulnerable to oxidation to the quinone species in neutral and alkaline conditions (10). Metanephrines do not have the catechol group, but have a methoxy group adjacent to a hydroxyl group, and are thus more stable. These compounds are highly polar and hydrophilic, with negative log D and log P values (3). These structural properties make sample preparation and analysis difficult.

A wide range of sample preparation techniques have been employed to analyze catecholamines and metanephrines in urine, most have been summarized in a recent review (3). Cation exchange mechanisms work well for metanephrines, but not the catecholamines because of their susceptibility to oxidation during elution with base. Solid phase extraction (SPE) with phenyl boronic acid (PBA SPE) columns work well for sample preparation of catecholamines because catechol groups bind with high affinity to the boronic acid groups to provide high recoveries. However, PBA SPE does not work well with metanephrines due to the absence of catechol groups. A method comparison published by Whiting, *et al*. reported reduced recoveries for catecholamines using cation exchange SPE, and no recovery for metanephrines on PBA SPE (8). The SPE method with the highest reported recoveries was that developed by Talwar, *et al*. (11), who found diphenyl boronic acid (DPBA) to complex and stabilize catecholamines in basic solution. The complex was then extracted using C_{18} sorbent, followed by acidic media to disrupt

the complex and elute the target compounds. DPBA forms reversible covalent bonds with the catechol of the catecholamines in basic solution; effectively minimizing oxidation and increasing lipophilicity for reversed phase retention (Figure 5.1). Whiting, *et al.*, also note that, although metanephrines do not have the cis-diol moiety necessary for the complexation with DPBA, they exhibited high recoveries with the same extraction procedure. Metanephrine recovery was decreased by a third without DPBA present during extraction, suggesting interaction as an affinity-pairing agent. We have adapted the Whiting method to design a DPX extraction that takes place within a pipette tip, which facilitates an easily automated alternative to traditional SPE requiring less sample and solvent volume. The objective of this study was to develop an automated sample preparation method utilizing the DPBA complexing agent to minimize sample preparation time (<15 min) and improve sensitivity (limit of detection < 0.25 ng/mL) for the analysis of free catecholamines and metanephrines in urine with LC-MS/MS.

Experimental Methods

Reagents and Standards.

Drug standards (catecholamine mix 1, catecholamine mix 2, dopamine, dopamine-d4, norepinephrine-d6, epinephrine-d6, normetanephrine-d3, and metanephrine-d3) were purchased from Cerilliant Corporation (Round Rock, TX). Ammonium chloride and diphenylborinic acid 2-aminoethyl ester (98%), were purchased from Acros Organics through Thermo Fisher Scientific (NJ). LC-MS grade formic acid was also purchased from Thermo Scientific (Waltham, MA). Level 1 and level 2 ClinChek® lyophilized biogenic amine urine controls were purchased from RECIPE (Munich, Germany).

Synthetic urine (Surine™) was purchased from DTI (Lenexa, KS). DPX CO-RE RP tips were purchased from DPX Technologies, LLC (Columbia, SC).

Instrumental Analysis.

Analyses were performed using a Thermo TSQ Vantage™ triple quadrupole mass spectrometer (Milwaukee, WI) coupled to an Agilent 1260 Series HPLC (Agilent Technologies, Santa Clara, CA) equipped with a Restek 3 µm Ultra PFPP column (100 mm × 2.1 mm) (Bellefonte, PA) with column temperature held at 40 °C. Sample injections of 10 µL were made using a 6 port (0.25 mm) Cheminert C2V injection valve (Houston, TX) incorporated on a dual rail GERSTEL MPS autosampler (Linthicum, MD).

The mobile phase was composed of 0.1% formic acid in water (A) and 0.1% formic acid in methanol (B). The gradient started at 4% B and was held for 2 min. It was ramped to 70% B at 3 min, where it remained until 3.75 min, then re-equilibrated to 4% B, for a total run time of 5.5 min. Eluent was diverted to waste during the intervals of 0-0.5 and 4.0-5.5 min. The column flow rate was 0.3 mL/min. Mass spectrometer parameters were: electrospray voltage, 3000 V; auxillary gas pressure, 8 psi; sheath gas pressure, 30 psi; vaporizer temperature was 325 °C and capillary temperature was 300 °C. The transitions monitored for each compound are listed in Table 5.1. The most abundant *m/z* was monitored, which for norepinephrine, normetanephrine and metanephrine was the water-loss ($M+H-H_2O$) product ion.

Sample Preparation.

In a well plate, 300 µL of synthetic urine, 0.2 M HCl calibrator, or quality control sample was spiked with internal standard (10 µL). The well plate was loaded onto a Hamilton NIMBUS96 system. Reservoirs of complexing agent (0.2% (w/v) diphenylborinic acid, 5 g/L EDTA in a 2 M NH_4Cl/NH_4OH pH 8.5 buffer), wash buffer (0.2 M NH_4Cl/NH_4OH pH 8.5), 100% methanol, and 1 M formic acid were also added to the deck of the Hamilton system. The liquid handling system used CO-RE 1 mL tips to add 600 µL of complexing agent to the urine sample well plate, 500 µL of wash buffer to a second "wash" well plate, 270 µL of 1 M formic acid to a third "elution" well plate, and 30 µL of methanol to the third "elution" well plate. The Hamilton robotic system discards the CO-RE tips and picks up 1 mL DPX RP (reverse phase) tips. Styrene divinyl benzene sorbent DPX RP tips are ideal for extracting these analytes. After conditioning by aspirating and dispensing 100% methanol twice, the tips were conditioned with wash buffer, and then the sample solution was aspirated and dispensed four times. Note that the DPBA complexing is essentially quantitative (8), and the mixing provided by aspirating and dispensing the sample solution insures complexation of catecholamines and efficient retention on the styrene divinyl benzene resin. After rinsing the tips with the wash buffer, analytes were eluted with the 1 M formic acid/10% methanol solution. The acidic solution reverses the diphenyl boronate complexes, and the methanol enhances elution of any remaining retained analytes via reverse phased interactions. Low methanol content is also beneficial for minimal removal of any retained matrix and maximizing selectivity. The "elution" well plate was then moved to the autosampler for LC-MS/MS injection. This automated process takes less than 15 min to complete.

Method Validation

Linearity and Sensitivity.

Linear least squares regression with a 1/x weighting was used to fit calibration models based on nine calibration points for each analyte spanning the concentration range from 0.5 ng/mL to 1000 ng/mL for norepinephrine and epinephrine, and 0.1 to 1000 ng/mL for dopamine, normetanephrine and metanephrine. Carryover was evaluated by running three replicate blank samples after each high calibrator. The limit of detection (LOD) was calculated using the estimated standard deviation of the y-intercept (s_{y0}) and the average slope of the calibration (avg_m):

$$LOD = (3.3\ s_y)/avg_m$$

The limit of quantitation (LOQ) was similarly estimated with a multiple of 10 instead of 3.3. The average slope and standard deviation of the y-intercept were taken from the analysis of three separate sets of extracted calibrators.

Accuracy and Precision.

The accuracy and precision of the method were determined by evaluating two external quality controls. The Level 1 control had mean values of 64 ng/mL for norepinephrine, 20 ng/mL for epinephrine, 194 ng/mL for dopamine, 325 ng/mL for normetanephrine, and 172 ng/mL for metanephrine. Level 2 had mean values of 174 ng/mL for norepinephrine, 39.8 ng/mL for epinephrine, 293 ng/mL for dopamine, 1568 ng/mL for normetanephrine, and 1017 ng/mL for metanephrine. Each control was analyzed in triplicate over three separate runs. The accuracy was calculated as shown below.

$$\frac{(\text{mean concentration measured} - \text{fortified concentration})}{\text{fortified concentration}} \; x \; 100\%$$

The within-run precision was determined by taking the standard deviation of a single run of triplicate quality control samples at a single concentration divided by the mean calculated value of that single run x 100%. The between-run precision was determined by taking the standard deviation of all observations (9 total) for each concentration divided by the grand mean for each concentration x 100%.

Extraction Efficiency and Matrix Effects.

Matrix effects were determined using a post-extraction addition technique. An unextracted neat solution of 100 ng/mL of each analyte was injected four times (set 1). These results were compared to the results from four replicate samples of extracted synthetic urine spiked containing analyte at the appropriate concentration post-extraction (set 2). Matrix effects were calculated as the mean area of set 2 divided by the mean area of set 1 subtracted from 1 and multiplied by 100%. A negative value represents ion suppression, while a positive value represents ion enhancement. Extraction efficiency was determined by comparing the matrix matched samples (set 2) to a set of synthetic urine samples that were fortified before extraction (set 3). Extraction efficiency was calculated as the mean area of set 3 divided by the mean area of set 2 multiplied by 100%.

Results and Discussion

Chromatography.

Figure 2 shows the separation of the analytes at a concentration of 10 ng/mL. The five analytes were easily separated on the 100 mm PFPP column. The highest water mobile phase percentage for initial conditions is ideal to promote the most retention and separation of these highly polar compounds. With the initial gradient conditions of methanol (mobile phase B) less than 4%, peak splitting arose due to the relatively large injection volume (10 uL) of the 10% methanol eluent. The initial gradient conditions were modified to prevent peak splitting of norepinephrine, and in some cases epinephrine. Larger initial methanol mobile phase percentages resulted in less separation between analytes and more interference peaks.

Sample pH and flow rates.

As previously reported by Talwar, *et al*, the pH of the complexed sample needs to be within the range of 7.5-9.5 to achieve reproducible high recoveries (> 81%). Sample loading and elution flow rates also affected recoveries. During aspiration and dispensing of each step of the extraction process, a slow flow rate was used to assure efficient mixing of the solution and the sorbent inside the tip. During dispensing steps especially, a slow flow allows the resin to settle first so the solution flows through the bed of resin at the bottom of the tip to maximize retention/elution. Higher flow rates resulted in inconsistent, lower recoveries.

Elution step.

Formic acid (1 M) was chosen for the elution step from DPX yielded better analyte signal intensities than acetic acid. While the acid disrupts the diphenyl boronic acid-catecholamine complex, residual reversed phase interactions between free catecholamines (and metanephrines) with the styrene divinyl benzene sorbent remained. Addition of methanol was necessary for disrupting the remaining reversed phase interactions to enhance elution efficiency and thus, enhance recovery. The addition of methanol to the elution solvent increased recoveries of all analytes with 10% performing better than 5%.

Linearity and Sensitivity.

Calibrations resulted in average coefficients of determination (R^2) values of 0.9992 for norepinephrine, 0.9996 for epinephrine, 0.9996 for dopamine, 0.9998 for normetanephrine, and 0.9982 for metanephrine. The average slope and y-intercept standard deviation values were used to determine the LODs and LOQs for each compound as described above and shown in Table 5.2. The limit of quantitation for each compound was similar to or better than those recently reported values (4-7, 12).

Accuracy and Precision.

Accuracy, as well as within-run and between-run precision (% CV) are provided in Table 5.3. The method was very accurate for quantitation of quality control samples with each average analyte concentration falling within the manufacturer's listed expected range of concentrations. The average within-run precision had a maximum CV of 6% for the level

1 of epinephrine control, and the between-run precision had a maximum CV of 7% for the level 2 metanephrine control.

Extraction Efficiency and Matrix Effects.

Matrix effects were relatively low for epinephrine, dopamine, normetanephrine and metanephrine with a range of ion suppression from 1-14%. Norepinephrine exhibited greater matrix effects with ion suppression at 39%, likely because it is the most polar compound with little to no retention on the PFPP column. Extraction efficiencies were higher than 96% for all analytes except dopamine, which resulted in 81% extraction recovery (Figure 3.3).

Conclusions

We report a fast and robust analytical method reported that achieves sensitive LC-MS/MS analysis of free catecholamines and metanephrines in urine. Extraction using dispersive pipette extraction with DPX tips facilitates seamless integration of SPE with the Hamilton NIMBUS96 platform for the rapid (< 15 min) extraction of DPBA complexed catecholamines and metanephrines from urine. This method provides the necessary sensitivities without an additional solvent evaporation step. Limits of detection for all analytes were below 0.25 ng/mL, and LOQs were below 0.70 ng/mL. The calibration was linear ($R^2 > 0.998$) over more than four orders of magnitude with concentrations ranging from 0.5-1000 ng/mL. Replicate analysis of two different levels of synthetic urine controls demonstrated % coefficients of variation less than 8%. This method is an excellent alternative to previously published methods, with the advantages of ease of implementation, robustness, high sensitivity due to effective sample clean-up,

and high throughput (96 samples extracted in less than 15 min) with a 5.5 min LC-MS/MS run time.

References

1. Kushnir, M., Urry, F., Frank, E., Roberts, W., Shushan, B. (2002) Analysis of catecholamines in urine by positive-ion electrospray tandem mass spectrometry. *Clinical Chemistry*, **48**, 323-331.
2. Peaston, R., Weinkove, C. (2004) Measurement of catecholamines and their metabolites. *Annals of Clinical Biochemistry*, **41**, 17-38.
3. Bicker, J., Fortuna, A., Alves, G., Falcao, A. (2013) Liquid chromatographic methods for the quantification of catecholamines and their metabolites in several biological samples—A review. *Analytica Chimica Acta*, **768**, 12-34.
4. Li, X., Li, S., Wynveen, P., Mork, K., Kellermann, G. (2014) Development ad validation of a specific and sensitive LC-MS/MS method for quantification of urinary catecholamines and application in biological variation studies. *Analytical and Bioanalytical Chemistry*, **406**, 7287-7297.
5. Woo, H., Yang, J., Oh, H., Cho, Y., Kim, J., Park, H., Lee, S. (2016) A simple and rapid analytical method based on solid-phase extraction and liquid chromatography-mass spectrometry for the simultaneous determination of free catecholamines and metanephrines. *Clinical Biochemistry*, **49**, 573-579.
6. Peitzsch, M., Pelzel, D., Glockner, S., Prejbisz, A., Fassnacht, M., Beuschlein, F., Januszewicz, A., Siegert, G., Eisenhofer, G. (2013) Simultaneous liquid chromatography tandem mass spectrometric determination of urinary free metanephrines and catecholamines with comparisons of free and deconjugated metabolites. *Clinica Chimica Acta*, **418**, 50-58.

7. Clark, Z., Frank, E. (2011) Urinary metanephrines by liquid chromatography tandem mass spectrometry: Using multiple quantification methods to minimize interferences in a high throughput method. *Journal of Chromatography B*, **879**, 3673-3680.
8. Whiting, M. (2009) Simultaneous measurement of urinary metanephrines and catecholamines by liquid chromatography with tandem mass spectrometric detection. *Annals of Clinical Biochemistry*, **46**, 129-136.
9. Boyle, J., Davidson, D., Perry, C., Connell, J. (2007) Comparison of diagnostic accuracy of urinary free metanephrines, vanillyl madelic acid, and catecholamines and plasma catecholamines for diagnosis of phaechromocytoma. *Journal of Clinical Endocrinology and Metabolism*, **92**, 4602-4608.
10. Miki, K., Sudo, A. (1998) Effect of Urine pH, Storage Time, and Temperature on Stability of Catecholamines, Cortisol, and Creatinine. *Clinical Chemistry*, **44**, 1759-1762.
11. Talwar, D., Williamson, C., McLaughlin, Gill, A., O'Reilly, D. (2002) Extraction and separation of urinary catecholamines as their diphenyl boronate complexes using C_{18} solid-phase extraction sorbent and high-performance liquid chromatography. *Journal of Chromatography B*, **769**, 341-349.
12. Diniz, M., Vilhena, L., Paulo, B., Barbosa, T., Mateo, E. (2015) Simultaneous determination of catecholamines and metanephrines in urine by liquid chromatography electrospray ionization tandem mass spectrometry: successful clinical application. *Journal of Brazilian Chemical Society*, **26**, 1684-1691.

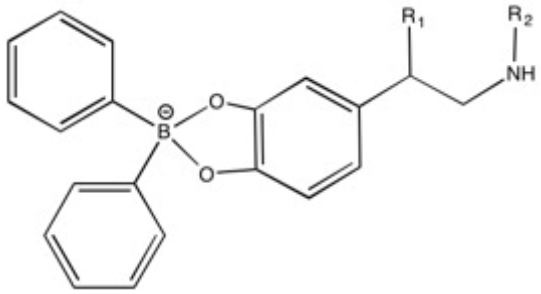

Figure 5.1. Diphenyl boronate-catecholamine complex structure. (For norepinephrine: R1 = OH, R2=H; for epinephrine: R1=OH, R2=CH_3; for dopamine: R1=H, R2=H).

Table 5.1. Selected ion transitions			
Compound	*m/z*	Quantifier	Qualifier
Norepinephrine	151.8	106.8	77
Norepinephrine-d6	157.8	80	111
Epinephrine	183.9	166	107
Epinephrine-d6	190.1	171.7	
Dopamine	153.8	136.8	90.9
Dopamine-d4	157.9	140.7	
Normetanephrine	165.8	121	133.8
Normetanephrine-d3	168.8	136.7	122.8
Metanephrine	180	148	165
Metanephrine-d3	182.8	120.9	150.8

Table 5.2. The standard deviation of the y-intercept (s_y), average slope (n=5) (avg_m), limit of detection (LOD) in ng/mL, limit of quantitation (LOQ) in ng/mL, and the average coefficient of determination (R^2) (n = 5).

Compound	s_y	avg_m	LOD	LOQ	avg R^2
Norepinephrine	0.0037	0.068	0.18	0.53	0.9992
Epinephrine	0.0058	0.088	0.22	0.65	0.9996
Dopamine	0.0055	0.12	0.15	0.46	0.9996
Normetanephrine	0.00019	0.19	0.003	0.01	0.9998
Metanephrine	0.0016	0.17	0.03	0.09	0.9982

Table 5.3. Accuracy and Precision of the method based on two levels of external quality control.				
Level 1				
Analyte	Expected Range	Mean	Within-run, CV	Between Run, CV
Norepinephrine	51.2-76.8	62.8	5%	5%
Epinephrine	16.0-24.0	19.6	6%	5%
Dopamine	155-233	186.2	3%	6%
Normetanephrine	260-390	264.5	5%	5%
Metanephrine	138-206	166.6	5%	7%
Level 2				
Analyte	Expected Range	Mean	Within-run, CV	Between Run, CV
Norepinephrine	139-209	168.3	3%	5%
Epinephrine	31.8-47.8	39.7	2%	2%
Dopamine	234-352	284.3	4%	5%
Normetanephrine	1254-1882	1493.7	4%	4%
Metanephrine	814-1220	1056.8	3%	4%

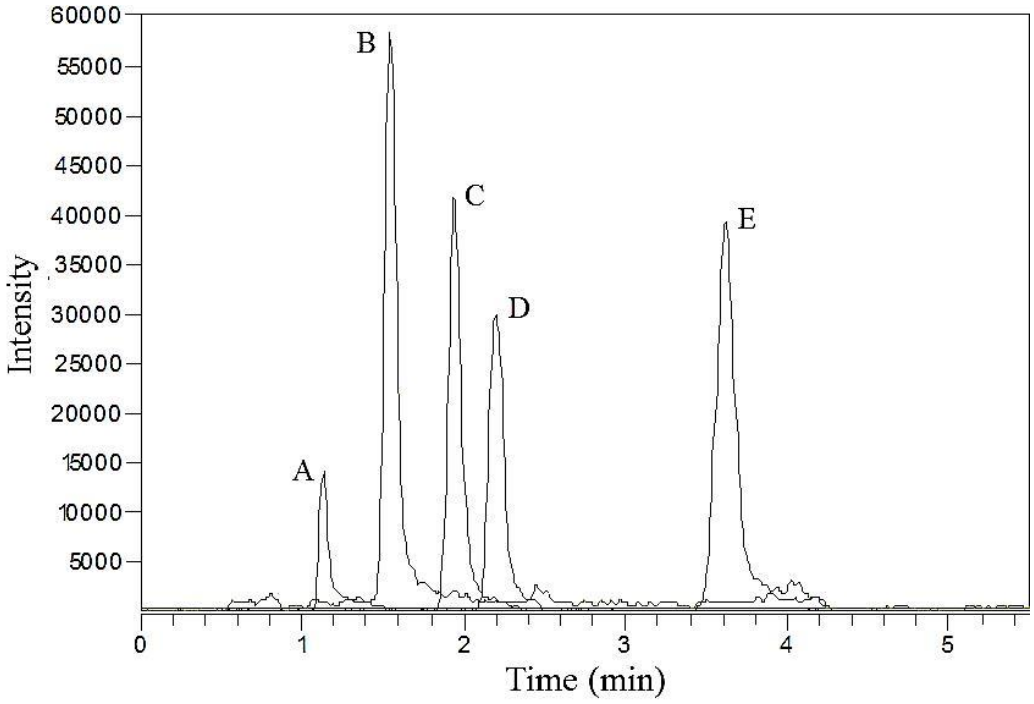

Figure 5.2. Separation of analytes at 10 ng/mL: (A) norepinephrine; (B) epinephrine; (C) normetanephrine; (D) is dopamine; and (E) metanephrine.

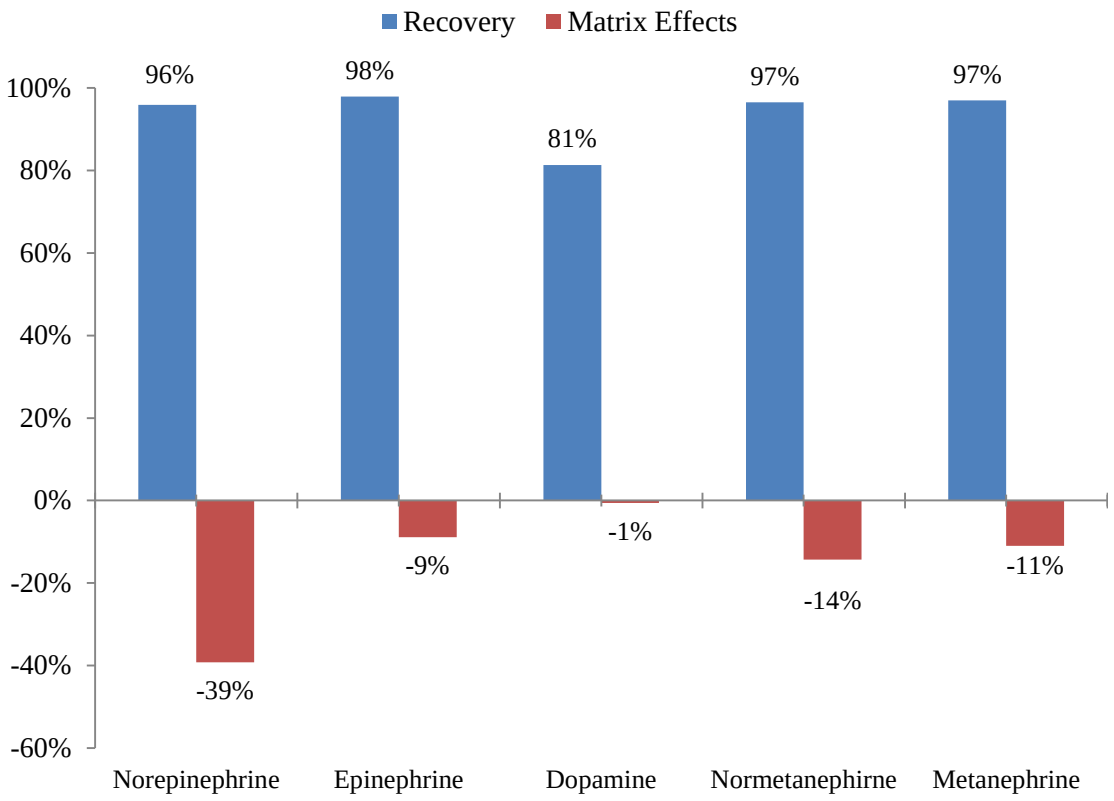

Figure 5.3. Recovery and matrix effects of catecholamines and metanephrines extracted using the automated DPX method.

CHAPTER 6

EVALUATIONS OF LIMIT OF DETECTION, WEIGHTED LEAST SQUARES REGRESSION, AND TOLERANCE INTERVALS IN A FORENSIC APPLICATION

Abstract

Limit of detection (LOD) is an important figure of merit, especially in forensic science where the question of detection has real world implications. However, ambiguity often exists in the choice of measurement standard deviation as a basis for the LOD (replicate blank measurements, residuals from the calibration relationship, etc.). Few sources discuss assumptions made with different choices of calibration regression on which the LOD is based (normality of data, homoscedasticity of variance, false positive/negative rates) (1-2), or the applicability of tolerance intervals to LOD calculations (3-5). This research stands to clarify these ambiguities and to demonstrate the application of tolerance intervals for calculating LOD in forensic dye analysis.

Introduction

The ubiquitous nature of fibers provides an information-rich evidence source for crime scene investigations; however, in cases of similarly dyed fibers, current fiber analysis techniques do not provide adequate chemical information for unambiguous match determinations to be made. We have targeted fiber sizes of 1 mm or less for our extraction procedure to offset the issue of damaging evidence, and we use UPLC-DAD (Ultra Performance Liquid Chromatography-Diode Array Detection) to achieve the necessary sensitivity. In association with taking the smallest fiber size possible, we also care to determine the limit of detection for each of the dyes.

Limit of detection (LOD, sometimes referred to as detection limit) does not carry a consistent definition throughout the literature. Accreditation organizations and governing bodies do not have specific definitions or defined ways to calculate LOD (6-14). Some may put forth suggestions, but do not have detailed procedures. There is a lack of consistent definitions, a lack of consistent notation, and calculations. In 1995, IUPAC (International Union of Pure and Applied Chemistry), in an attempt to standardize nomenclature, defined detection limit as "the measure of the inherent detection capability of a chemical measurement process" (11). In 1997, IUPAC defined "the limit of detection, expressed as the concentration, c_L, or the quantity, q_L, is derived from the smallest measure, x_L, that can be detected with reasonable certainty for a given analytical procedure. The value of x_L is given by the equation, $x_L = \bar{x}_{bi} + ks_{bi}$, where $\bar{x}_{bi}$ is the mean of the blank measures, s_{bi} is the standard deviation of the blank measures, and k is a numerical factor chosen according to the confidence level desired" (7). The factor k does not have a defined value and values in the literature range from 2 to 3.3.[6] IUPAC

specifically gives an arbitrary value of k=3 (9). This IUPAC methodology is different from that documented in ICH (International Conference on Harmonization) (14), the Scientific Working Group for Forensic Toxicology (SWGTOX) (8), the Analytical Methods Committee of the Royal Society of Chemistry (9), and countless other guidelines and literature references. These inconsistencies lead to chemists unknowingly making statistical errors and misguided laboratory comparisons. Most guidelines for LOD gloss over two important issues: how can both false positive and false negative errors be controlled, and how one handles calibration data that is heteroscedastic (variability not the same at different analyte levels).

The research objective of this work is to demonstrate the forensic value of a statistically sound approach for calculating the limit of detection with control of both false positive and negative rates using statistical tolerance intervals and to evaluate the performance of weighted least squares for a calibration model for heteroscedastic data.

Theory

LOD Meaning and Calculation

Limit of detection is the smallest measure, on the y-axis, that can be extrapolated to an x-axis concentration or quantity that can be reliably detected for an analytical method. A limit of detection, traditionally a point estimate, has related false negative and false positive error rates. A false negative is the error of not detecting analyte when it is, in fact, present. A false positive is the error of detecting an analyte when it is, in fact, not present. These concepts are shown in Table 6.1.

Most existing LOD guidelines lack a detailed procedure for calculation of the limit of detection, thus impeding inter-laboratory comparisons. Two laboratories may use the same instrumental method, but the way in which LOD was calculated, if not identical, skews the comparison. Even if the equation used in both cases is the same, interpretation of the variables could vary. The largest variation in interpretation involves the source of uncertainty employed in the LOD calculation: where should the standard deviation be evaluated? As shown in Table 6.2, the variety of choices for calculation of the standard deviation results in different LOD values. The measurement variability has been estimated using the standard deviation of the blank and of the measurements, the lowest non-zero calibrator, and the standard deviation of the residuals.

The number of standard deviations, *k*, above the mean of the blank measurements at which the LOD is defined, determines the probability of false positive detection. No single value for LOD is appropriate for all situations and, ultimately, the analyst should think about the consequences of false positives and set LOD accordingly. LOD is often defined as $\mu_b + 3\sigma_b$, or as $\mu_b + 3.3\sigma_b$, where μ_b and σ_b are the mean of the blank replicates and a measure of the measurement uncertainty, respectively. The former is generally a result of the rounding of the latter.[2] If LOD is set at $\mu_b + 3.3\sigma_b$, this point is also known as the critical level when not being used as the LOD (3), the fractional risk, α, of detecting analyte when, in fact, it is absent (false positive) is 0.0005. Thus, LOD is based on setting the false positive risk to an acceptably low level by using an appropriately high value for the *k*-multiplier. Historically, k values as low as 2 have been used (6). However, the false negative error rate is 50% at any limit of detection so defined (2). This concept is illustrated in Figure 1.

The false negative rate decreases as the number of standard deviations, k, from the mean that the LOD is determined to lie increases. The fractional false negative rate, β, falls to 0.0005, at $6.6\sigma_b$ above the mean of the blank (Figure 6.2). At which level, analyte can be detected *consistently*. The value at $6.6\sigma_b$ gives sufficiently consistent detection, 99.95% of the time, and is called the "minimum-consistently-detectable amount" (MCDA) (15). If the analyte is present at the MCDA repeatedly, then it would only be incorrectly assessed as absent (a false negative result) 0.05% of the time. However, there is no confidence level associated with the MCDA.

Tolerance Intervals

If controlling both false positive *and* false negative error rates is of concern, with a designated degree of confidence, then a tolerance interval is required. Statistical tolerance intervals have not been often applied in practice, partly because of the paucity of statistical tables for the asymmetric functions needed, and the complex calculations required (1,3,16). However, sample calculations are available (5,10).

A tolerance interval is defined as an interval that contains at least a defined portion, p, of the population with a defined degree of confidence, 100(1-α)%. As a result, there is 100(1-α)% confidence that the tolerance interval includes 100p% of the population (16). The confidence level associated with the tolerance interval takes into account the fact that the samples do not perfectly reflect the true population. Adjusting the confidence and spread inherently adjusts the false negative and false positive rates, which can later be determined. The higher the confidence and the spread, the lower the false positive and false negative error rates. Adjusting the confidence and spread can be valuable when

either the false positive or false negative result may have significant consequences (i.e., forensic cases that go to trial based on laboratory results). The tolerance interval can also be adjusted to determine an upper or lower bound of a portion of the data. These upper limits can help generate more accurate limits of detection. Statistical tolerance intervals typically produce LODs higher than estimated using other approaches. Tolerance intervals provide the best option for calculating limit of detection because it provides a value that can be used for a "large and potentially unknown number of detection decisions with a high, specified, degree of confidence" (3).

Assumptions

Most analysts use ordinary least squares (OLS) as a regression analysis technique. In doing this, there are some basic assumptions that are made. Miller[2] provides a description of the three major assumptions: (1) errors made in measuring instrumental signals (y-direction error) are greater than all other errors, (2) y-direction error is normally distributed, and (3) the data is homoscedastic. In general, if the OLS model does not pass a lack-of-fit test, then a better investigation of the required assumptions may be informative. If any of these assumptions cannot be upheld, then the OLS regression is not the appropriate model.

The validity of the first assumption relies on the error of the standards versus error of the instrumentation. Previously, the first assumption was generally taken as valid because the instrumentation error outweighed the error of the standards. However, with modern day instrumentation and standard reference materials, the two errors may be closer than most would think. One can simply assess the relative standard deviation of the instrumental

method compared to the relative standard deviation (RSD) of the reference material or the in-house calibrators (propagation of error). If the instrumental RSD is not greater than the calibrator RSD, then the assumption fails.

The residuals must be normally distributed. Normality can be easily detected by examination of the plot of residuals. The data is normally distributed if the points lie primarily at the predicted value with some residuals trailing off symmetrically. More formal statistical tests exist that examine normality including an Anderson-Darling test or a Shapiro-Wilks test.

The importance of the third assumption, homoscedasticity, lies in the fact that OLS regression minimizes the sum of squares of residuals. If certain concentrations have disproportionately high variance, then the regression coefficients estimation will be unreasonably effected. Bartlett's Test and Levene's Test are useful for testing homogeneity of the data. Another easy way of checking for constant variance is to simply look at the residuals. A common way to counteract the heterogeneity of the variance is to weight the dependent variable, as done with weighted least squares regression (WLS). The weighting scheme generally results in homogenous variance which allows OLS to be performed on the weighted regression.

Weighted Least Squares

The main assumption that generally does not hold with OLS, and is usually not tested for, is homoscedasticity. When the data does not exhibit constant variance, OLS estimation is still linear and unbiased, but it is not the minimum variance estimate which means that it is inefficient (3). Weighted least squares (WLS) is a great technique when the data is heteroscedastic and the analyst would prefer not to use a transformation model or one

does not fit the data appropriately. Weighted least squares is an adaptation of OLS that accounts for heterogeneity in variance. Weighted least squares regression is used by applying a weight to each set of data points. Recommended weights vary, but the most cited and most reflective of the data is a weight of the inverse of the variance at each set of data points (4). By using the inverse of the variance as a weight, more weight is given to the sets of data points with the least amount of variance and less weight to the sets of data points with more uncertainty. In the present research, true variance was estimated from the replicates, but variance modeling is a good alternative when replicate number is small (4). Variance modeling can also be used to determine uncertainty between data points. Another benefit of WLS is that the original data remain unchanged, i.e. there is no need to refit response versus concentration. The model used in the present work is explained by Zorn *et al* (3).

Experimental Section

Materials

Dyed fabric and textile dye standards were sampled from our collection of production samples, which were donated by textile and dyestuff manufacturers from the southeastern United States. The nine dyes selected for this study included three dyes from each of the acid, basic, and disperse classes.

Fiber sample preparation

Individual fibers 5-mm in length were cut using a fiber guillotine; 1 mm and 0.5 mm fibers were cut by hand using a table-mounted magnifying glass and scalpel. Each fiber length was cut in triplicate. Cut fibers were then loaded into Waters Total Recovery®

vials for extraction. These vials enable extractions to be performed with low solvent volumes (< 50 μL), enabling concentration of dyes in the resulting extract.

Calibration design

Experimental designs for UPLC-DAD calibration were constructed for all nine dyes based on 5 replicate experiments at 7 levels of dye concentration (0 ppb, 100 ppb, 500 ppb, 1000 ppb, 1500 ppb, 2000 ppb, and 2500 ppb). A blank sample was measured 15 times as a quality control sample interspersed through the runs. A lower concentration design was also performed based on five replicate experiments using standard mixtures of the 9 dyes at concentrations 10 ppb, 20 ppb, 30 ppb, 40 ppb, 50 ppb, and 18 blank injections to better characterize low limits of detection. For each dye peak, QuanLynx™, data management software included with MassLynx™ (Waters Corporation, Milford, MA) was used to integrate peak areas above corrected baselines. For each dye standard at 1000 ppb concentration, the retention time window encompassing the baseline peak width was determined; this window was then employed as the dye peak integration window for all samples, including blanks.

Instrumentation

Dye standards and extracts were separated and detected using a Waters Acquity™ UPLC H-Class equipped with a quaternary solvent pump system and a Waters PDA eλ detector. The column was a 2.1 X 50 mm I.D. 1.7 μm particle size Waters Acquity™ BEH C18 column with a 2.1 X 5 mm I.D. 1.7 μm particle size Waters Acquity UPLC® BEH C18 VanGuard precolumn. The mobile phase gradient was based on mixtures of 50 mM ammonium acetate in water and 0.15% formic acid in methanol. The column temperature

was set at 40 °C. The diode array detector scanned the wavelength range from 325 nm to 675 nm at a rate of 40 Hz and 1.2 nm resolution. The sample injection volume was10 µL.

Results and Discussion

A fiber dye extraction method was calibrated at five different concentration points. After looking at the residuals and calculating an F-test based on the OLS regression, it was obvious that the data was heteroscedastic and did not fit the OLS model, shown in Figure 6.3. A WLS model was produced for each dye, yielding better residual standard deviations in every case. Four examples of this are shown in Table 6.3. The residual standard deviations of the WLS regression were all less than 0.1 suggesting a very good correlation between the data and the model. According to Zeng, this behavior may be a result of the chromatographic technique. "A growing body of evidence indicates that chromatographic techniques are dominated by this type of heteroscedasticity over sampling regions used in routine analytical work. Neglect of heteroscedasticity in calibration, through use of unweighted or "ordinary" least squares (OLS) instead of weighted least squares (WLS), can lead to significant loss of precision, especially in the low signal limit which is often important in quantitating substances present at trace levels" (17).

The limits of detection were calculated for the dyes as well; three examples are shown in Table 6.4. It is made clear that the LOD values vary with the method used. $LOD_{1\text{-}3}$ are calculated via $3.3\sigma_b$ (this calculation was used for comparison purposes because it the most common calculation used) but differ in the method of calculating σ_b, the standard deviation of the blank. LOD_1 estimates σ_b using the standard deviation of the integrated

blank signals across the width of the peak. LOD_2 estimates σ_b using the standard deviation of the lowest non-zero calibrator (10 ppb). LOD_3 estimates σ_b based on the standard error of the y-intercept of the calibration model, i.e. the standard deviation of the residuals. However, for LOD_4, an upper one-sided tolerance interval was used.

A sample calculation of a simple non-simultaneous upper-limit tolerance interval based on Acid Red 337 is shown below.

According to NIST (20), Upper One Sided Tolerance Interval:

$$Y_U = \bar{Y} + k_1 s$$

$$k_1 = \frac{z_p + \sqrt{z_p^2 - ab}}{a}$$

$$a = 1 - \frac{z_\gamma^2}{2(N-1)}$$

$$b = z_p^2 - \frac{z_\gamma^2}{N}$$

95% confidence (γ=0.99) & 99.95% population (p=0.95)

$z_p = 3.291 \quad z_p^2 = 10.831 \quad z_\gamma = 1.645 \quad z_\gamma^2 = 2.706$

$$a = 1 - \frac{2.706}{2(18-1)} = 0.92041$$

$$b = 10.831 - \frac{2.706}{18} = 10.68067$$

$$k_1 = \frac{3.291 + \sqrt{10.831 - (0.92041)(10.68067)}}{0.92041} = 4.6623$$

$$Y_U = \bar{Y} + k_1 s$$

$$Y_U = 0.7126 + 4.6623(1.36) = 7.06\, ppb\ (LOD)$$

The calculation requires a mean and standard deviation and a confidence and population designation. The mean of this calculation must be the critical level, L_C, ($\mu_b + 3.3\sigma_b$) because the LOD justified by the tolerance interval needs to be shifted to the right of the critical level (where β is 0.5) to decrease the false negative rate, as is done with MCDA. This "shift to the right" is shown by the variable k_1 in the tolerance interval and represents the number of standard deviations from the critical level that the LOD will be. In total, the LOD will be $3.3 + k_1$ standard deviations from the blank. The standard deviation used in the calculation is the standard deviation of the blank, which is assuming homoscedasticity. In the future, variance modeling will be used to predict a more accurate uncertainty at the L_C and the LOD, as mentioned below. The confidence and population coverage were set at 95% and 99.95%, respectively.

A population coverage of 99.95% (below the interval specified) allows for 0.0005 false negative risk, shown in Figure 6.4. This is known because the standard deviation of the two curves is equal. A false negative rate of 0.0005 makes the tolerance interval LOD comparable to the MCDA. However, giving the tolerance interval a confidence level makes it inherently more reliable than the MCDA. As a result, LOD generally lies further from the blank than the MCDA. (i.e. $3.3 + k_1$ is greater than 3.3 + 3.3) With the specified conditions, k_1 is 4.6623, which means that the tolerance interval LOD is actually 1.3623 standard deviations further than the MCDA.

The point at which the LOD normal distribution and the distribution of the blank overlap is called the critical level ($\mu_b + 3.3\sigma_b$). The area of each curve that overlaps into the other at the critical level represents either the false positive or false negative error, shown in Figure 6.5. The rate of these errors decreases with the increase in number of standard

deviations from the blank in which the LOD lies. Here this distance is controlled primarily by the confidence and population spread chosen in the tolerance interval. In other words, by increasing the confidence and the population percentages, the number of standard deviations between the LOD and the blank will increase, thus decreasing the false positive and false negative error rates. In general, the tolerance interval based LODs were more conservative, which is to be expected.

Other means of calibration analysis include generalized least squares (GLS), simultaneous tolerance intervals and modeling weights for least squares. GLS includes uncertainties in the x-axis and the y-axis, unlike WLS (i.e. in GLS, there is no assumption that errors in the y direction need to be larger than the errors in the x direction) (18). However, there is the opposite assertion: there are errors in both the x and y direction; therefore, GLS calibration requires uncertainty profiles for both the calibration solutions (x direction) and their corresponding instrumental responses (y direction) (18). Once the standard deviation in each direction is determined, the inverse variance weights can be determined and applied.

The tolerance intervals described thus far have been non-simultaneous intervals. However, simultaneous tolerance intervals can also be useful and can be broken down into ordinary least squares intervals and weighted least squares intervals. Simultaneous intervals span the entire calibration model and, in the case of tolerance intervals, give a sense of uncertainty along the calibration. (i.e., for the future, the model will show an interval where, for instance, 99.95% of the population will lie, at any given concentration along the model, with 95% confidence). The simultaneous tolerance intervals require a correlation between variance and concentration. In the OLS case, this is rather simple due

to the homoscedasticity. However, with WLS tolerance intervals, a proper model must be fit to the relationship (described further in "modeling weights" below). Zorn and Gibbons both discuss calculations for the weighted tolerance intervals (3-4). As a result of the modeling of the variance, weighted tolerance interval width varies with concentration (4). Because error generally increases with concentration, weighted tolerance intervals allow for tighter tolerance intervals at lower concentrations which would result in lower and more accurate limits of detection (3).

In the case of the weighted and generalized least squares regressions and the weighted tolerance intervals, the weights are presumed to be known via analysis of the replicates or by propagation of error. However, when the number of replicates is low or when the propagation of error is too timely, the use of models to estimate the variance as a function of concentration should be explored. Obviously, the best fit model should be used and potential models include, but are not limited to, the Rocke and Lorenzo model, exponential model, and a linear model (32). Modeling variance as a function of concentration will also help to interpolate variances for future figures, including limit of detection.

Conclusion

Limit of detection is an important figure of merit in forensic trace analysis. A consistent limit of detection can be skewed through improper calculations. Firstly, it is imperative that the proper regression model be chosen for the calibration data. Heteroscedasticity is frequently overlooked and in its presence, weighted least squares regression is an appropriate alternative to ordinary (unweighted) least squares. Tolerance intervals,

specifically upper limit tolerance intervals, should be employed to determine the limit of detection value. At this time, tolerance intervals are calculated with an assumption of homoscedasticity, thus can only be used with OLS. Therefore, any extrapolation (converting from the y-axis to the x-axis) during the tolerance interval calculation should be done with the OLS regression model. Tolerance intervals give a conservative estimation of limit of detection that can be implemented for an extended period of time.

References

1. Currie, L. (1997) Detection: international update, and some emerging di-lemmas involving calibration, the blank, and multiple detection decisions. *Chemometrics and Intelligent Laboratory Systems*, **37**, 151-181.
2. Miller, J. (1991) Basic Statistical Methods for Analytical Chemistry Part 2. Calibration and Regression Methods. *Analyst*, **116**, 3-14.
3. Zorn, M., Gibbons, R., Sonzogni, William C. (1997) Weighted Least Squares Approach to Calculating Limits of Detection and Quantification by Modeling Variability as a Function of Concentration. *Analytical Chemistry*, **69**, 3069-3075.
4. Gibbons, R., Coleman, D. *Statistical Methods for Detection and Quantification of Environmental Contaminants*, John Wiley, New York, 2001.
5. Lavagnini, I., Magno, F. (2006) A Statistical Overview on Univariate Calibration, Inverse Regression, and Detection Limits: Application to GC/MS Technique. *Mass Spectrometry Reviews*, **26**, 1-18.
6. Currie, L. (1999) Detection and Quantification Limits: Origins and Historical Overview. *Analytica Chimica Acta*, **391**, 127-134.
7. IUPAC. Compendium of Chemical Terminology, 2nd ed. (the "Gold Book"). Compiled by A. D. McNaught and A. Wilkinson. Blackwell Scientific Publications, Oxford (1997)
8. Scientific Working Group for Forensic Toxicology (2013) Standard Practices for Method Validation in Forensic Toxicology. *Journal of Analytical Toxicology*, **37**, 452-474.

9. Analytical Methods Committee. (1987) Recommendations for the Definition, Estimation and Use of the Detection Limit. *Analyst*, **112**, 199-204.
10. *Engineering Statistics Handbook*, National Institute of Standards, Washington, DC [URL: http://www.itl.nist.gov/div898/handbook/index.htm].
11. Currie, L. (1995) Nomenclature in Evaluation of Analytical Methods Including Detection and Quantification Capabilities. *Pure & Applied Chemistry*, **67**, 1699-1723.
12. Inczedy, J., Lengyel, T., Ure, A. IUPAC Compendium of Analytical Nomenclature: Definitive Rules. 3rd Edition. 1997. Chapter 18 Section 4.3.7
13. U.S. Department of Health and Human Services, Food and Drug Administration. "Guidance for Industry: Bioanalytical Method Validation," **2001**.
14. U.S. Department of Health and Human Services, Food and Drug Administration. "Guidance for Industry: Q2B Validation of Analytical Procedures: Methodology," **1996**.
15. Deming, S., Morgan, S. Statistical Analysis of Laboratory Data, ACS Short Course, American Chemical Society, Washington D.C., 2006.
16. Hahn, G., Meeker, W. *Statistical Intervals: A Guide for Practitioners*, John Wiley & Sons, Inc. New York, 1991.
17. Zeng, Q., Zhang, E., Dong, H., Tellinghuisen, J. (2008) Weighted Least Squares in Calibration: Estimating data variance functions in high-performance liquid chromatography. *Journal of Chromatography A*, **1206**, 147-152

18. Duer, W., Ogren, P. et. Al. (2008) Comparison of ordinary, weighted, and generalized least-squares straight-line calibrations for LC-MS-MS, GC-MS, HPLC, GC, and enzymatic assay. *Journal of Analytical Toxicology*, **32**, 329-338.

19. Currie, L. A. (Ed.) Detection in Analytical Chemistry: Importance, Theory, and Practice, ACS Symp. Series 361, American Chemical Society, Washington, DC, 1988.

20. Rozet, E., Ziemons, E., Marini R., Boulanger B., Hubert, P. (2012) Quality by Design Complaint Analytical Method Validation. *Analytical Chemistry*, **84**, 106-112.

21. Zorn, M., Gibbons, R., Sonzogni, W. (1999) Evaluation of Approximate Methods for Calculating the Limit of Detection and Limit of Quantitation. *Environmental Science and Technol*ogy, **33**, 2291-2295.

22. Garber, C. (1995) Statistics. *Analytical Chemistry*, **67**, 443R-448R.

23. Long, G., Winefordner, J. (1983) Limit of Detection: A Closer Look at the IUPAC Definition. *Analytical Chemistry*, **55**, 712A-724A.

24. Voigtman, E. (2008) Limits of Detection and Decisions. Part 4. *Spectrochimica Acta Part B*, **63**, 154-165.

25. Bocio, J., Riu, J., Boque, R., Ruis, F., (2003) Limits of detection in linear regression with errors in the concentration. *Journal of Chemometrics*, **17**, 413-421.

26. Vial, J., Jardy, A. (1999) Experimental Comparison of the Different Approaches to Estimate LOD and LOQ of an HPLC Method. *Analytical Chemistry*, **71**, 2672-2677.

27. Thompson, M. (1989) Robust Statistics and Functional Relationship Estimation for Comparing the Bias of Analytical Procedures over Extended Concentration Ranges. *Analytical Chemistry,* **61**, 1942-1945.

28. Gonzalez, A., Herrador, M. (2007) A Practical Guide to Analytical Method Validation, Including Measurement Uncertainty and Accuracy Profiles. *Trends in Analytical Chemistry*, **26**, 227-238.

29. Almeida, A., Castel-Branco, M., Falcao, A. (2002) Linear regression for calibration lines revisited: weighting schemes for bioanalytical methods. *Journal of Chromatography B*, **774**, 215-222

30. Sadray, S., Rezaee, S., Rezakhah, S. (2003) Non-linear heteroscedastic regression model for determination of methotrexate in human plasma by high performance liquid chromatography. *Journal of Chromatography B*, **787**, 293-302.

31. Danzer, K., Currie, L. (1998) IUPAC: Guidelines for Calibration in Analytical Chemistry Part 1. Fundamentals and Single Component Calibration. *Pure and Applied Chemistry,* **70**, 993-1014

32. Currie, L. (1997) Detection: International update, and some emerging di-lemmas involving calibration, the blank, and multiple detection decisions. *Chemometrics and Intelligent Laboratory Systems*, **37**, 151-181.

Table 6.1. Confusion Matrix of False Positives and False Negatives

		PREDICTED	
		Positive	Negative
TRUE	Positive	True Positive	False Negative
	Negative	False Positive	True Negative

Table 6.2.
Effects on the limit of detection by estimating variability from different sources.

Acid Red 337		
σ_b	LOD Basis	LOD
standard deviation of replicate measurements of blanks, df = 14	$3.3\sigma_b$	3.07
standard deviation of the lowest non-zero calibrator, df = 5		1.89
standard deviation of the residuals, df = 43		0.86

Table 6.3.
Comparison of Calibration Parameters based on Unweighted versus Weighted Least Squares Analysis

Least Squares Regression Parameters						
	Unweighted			Weighted		
Dye	Intercept	Slope	S, residuals	Intercept	Slope	S, residuals
Acid Red 337	11.39	55.45	68.48	105.6	57.34	0.023
BasicYellow 28	93.52	56.32	62.68	110.7	55.02	0.046
Disperse Yellow 114	13.84	86.45	46.64	46.71	14.52	0.069
Basic Violet 16	93.65	109.7	122.5	95.97	93.94	0.037

Table 6.4. Comparison of UPLC with UV/visible detection LODs for textile dyes (in ppb) ($x_{LOD} = \bar{x}_{blank} + 3.3s$) based on: (1) s_b ; (2) s of the lowest non-zero concentration replicates; (3) s of the y-intercept of the calibration line; and (4) a statistical tolerance interval.

DYE	LOD_1	LOD_2	LOD_3	LOD_4
Basic Violet 16	1.84	2.09	0.91	4.36
Basic Yellow 28	2.69	0.93	0.77	6.50
Acid Red 337	3.07	1.89	0.86	7.06

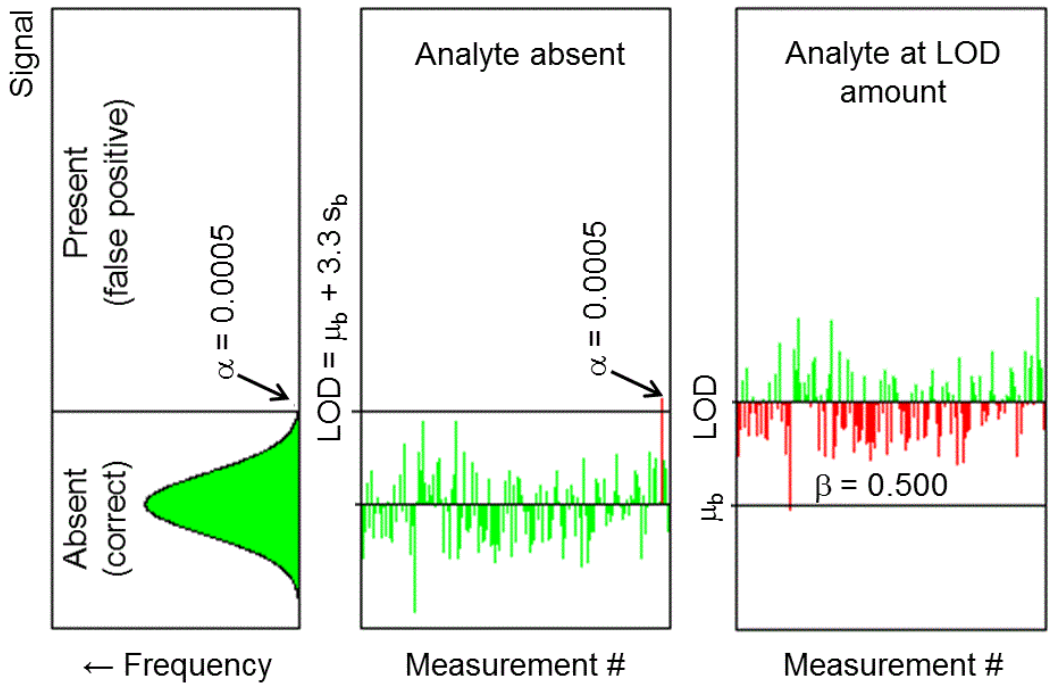

Figure 6.1. False positive and false negative risks for a sample containing analyte equivalent to the amount at the limit of detection.

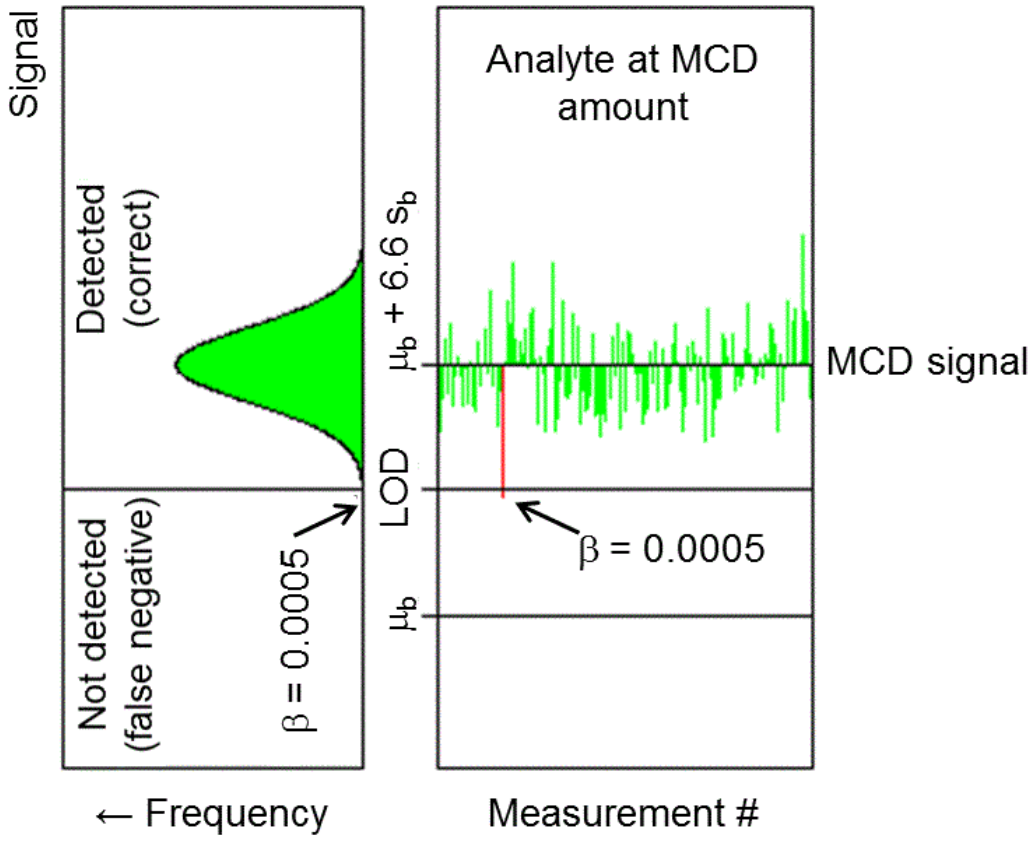

Figure 6.2. For a sample that contains an amount of analyte that gives a signal equal to the mean of the blank plus 6.6 standard deviations of the blank signal (twice that for LOD), it can be said that analyte has been confidently detected (at or above the LOD), and that the analyte is also consistently detected (at or above the MCDA).

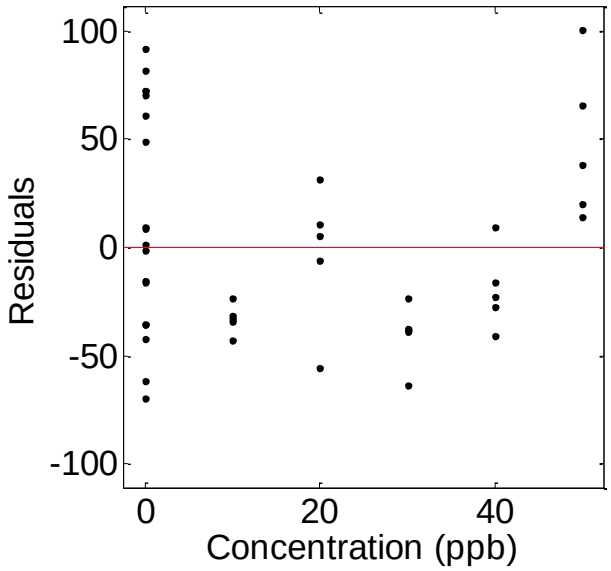

Figure 6.3. An example of heteroscedasticity in the Disperse Yellow 114 data. The critical value of the F-Statistic with 41 degrees of freedom is 4.0785 at 95% confidence. The calculated F-statistic for this data is 1268.7695. This exemplifies the lack of fit of the ordinary least squares model.

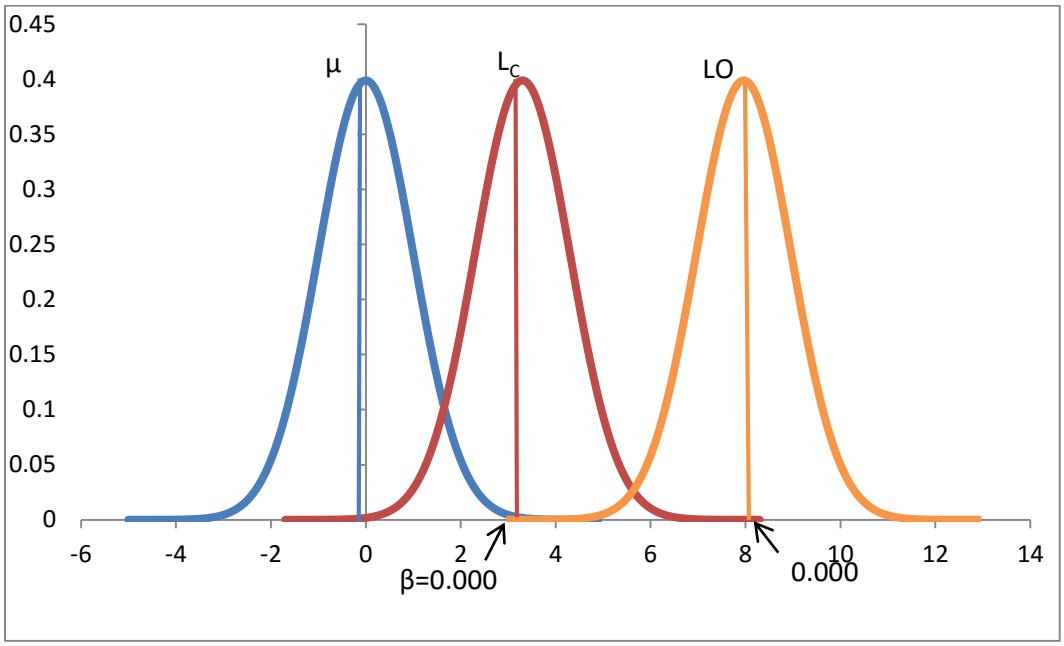

Figure 6.4. Comparison of the blank, critical level, and LOD distributions.

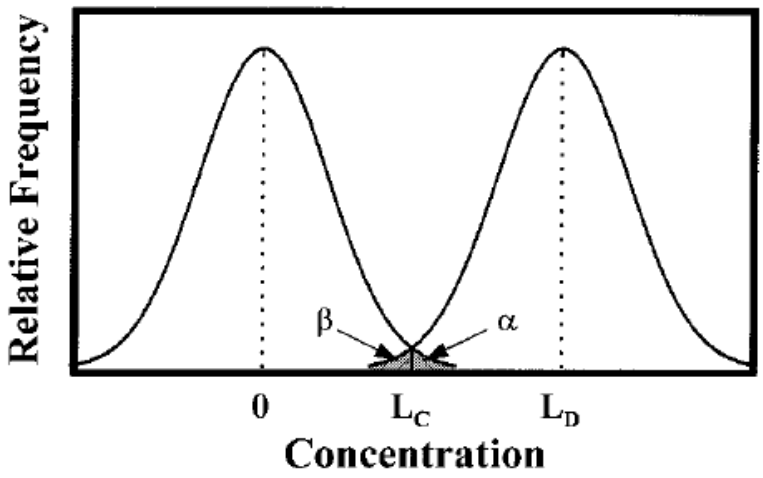

Figure 6.5. Relationship between the blank, limit of detection, and the critical level. Representation of the false positive and false negative error. L_D is the limit of detection, L_C is the critical level, and the blank mean is shown to be zero (3).

REFERENCES

Aderjan, R., Skopp, G. (1998) Formation and Clearance of Active and Inactive Metabolites of Opiates in Humans. *Therapeutic Drug Monitoring*. **20**, 561-569.

Almeida, A., Castel-Branco, M., Falcao, A. (2002) Linear regression for calibration lines revisited: weighting schemes for bioanalytical methods. *Journal of Chromatography B*, **774**, 215-222

Analytical Methods Committee. (1987) Recommendations for the Definition, Estimation and Use of the Detection Limit. *Analyst*, **112**, 199-204.

Bar-Oz, B. (2003) Comparison of Meconium and Neonatal Hair Analysis for Detection of Gestational Exposure to Drugs of Abuse.*Archives of Disease in Childhood. Fetal and Neonatal Edition*, **88**, F98-F100.

(2012) Bcnc.org.uk. Benzodiazepine use in pregnancy. http://www.bcnc.org.uk/BZ_pregnancy.pdf (accessed 1 January 2015)

Bicker, J., Fortuna, A., Alves, G., Falcao, A. (2013) Liquid chromatographic methods for the quantification of catecholamines and their metabolites in several biological samples—A review. *Analytica Chimica Acta*, **768**, 12-34.

Boerner, U., Abbott, S., Roe, R. (1975) The Metabolism of Morphine and Heroin in Man. *Drug Metabolism Reviews*. **4**, 39-73.

Bogusz, M., Maier, R., Driessen, S. (1997) Morphine, Morphine-3-Glucuronide, Morphine-6-Glucuronide, and 6-Monoacetylmorphine Determined by Means of Atmospheric Pressure Chemical Ionization-Mass Spectrometry-Liquid Chromatography in Body Fluids of Heroin Victims. Journal of Analytical Toxicology, 21, 346-355.

Bordin, D., Alves, M., Cabrices, O., Campos, E., De Martinis, B. (2013)A Rapid Assay for the Simultaneous Determination of Nicotine, Cocaine, and Metabolites in Meconium Using Disposable Pipette Extraction and Gas Chromatography-Mass Spectrometry. *Journal of Analytical Toxicology*, **38**, 31-38.

Boyle, J., Davidson, D., Perry, C., Connell, J. (2007) Comparison of diagnostic accuracy of urinary free metanephrines, vanillyl madelic acid, and catecholamines and plasma catecholamines for diagnosis of phaechromocytoma. *Journal of Clinical Endocrinology and Metabolism*, **92**, 4602-4608.

Bocio, J., Riu, J., Boque, R., Ruis, F., (2003) Limits of detection in linear regression with errors in the concentration. *Journal of Chemometrics*, **17**, 413-421.

Breyer-Pfaff, U. (2004) The metabolic fate of amitriptyline, nortriptyline, and amitriptylinoxide in man. *Drug Metabolism Reviews*, **36**, 723-746.

Chabria, S. (2006) Rhabdomyolysis: a manifestation of cyclobenzaprine toxicity. *Journal of Occupational Medicine and Toxicology*, **1**, 1-2.

Cimolai, N. (2009) Cyclobenzaprine: a new look at an old pharmacological agent. *Expert Reviews in Clinical Pharmacology*, **2**, 255-263.

Clark, Z., Frank, E. (2011) Urinary metanephrines by liquid chromatography tandem mass spectrometry: Using multiple quantification methods to minimize interferences in a high throughput method. *Journal of Chromatography B*, **879**, 3673-3680.

Compton, R., Berning, A. (2009) Results of the 2007 national roadside survey of alcohol and drug use by drivers. COT HS 811 175. NHTSA, Washington, DC.

Cone, E., Welch, P. (1991) Forensic Drug Testing for Opiates: I. Detection of 6-Acetylmorphine in Urine as an Indicator of Recent Heroin Exposure; Drug and Assay Considerations and Detection Times. *Journal of Analytical Toxicology*, **15**, 1-7.

Cone, E., Jufer, R., Darwin, W. (1996) Forensic Drug Testing for Opiates. VII. Urinary Excretion Profile of Intranasal (Snorted) Heroin. *Journal of Analytical Toxicology*. **20**, 379-392.

Coulter, C., Miller, E., Crompton, K., Moore, C. (2008) Tetrahydrocannabinol and two of its metabolites in whole blood using liquid chromatography-tandem mass spectrometry. *Journal of Analytical Toxicology*, **32**, 653-658.

Couper, F., Peterson, B. (2014) The prevalence of marijuana in suspected impaired driving cases in Washington state. *Journal of Analytical Toxicology*, **38**, 569-574.

Currie, L. (Ed.) Detection in Analytical Chemistry: Importance, Theory, and Practice, ACS Symp. Series 361, American Chemical Society, Washington, DC, 1988.

Currie, L. (1995) Nomenclature in Evaluation of Analytical Methods Including Detection and Quantification Capabilities. *Pure & Applied Chemistry*, **67**, 1699-1723.

Currie, L. (1997) Detection: International update, and some emerging di-lemmas involving calibration, the blank, and multiple detection decisions. *Chemometrics and Intelligent Laboratory Systems*, **37**, 151-181.

Currie, L. (1999) Detection and Quantification Limits: Origins and Historical Overview. *Analytica Chimica Acta*, **391**, 127-134.

Dahl-Puustinen, M., Aberg-Wistedt, A., Bertilsson, L. (1989) Glucuronidation of Amitriptyline in Man *in Vivo*. *Pharmacology and Toxicology*, **65**, 37-35.

Danzer, K., Currie, L. (1998) IUPAC: Guidelines for Calibration in Analytical Chemistry Part 1. Fundamentals and Single Component Calibration. *Pure and Applied Chemistry*, **70**, 993-1014

Deming, S., Morgan, S. Statistical Analysis of Laboratory Data, ACS Short Course, American Chemical Society, Washington D.C., 2006.

Diniz, M., Vilhena, L., Paulo, B., Barbosa, T., Mateo, E. (2015) Simultaneous determination of catecholamines and metanephrines in urine by liquid chromatography electrospray ionization tandem mass spectrometry: successful clinical application. *Journal of Brazilian Chemical Society*, **26**, 1684-1691.

Duer, W., Ogren, P. et. Al. (2008) Comparison of ordinary, weighted, and generalized least-squares straight-line calibrations for LC-MS-MS, GC-MS, HPLC, GC, and enzymatic assay. *Journal of Analytical Toxicology*, **32**, 329-338.

Elian, A., Hackett, J. (2009) Solid-phase extraction and analysis of THC and Carboxy-THC from whole blood using a novel fluorinated solid-phase extraction sorbent and fast liquid chromatography-tandem mass spectrometry. *Journal of Analytical Toxicology*, **33**, 461-468.

Engineering Statistics Handbook, National Institute of Standards, Washington, DC [URL: http://www.itl.nist.gov/div898/handbook/index.htm].

Fabritius, M. et al. (2013) Comparison of cannabinoid concentrations in oral fluid and whole blood between occasional and regular cannabis smokers prior to and after smoking a cannabis joint. *Analytical and Bioanalytical Chemistry*, **405**, 9791-9803.

Fernandez, M., Boeck, G., Wood, M., Lopez-Rivadulla, M., Samyn, N. (2008) Simultaneous analysis of THC and its metabolites in blood using liquid chromatography-tandem mass spectrometry. *Journal of Chromatography B*, **875**, 465-470.

Fischer, D., Breyer-Pfaff, U. (1995) Comparison of procedures for measuring the quaternary N-glucuronides of amitriptyline and diphenhydramine in human urine with and without hydrolysis. *Journal of Pharmacy and Pharmacology*, **47**, 534-538.

Garber, C. (1995) Statistics. *Analytical Chemistry*, **67**, 443R-448R.

Garcia-Algar, O., Lopez-Vilchez, M.A., Martin, I., Mur, A., Pellegrini, M., Pacifici, R., Rossi, S., Pichini, S. (2007) Confirmation of gestational exposure to alprazolam by analysis of biological matrices in a newborn with neonatal sepsis. *Clinical Toxicology*, **45**, 295-298.

Gareri, J., Klein, J., Koren, G. (2006) Drugs of abuse testing in meconium. *Clinica Chimica Acta*, **366**, 101-111.

Gibbons, R., Coleman, D. *Statistical Methods for Detection and Quantification of Environmental Contaminants*, John Wiley, New York, 2001.

Gonzalez, A., Herrador, M. (2007) A Practical Guide to Analytical Method Validation, Including Measurement Uncertainty and Accuracy Profiles. *Trends in Analytical Chemistry*, **26**, 227-238.

Gray, T., Shakleya, D., Huestis, M. (2009) A liquid chromatography tandem mass spectrometry method for the simultaneous quantification of 20 drugs of abuse and metabolites in human meconium. *Analytical and Bioanalytical Chemistry*, **393**, 1977-1990.

Grotenhermen, F. (2003) Pharmacokinetics and pharmacodynamics of cannabinoids. *Clinical Pharmacokinetics*, **42**, 327–360.

Hahn, G., Meeker, W. *Statistical Intervals: A Guide for Practitioners*, John Wiley & Sons, Inc. New York, 1991.

Hawes, E. (1998) N+-glucuronidation, a common pathway in human urine of drugs with a tertiary amine group. *Drug Metabolism and Disposition*, **26**, 830-837.

Heideloff, C., Gabler, J., Yuan, C., Zhang, L., Wang, S. (2014) In Vitro Conversion of Morphine to 6-Acetylmorphine in Urine Samples during Enzymatic Hydrolysis. *Clinical Chemistry*. **60**, 1234-1235.

Hucker, H., Balletto, A., Arison, B., Zacchei, A. Arison, B. (1978) Physiological disposition and metabolism of cyclobenzaprine in the rat, dog, rhesus monkey, and man. *Drug Metabolism and Disposition*, **6**, 659-672.

Huestis, M.A. (2007) Human cannabinoid pharmacokinetics. *Chemistry and Biodiversity*, **4**, 1770–1804.

Inczedy, J., Lengyel, T., Ure, A. IUPAC Compendium of Analytical Nomenclature: Definitive Rules. 3rd Edition. 1997. Chapter 18 Section 4.3.7

Iqbal, M.M., Sobhan, T., Ryals, T. (2002) Effects of commonly used benzodiazepines on the fetus, the neonate, and the nursing infant. *Psychiatric Services*, **53**, 39-49.

IUPAC. Compendium of Chemical Terminology, 2nd ed. (the "Gold Book"). Compiled by A. D. McNaught and A. Wilkinson. Blackwell Scientific Publications, Oxford (1997)

Jagerdeo, E., Schaff, J., Montgomery, M., LeBeau, M. (2009) A semi-automated solid-phase extraction liquid chromatography/tandem mass spectrometry method for the analysis of tetrahydrocannabinol and metabolites in whole blood. *Rapid Communications in Mass Spectrometry*, **23**, 2697-2705.

Jamey, C., Szwarc, E., Tracqui, A., Ludes, B., (2008) Determination of cannabinoids in whole blood by UPLC-MS-MS. *Journal of Analytical Toxicology*, **32**, 349-354.

Kowalczyk, I., Hawes, E., McKay, G. (2000) Stability and enzymatic hydrolysis of quaternary ammonium-linked glucuronide metabolites of drugs with an aliphatic tertiary amine-implications for analysis. *Journal of Pharmaceutical and Biomedical Analysis*, **22**, 803-811.

Krouwer, J., Rabinowitz, R. (1984) How to Improve Estimates of Imprecision. *Clinical Chemistry*, **30**, 290-292.

Kushnir, M., Urry, F., Frank, E., Roberts, W., Shushan, B. (2002) Analysis of catecholamines in urine by positive-ion electrospray tandem mass spectrometry. *Clinical Chemistry*, **48**, 323-331.

LaCroix, C., Saussereau, E. (2012) Fast liquid chromatography/tandem mass spectrometry determination of cannabinoids in micro volume blood samples after dabsyl derivatization. *Journal of Chromatography B*, **905**, 85-95.

Lavagnini, I., Magno, F. (2006) A Statistical Overview on Univariate Calibration, Inverse Regression, and Detection Limits: Application to GC/MS Technique. *Mass Spectrometry Reviews*, **26**, 1-18.

Lebby, T., Dugger, K. (1990) Skeletal muscle relaxant ingestion. *Veterinary and Human Toxicology*, **32**, 133-135.

Li, X., Li, S., Wynveen, P., Mork, K., Kellermann, G. (2014) Development ad validation of a specific and sensitive LC-MS/MS method for quantification of urinary catecholamines and application in biological variation studies. *Analytical and Bioanalytical Chemistry*, **406**, 7287-7297.

Linden, C., Mitchener, J., Lindzon, R., Rumack, B. (1983) Cyclobenzaprine overdosage. *Clinical Toxicology*, **20**, 281-288.

Logan, B., Lowric, K., Turri, J., Yeakel, J., Limoges, J., Miles, A., Scarneo, C., Kerrigan, S., Farrell, L. (2013) Recommendations for Toxicological Investigation of Drug-Impaired Driving and Motor Vehicle Fatalities. *Journal of Analytical Toxicology*, **37**, 552-558.

Long, G., Winefordner, J. (1983) Limit of Detection: A Closer Look at the IUPAC Definition. *Analytical Chemistry*, **55**, 712A-724A.

Marin, S.J. (2008) Quantitation of Benzodiazepines in Urine, Serum, Plasma, and Meconium by LC-MS-MS. *Journal of Analytical Toxicology*, **32**, 492-498.

Marin S and McMillin G (2010). LC-MS/MS Analysis of 13 Benzodiazepines and Metabolites in Urine, Serum, Plasma and Meconium. In Hammett-Stabler C, Garg U (Eds.), *Clinical Applications of Mass Spectrometry* (pp. 89-105). Totowa NJ: Humana Press.

Masten, S., Guenzburger, G. (2014) Changes in driver cannabinoid prevalence in 12 U.S. states after implementing medical marijuana laws. *Journal of Safety Research*, **50**, 35-52.

McMillin, G.A., Wood, K.E., Strathmann, F.G., Krasowski, M.D. (2015) Patterns of Drugs and Drug Metabolites Observed in Meconium; What Do They Mean? *Therapeutic Drug Monitoring*, 37, 568-80.

Miki, K., Sudo, A. (1998) Effect of Urine pH, Storage Time, and Temperature on Stability of Catecholamines, Cortisol, and Creatinine. *Clinical Chemistry*, **44**, 1759-1762.

Miller, J. (1991) Basic Statistical Methods for Analytical Chemistry Part 2. Calibration and Regression Methods. *Analyst*, **116**, 3-14.

Mitchell, J., Paul, B. (1991) Forensic Drug Testing For Opiates. II. Metabolism and Excretion Rate of Morphine in Humans After Morphine Administration. *Journal of Analytical Toxicology*. **15**, 49-53.

Morris, A.A., Chester, S.S., Strickland, E.C., McIntire, G.L. (2014) Rapid enzymatic hydrolysis using a novel β-glucuronidase in benzodiazepine urinalysis. *Journal of Analytical Toxicology*, **38**, 610-614.

Nakamura, M. (2011) Analyses of benzodiazepines and their metabolites in various biological matrices by LC-MS(/MS). *Biomedical Chromatography*, **25**, 1283-1307.

O'Riordan, W., Gillette, P., Calderon, J., Stennes, R. (1986) Overdose of cyclobenzaprine, the tricyclic muscle relaxant. *Annals of Emergency Medicine*, **15**, 592-593.

Peaston, R., Weinkove, C. (2004) Measurement of catecholamines and their metabolites. *Annals of Clinical Biochemistry*, **41**, 17-38.

Peitzsch, M., Pelzel, D., Glockner, S., Prejbisz, A., Fassnacht, M., Beuschlein, F., Januszewicz, A., Siegert, G., Eisenhofer, G. (2013) Simultaneous liquid chromatography tandem mass spectrometric determination of urinary free metanephrines and catecholamines with comparisons of free and deconjugated metabolites. *Clinica Chimica Acta*, **418**, 50-58.

Pichini, S., Cortes, L., Marchei, E., Solimini, R., Pacifici, R., Gomez-Roig, M., Garcia-Algar, O., (2016) Ultra-high-pressure liquid chromatography tandem mass spectrometry determination of antidepressant and anxiolytic drugs in neonatal meconium and maternal hair. *Journal of Pharmaceutical and Biomedical Analysis*, **118**, 9-16.

Rana, S., Uralets, V., Ross, W. (2008) A new method for simultaneous determination of cyclic antidepressants and their metabolites in urine using enzymatic hydrolysis and fast GC-MS. *Journal of Analytical Toxicology*, **32**, 355-363.

Rozet, E., Ziemons, E., Marini R., Boulanger B., Hubert, P. (2012) Quality by Design Complaint Analytical Method Validation. *Analytical Chemistry*, **84**, 106-112.

Sadray, S., Rezaee, S., Rezakhah, S. (2003) Non-linear heteroscedastic regression model for determination of methotrexate in human plasma by high performance liquid chromatography. *Journal of Chromatography B*, **787**, 293-302.

Schwope, D., Scheidweiler, K. (2011) Direct quantification of cannabinoids and cannabinoid glucuronides in whole blood by liquid chromatography-tandem mass spectrometry. *Analytical and Bioanalytical Chemistry*, **401**, 1273-1283.

Scientific Working Group for Forensic Toxicology (2013) Standard Practices for Method Validation in Forensic Toxicology. *Journal of Analytical Toxicology*, **37**, 452-474.

Simoes, S., Ajenjo, A., Dias, M. (2011) Qualitative and quantitative analysis of THC, 11-hydroxy-THC, and 11-nor-9-carboxy-THC in whole blood by ultra-performance liquid chromatography/tandem mass spectrometry. *Rapid Communications in Mass Spectrometry*, **25**, 2603-2610.

Smith, M., Shimomura, E., Summers, J., Paul, B. (2001) Urinary Excretion Profiles for Total Morphine, Free Morphine, and 6-Acetylmorphine Following Smoked and Intravenous Heroin. *Journal of Analytical Toxicology*. **25**, 504-514.

Spiller, H., Winter, M., Mann, K., Borys, D., Muir, S., Krenzelok, E. (1995) Five-year multicenter retrospective review of cyclobenzaprine toxicity. *Journal of Emergency Medicine*, **13**, 781-785.

Spiller, H., Cutino, L. (2003) Fatal cyclobenzaprine overdose with postmortem values. *Journal of Forensic Science*, **48**, 883-884.

Substance Abuse and Mental Health Services Administration, Results from the 2013 National Survey on Drug Use and Health: Summary of National Findings, NSDUH Series H-48, HHS Publication No. (SMA) 14-4863. Rockville, MD: Substance Abuse and Mental Health Services Administration, 2014.

Talwar, D., Williamson, C., McLaughlin, Gill, A., O'Reilly, D. (2002) Extraction and separation of urinary catecholamines as their diphenyl boronate complexes using C_{18} solid-phase extraction sorbent and high-performance liquid chromatography. *Journal of Chromatography B*, **769**, 341-349.

Thompson, M. (1989) Robust Statistics and Functional Relationship Estimation for Comparing the Bias of Analytical Procedures over Extended Concentration Ranges. *Analytical Chemistry*, **61**, 1942-1945.

Urfer, S., Morton, J., Beall, V., Feldmann, J., Gunesch, J. (2014) Analysis of Δ9-tetrahydrocannabinol Driving Under the Influence of Drugs Cases in Colorado from January 2011 to February 2014. *Journal of Analytical Toxicology*, **38**, 575-581.

U.S. Department of Health and Human Services, Food and Drug Administration. "Guidance for Industry: Bioanalytical Method Validation," **2001**.

U.S. Department of Health and Human Services, Food and Drug Administration. "Guidance for Industry: Q2B Validation of Analytical Procedures: Methodology," **1996**.

Vial, J., Jardy, A. (1999) Experimental Comparison of the Different Approaches to Estimate LOD and LOQ of an HPLC Method. *Analytical Chemistry*, **71**, 2672-2677.

Voigtman, E. (2008) Limits of Detection and Decisions. Part 4. *Spectrochimica Acta Part B*, **63**, 154-165.

Von Euler, M., Villen, T., Svensson, J., Stahle, L. (2003) Interpretation of the Presence of 6-Monoacetylmorphine in the Absence of Morphine-3-glucuronide in Urine Samples: Evidence of Heroin Abuse. *Therapeutic Drug Monitoring*. **25**, 645-648.

Whiting, M. (2009) Simultaneous measurement of urinary metanephrines and catecholamines by liquid chromatography with tandem mass spectrometric detection. *Annals of Clinical Biochemistry*, **46**, 129-136.

Wilkner, B.N., Stiller, C., Bergamn, U., Asker, C., Kallen, B. (2007) Use of benzodiazepines and benzodiazepine receptor agonists during pregnancy: neonatal outcome and congenital malformations. *Pharmacoepidemiology and Drug Safety*, **16**, 1203-1210.

Williamson, S. (2006) Determination of the Prevalence of Drug Misuse by Meconium Analysis. *Archives of Disease in Childhood. Fetal and Neonatal Edition*, **91**, F291-F292.

Woo, H., Yang, J., Oh, H., Cho, Y., Kim, J., Park, H., Lee, S. (2016) A simple and rapid analytical method based on solid-phase extraction and liquid chromatography-mass spectrometry for the simultaneous determination of free catecholamines and metanephrines. *Clinical Biochemistry*, **49**, 573-579.

Wood, E., Brooks-Russell, A., Drum, P. (2016) Delays in DUI blood testing: Impact on cannabis DUI assessments. *Traffic Injury Prevention*, **17**, 105-108.

Wu, F. Marin, S. Clark, C., McMillin, G. Stability of 21 cocaine, opioid and benzodiazepine drug analytes in meconium at three temperatures. Presented at: 51st Annual Academy of Clinical Laboratory Physicians and Scientists Meeting; 2016 Jun 2-4; Birmingham, AL

Yeh, S., Gorodetzky, C., McQuin, R. (1976) Urinary Excretion of Heroin and Its Metabolites in Man. *Journal of Pharmacology and Experimental Therapeutics*. **196**, 249-256.

Zeng, Q., Zhang, E., Dong, H., Tellinghuisen, J. (2008) Weighted Least Squares in Calibration: Estimating data variance functions in high-performance liquid chromatography. *Journal of Chromatography A*, **1206**, 147-152

Zorn, M., Gibbons, R., Sonzogni, William C. (1997) Weighted Least Squares Approach to Calculating Limits of Detection and Quantification by Modeling Variability as a Function of Concentration. *Analytical Chemistry*, **69**, 3069-3075.

Zorn, M., Gibbons, R., Sonzogni, W. (1999) Evaluation of Approximate Methods for Calculating the Limit of Detection and Limit of Quantitation. *Environmental Science and Technol*ogy, **33**, 2291-2295.

Zuccaro, P., Ricciarello, R., Pichini, S., Pacifici, R., Altieri, I., Pellegrini, M. Ascenzo, G. (1997) Simultaneous Determination of Heroin, 6-Monoacetylmorphine, Morphine, and its Glucuronides by Liquid Chromatography-Atmospheric Pressure Ionspray-Mass Spectrometry. *Journal of Analytical Toxicology*. **21**, 268-277.